ICE PACK HEAT SINK SUBSYSTEM - PHASE II

FINAL REPORT

BY
GEORGE J. ROEBELEN JR.
AND
JORDAN D. KELLNER

PREPARED UNDER CONTRACT NO. NAS 2-7011

By
HAMILTON STANDARD
DIVISION OF UNITED AIRCRAFT CORPORATION
WINDSOR LOCKS, CONNECTICUT

For
NATIONAL AERONAUTICS AND SPACE ADMINISTRATION
AMES RESEARCH CENTER
MOFFET FIELD, CALIFORNIA 94035

JANUARY 1975

Hamilton Standard DIVISION OF UNITED AIRCRAFT CORPORATION

CR 137611
SVHSER 6525

ABSTRACT

ICE PACK HEAT SINK SUBSYSTEM - PHASE II

by

George J. Roebelen, Jr.

and

Jordan D. Kellner

Contract No. NAS 2-7011

This report describes the design, development, fabrication, and test at one gravity of a prototype Ice Pack Heat Sink Subsystem to be used eventually for astronaut cooling during manned space missions; the investigation of thermal storage material with the objective of uncovering materials with heats of fusion and/or solution in the range of 300 Btu/lb (700 kilojoules/kilogram); and the planned procedure for implementing an Ice Pack Heat Sink Subsystem Flight Experiment.

In normal use, excess heat in the liquid cooling garment (LCG) coolant is transferred to a reusable/regenerable ice pack heat sink. For emergency operation, or for extension of extravehicular activity mission time after all the ice has melted, water from the ice pack is boiled to vacuum, thereby continuing to remove heat from the LCG coolant. This subsystem incorporates a quick disconnect thermal interface between the ice pack heat sink and the subsystem heat exchanger.

Hamilton Standard
DIVISION OF UNITED AIRCRAFT CORPORATION

CR 137611
SVHSER 6525

ICE PACK HEAT SINK SUBSYSTEM - PHASE II

FINAL REPORT

BY

GEORGE J. ROEBELEN, JR.

AND

JORDAN D. KELLNER

PREPARED UNDER CONTRACT NO. NAS 2-7011

BY

HAMILTON STANDARD

DIVISION OF UNITED AIRCRAFT CORPORATION

WINDSOR LOCKS, CONNECTICUT

FOR

NATIONAL AERONAUTICS AND SPACE ADMINISTRATION

AMES RESEARCH CENTER

MOFFETT FIELD, CALIFORNIA 94035

DECEMBER 1974

Hamilton Standard DIVISION OF UNITED AIRCRAFT CORPORATION UA

FOREWORD

This report has been prepared by the Hamilton Standard Division of the United Aircraft Corporation for the National Aeronautics and Space Administration's Ames Research Center in accordance with the requirements of Contract NAS 2-7011, Ice Pack Heat Sink Subsystem - Phase II.

Appreciation is expressed to the NASA Technical Monitor, Mr. James R. Blackaby of the Ames Research Center, for his guidance and advice.

Hamilton Standard personnel responsible for the conduct of this program were Mr. F. H. Greenwood, Program Manager, and Mr. G. J. Roebelen, Jr., Program Engineer. Appreciation is expressed to Mr. J. S. Lovell, Chief, Advanced Engineering; Mr. P. F. Heimlich, Design Engineer; and Mr. E. H. Tepper, Analytical Engineer, whose efforts made the successful completion of this program possible.

United Aircraft Research Laboratories personnel responsible for the Thermal Storage Materials Evaluation portion of this program were Dr. Jordan Kellner, principal investigator, and D. G. McMahon, Chief, Chemical Sciences.

A Flight Experiment Plan has been prepared as a result of effort expended during the period covered by this report. This plan, which outlines the steps necessary for developing the Ice Pack Heat Sink Subsystem into a Shuttle/Spacelab flight experiment, is contained under separate cover, Ice Pack Heat Sink Subsystem - Phase II, Flight Experiment Plan, SVHSER 6526.

Hamilton Standard DIVISION OF UNITED AIRCRAFT CORPORATION UA

TABLE OF CONTENTS

TABLE OF CONTENTS (Continued)

TABLE OF CONTENTS (Continued)

TABLE OF CONTENTS (Concluded)

LIST OF FIGURES

LIST OF FIGURES (Continued)

LIST OF FIGURES (Concluded)

LIST OF TABLES

LIST OF TABLES (Concluded)

INTRODUCTION

Future manned space exploration missions are expected to include requirements for astronaut life support equipment capable of repeated use and regeneration for many extravehicular activity sorties. In anticipation of these requirements, NASA ARC funded two contracts (NAS 2-6021 and NAS 2-6022) for the study of Advanced Extravehicular Protective Systems. The purpose of these studies was to determine the most practical and promising concepts for manned space flight operations projected for the late 1970's and 1980's, and to identify areas where concentrated research would be most effective in the development of these concepts.

One regenerative concept for astronaut cooling utilizes an ice pack as the primary heat sink for a liquid cooling garment (LCG) cooling system. In an emergency, or for extended operations, water from the melted ice pack could be evaporated (boiled) directly to space vacuum. NASA ARC funded contract NAS 2-7011 Phase I to design, develop, fabricate, and test at one gravity a functional laboratory model of such an Ice Pack Heat Sink Subsystem.

This report describes the effort funded by NASA ARC under contract NAS 2-7011 Phase II whereby the Ice Pack Heat Sink Subsystem prototype system was designed, fabricated, and performance tested at one gravity. Further, this report describes the work expended to uncover a material or materials that might be substituted for water/ice as the thermal sink thereby reducing system weight and volume.

Calculations and data pertaining to the execution of this program were made in U.S. customary units and then converted to SI units.

SUMMARY

The objectives of the Ice Pack Heat Sink Subsystem - Phase II program are to improve the design and performance of the ice chest/heat exchanger interface; to design, fabricate, and performance test at one gravity a prototype system; to investigate thermal storage material with the objective of uncovering materials with heats of fusion and/or heats of solution in the range of 300 Btu/lb (700 kilojoules/kilogram); and to prepare a plan for a candidate Shuttle/Spacelab flight experiment capable of demonstrating the performance of an Ice Pack Heat Sink Subsystem for astronaut cooling in zero-gravity, as well as providing data on the physical phenomena associated primarily with the heat transfer aspects of the operation of such a system.

The basic purposes for conducting the Interface Development portion of the program were to develop a heat transfer interface surface combination that is sufficiently durable in construction to allow many (100 plus) couplings and uncouplings without degradation of performance, and to investigate surface configurations and preloading pressures with the intent of generating sufficient data to allow selection of optimum surface configurations and preload pressure. Additionally, a computer program has been prepared to allow optimization of Ice Pack geometry.

Based on the results of the Interface Development effort, as well as on the experience gained in the laboratory model development program (NAS 2-7011 Phase I), a prototype system has been designed, fabricated, and acceptance tested. Two prototype ice chests were designed and fabricated: one with and one without the requirement that the ice chest function as a water boiler for emergency cooling. A heat exchanger has been designed and fabricated to be capable of mating with each of the ice chests developed in this task. Performance requirements for this subsystem consist of providing a heat sink for the LCG coolant for one hour at a 1500 Btu/hr (1600 kilojoules/hr) heat rejection rate and with an LCG inlet temperature compatible to astronaut comfort. The tests completed during this series have confirmed the adequacy of the design.

Math model correlation has been established and has been utilized to create a simple procedure to schedule ice chest water flow as a function of heating rate, inlet water temperature and fraction of ice melted.

The thermal storage material work has shown that a 30 percent solution of potassium bifluoride (KHF_2) in water can be used to provide approximately 52 percent more heat absorption than an equal weight of

water-ice, and approximately 79 percent more heat absorption than an equal volume of water-ice. The regeneration of the KHF_2 water system can be accomplished easily by the same technique used presently for water-ice. Heat absorption begins at a lower temperature, however, than that for water-ice, 10.4°F (261K) as compared to 32°F (273K) for water-ice. Results of measurements of the heat of fusion of some likely candidate compounds and eutectic mixtures are also included in this report; however, none were found to approach the heat of fusion of water-ice in the temperature range of 14° to 158°F (263-343K).

Resulting from the effort to prepare a plan for a candidate Shuttle/Spacelab flight experiment is a comprehensive outline, Ice Pack Heat Sink Subsystem - Phase II, Flight Experiment Plan, SVHSER 6526, which describes the steps necessary to develop the concepts to flight experiment status. This report is contained under separate cover to allow its circulation independent of this final report.

Based on the results of this program the Ice Pack Heat Sink Subsystem prototype hardware has been developed to a point where it has shown itself to be acceptable for astronaut cooling during EVA.

CONCLUSIONS

Completion of the hardware portion of this program has led to the development of a prototype Ice Pack Heat Sink Subsystem with the following characteristics:

- The unit holds 10.45 lbm (4.75 kg) of water.
- Cooling loads of 750, 1500, and 2000 Btu/hr (800, 1600, and 2130 kJ/hr) can be satisfied for both the normal melting ice and emergency water boiling modes of operation.
- The interfaces between the ice chest/boiler and the heat exchangers are sufficiently durable to withstand repeated removal/installation cycles.

Completion of the thermal storage materials portion of this program has shown that a 30 percent solution of potassium bifluoride (KHF_2) in water can provide approximately 52 percent more heat absorption than an equal weight of water-ice, and approximately 79 percent more heat absorption than an equal volume of water-ice, with heat absorption beginning at 10.4°F (261K) as compared to 32°F (273K) for water-ice.

RECOMMENDATIONS

The studies and test results of this program evolved the following recommendations.

- Continuation of the basic hardware configuration generated by this program phase is recommended.

- Additional effort is recommended to study the impact of replacing water with a 30 percent solution of potassium bifluoride (KHF_2) in water as the heat sink material in the ice chest/boiler.

NOMENCLATURE

Btu	British thermal unit
Btu/hr	British thermal unit per hour
Btu/hr-^{o}F	British thermal unit per hour-degree Fahrenheit
Btu/hr-ft^{2}-^{o}F	British thermal unit per hour-square foot-degree Fahrenheit
C	connection
cm	centimeter
cp	water specific heat
EVA	extravehicular activity
^{o}F	degree Fahrenheit
g	gram
g/s	gram per second
gpm	gallons per minute
H/X, HX	heat exchanger
hr	hour
H_2O	water
in	inch
J	joule
J/s	joule per second
J/s-K	joule per second-degree kelvin
J/s-m^{2}-K	joule per second-square meter-degree kelvin
K	degree kelvin
k	thermal conductivity
kg	kilogram
kN	kilonewton
kN/m^{2}	kilonewton per square meter
kJ	kilojoule
kJ/hr	kilojoule per hour
kN/m$^{2}\Delta$	kilonewton per square meter delta
ks	kilosecond
LCG	liquid cooling garment
lbm, lb	pound mass (avoirdupois)
lbm/hr, lb/hr	pound mass per hour

m	meter, milli
mm	millimeter
mm Hg	millimeters of mercury
min	minutes
N	newton
psi	pounds force per square inch
psia	pounds force per square inch absolute
psid	pounds force per square inch delta
Q,q	heat transfer rate, heat load
rpm	revolutions per minute
s	second
T	temperature
T_{in}	water inlet temperature
T_{out}	water outlet temperature
torr	pressure measured in millimeters Hg
UA	overall subsystem thermal conductance
W, $\dot{W}$	water mass flow rate
W/mK	watts per meter-degree kelvin
X	fin height, length of heat transfer path
Δ T	temperature difference
η	fin efficiency, dimensionless conductance
μ	pressure measured in micron Hg
ϵ	effectiveness, heat exchanger or ice chest

INTERFACE DEVELOPMENT

The basic purposes for conducting the Interface Development portion of the program were to develop a heat transfer interface surface combination that is sufficiently durable in construction to allow many (100 plus) couplings and uncouplings without degradation of performance, and to investigate surface configurations and preloading pressures with the intent of generating sufficient data to allow selection of optimum surface configurations and preload pressure.

SURFACE CONFIGURATION SELECTION

Eight surface configurations were selected for test:

1. Plain aluminum on plain aluminum - this configuration is to be used as a baseline.

2. Lead plated aluminum on plain aluminum - this configuration represents the Phase I configuration.

3. Lead plated aluminum on plain aluminum with the lead plated part grooved to produce square pads approximately 0.25 in. (0.635 cm) x 0.25 in. (0.635 cm). Figure 1 illustrates this configuration.

4. Same as (3) but with every other pad removed to produce a checkerboard pattern. Figure 2 illustrates this configuration.

5. Same as (3) but with square pads approximately 1.5 in. (3.81 cm) x 1.5 in. (3.81 cm). Figure 3 illustrates this configuration.

6. Same as (5) but with every other pad removed to produce a checkerboard pattern. Figure 4 illustrates this configuration.

7. Lead plated aluminum on plain aluminum, displaced 0.062 in. (0.157 cm) laterally after pressure mating.

8. Lead plated aluminum on hard-coated aluminum.

Configurations 3 through 6 were designed to evaluate the self-cleaning effect of grooves in the lead plated surface. These grooves allow bits of grit to drop off the mating surface without being dragged across the entire surface. Further, these configurations were intended to help evaluate the improvement, if any, gained by allowing the lead plate to more easily flow (into the grooves) and thereby obtain better surface conformation.

Configuration 7 was designed to evaluate the improvement, if any, gained by scuffing the plates together under pressure.

Configuration 8 was intended to evaluate what loss, if any, would be encountered by hard-coating the plain aluminum surface. The hard-coating would be desirable to provide protection for the plain aluminum surface since this surface will be somewhat exposed in the actual hardware.

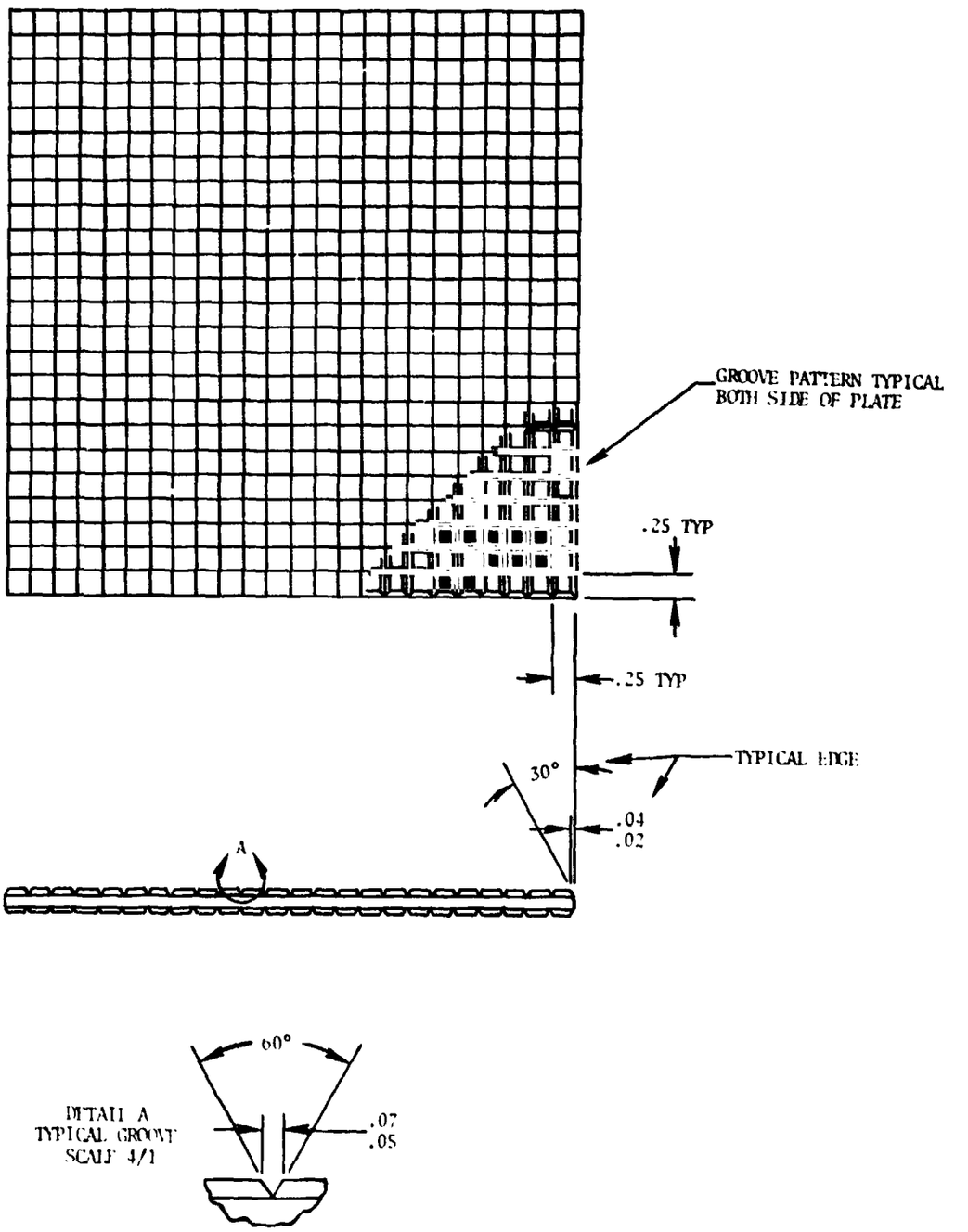

FIGURE 1 TEST CONFIGURATION 3

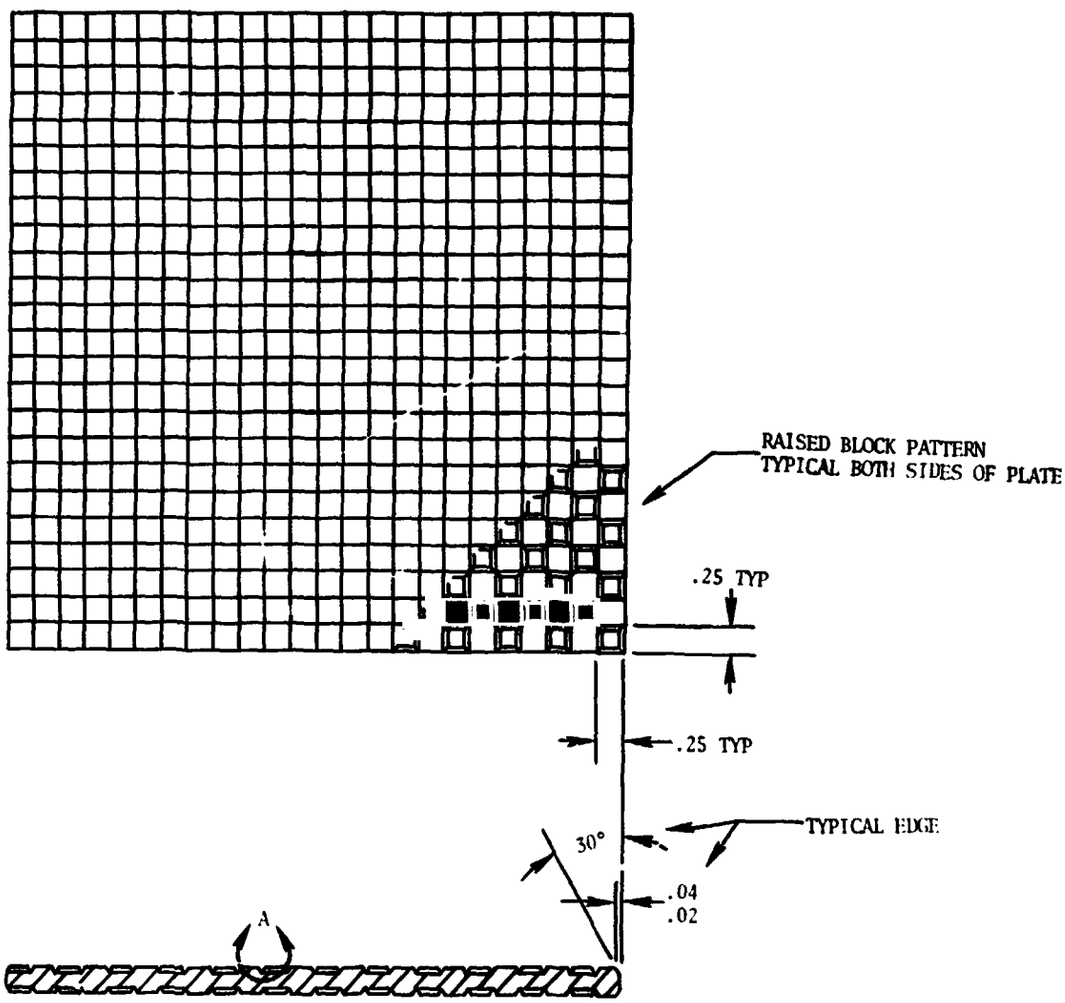

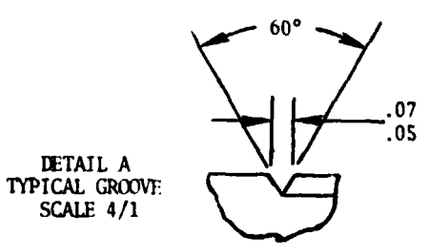

DETAIL A
TYPICAL GROOVE
SCALE 4/1

FIGURE 2 TEST CONFIGURATION 4

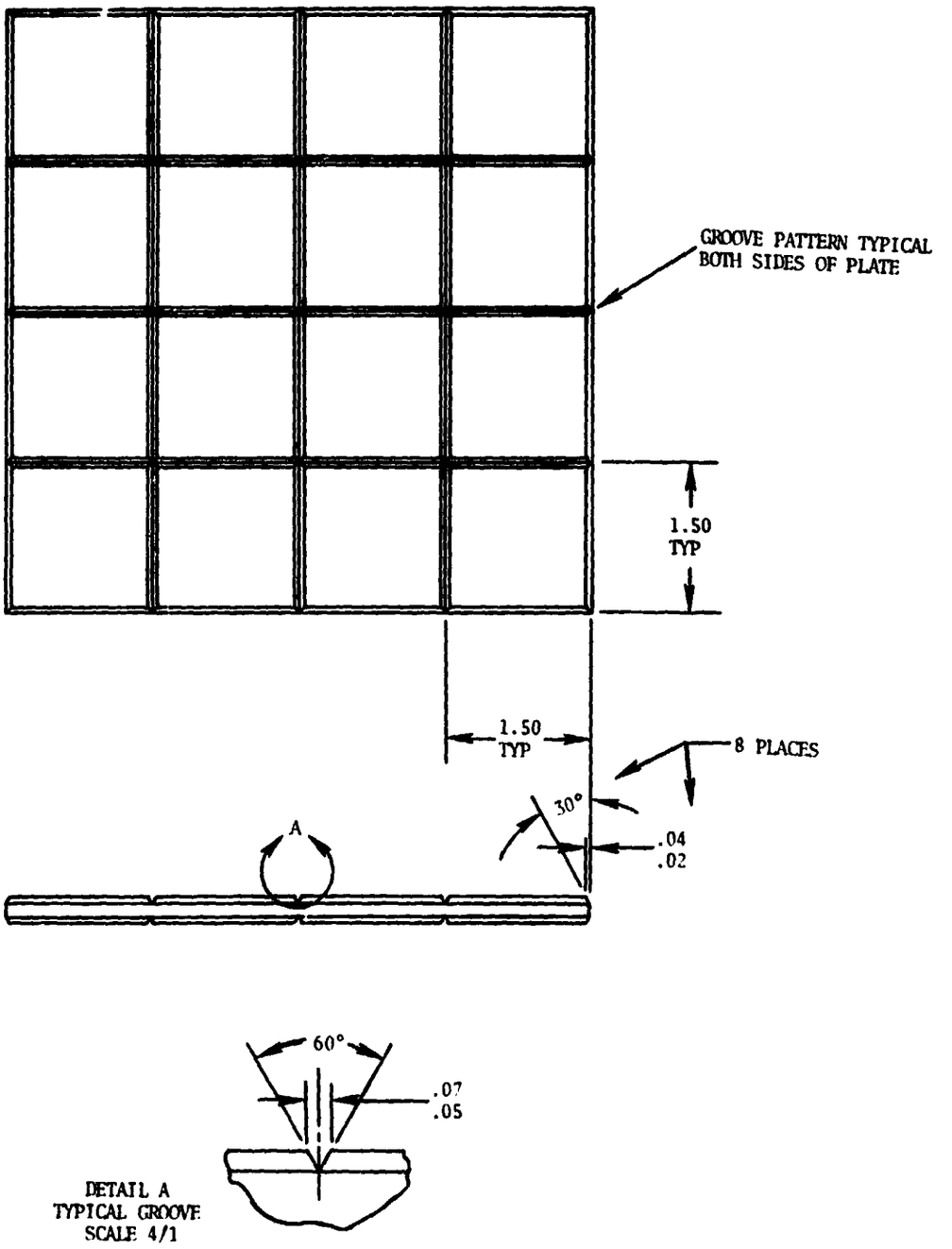

FIGURE 3 TEST CONFIGURATION 5

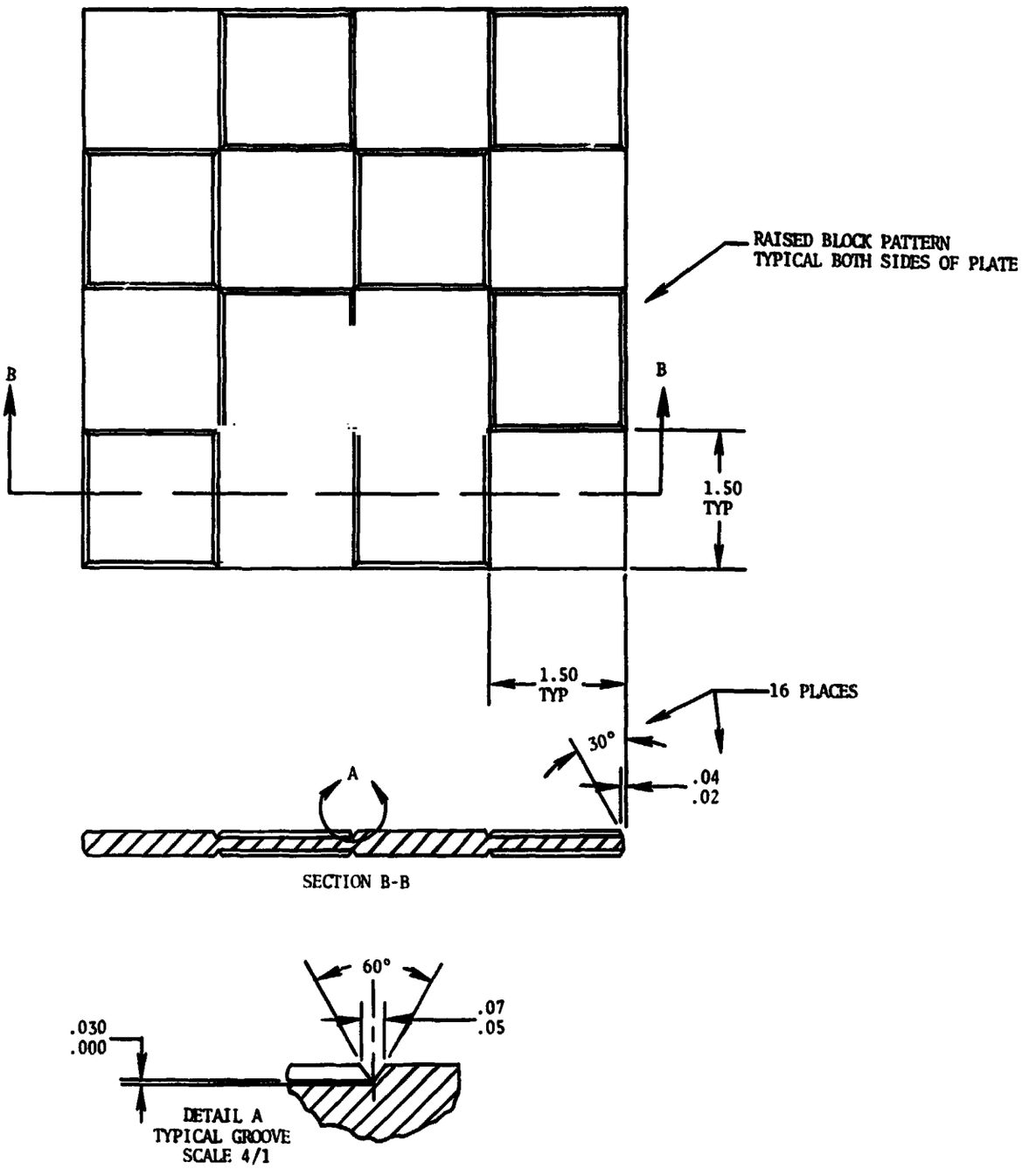

FIGURE 4 TEST CONFIGURATION 6

TEST PROGRAM

The interface development test program was revised after its initiation to make the most efficient use of available funding in light of contract change #9 which reduced the prototype design heat load to a maximum heat rejection rate of 2000 Btu/hr (586.7 J/s), and a total heat absorption of 1500 Btu (1584 kJ). The revised heat loads were lowered to the point where the required heat transfer surface size is approximately 8 inches (20.3 cm) by 12 inches (30.5 cm) as compared with the previous heat transfer surface size of 12 inches (30.5 cm) by 12 inches (30.5 cm). This new heat transfer surface size was sufficiently close to the 6 inches (15.2 cm) by 6 inches (15.2 cm) small scale test samples that the results of the small scale testing are sufficient to allow full scale configuration evaluation. Hence, the full scale testing was eliminated and a complete test sequence was run on each of the eight 6 x 6 configurations.

The Small/Large Scale Interface Development Test Plan is included in this report as Appendix A. Figure 5 shows the small/large scale interface development test fixture. Figures 6 and 7 show the 6 x 6 interface surfaces of the heater block and heat exchanger. The surfaces shown in these figures are hard-coated aluminum. Figures 8, 9, and 10 show thermocouple locations on the heater block, heat exchanger, and 6 x 6 configuration plates. The test fixture is designed to produce two interfaces in series, each interface with the same combination of surfaces in contact. This arrangement is particularly convenient because it allows the configuration to be changed by merely changing the configuration plate, since the heater surface and heat exchanger surface are plain aluminum (or hard-coated for the final tests).

Figure 11 shows the 6 x 6 configuration plate which, when installed with the test fixture, produces the plain aluminum on plain aluminum interface.

Figure 12 shows the lead-plated aluminum on plain aluminum configuration plate.

Figure 13 shows the lead-plated aluminum with 0.25 in. (0.635 cm) x 0.25 in. (0.635 cm) square pads on plain aluminum configuration plate.

Figure 14 shows the lead-plated aluminum with 0.25 in. (0.635 cm) x 0.25 in. (0.635 cm) alternate square pads on plain aluminum configuration plate.

Figure 15 shows the lead-plated aluminum with 1.5 in. (3.81 cm) x 1.5 in. (3.81 cm) square pads on plain aluminum configuration plate.

Figure 16 shows the lead-plated aluminum with 1.5 in. (3.81 cm) x 1.5 in. (3.81 cm) alternate square pads on plain aluminum configuration plate.

FIGURE 5 SMALL/LARGE SCALE INTERFACE DEVELOPMENT TEST FIXTURE

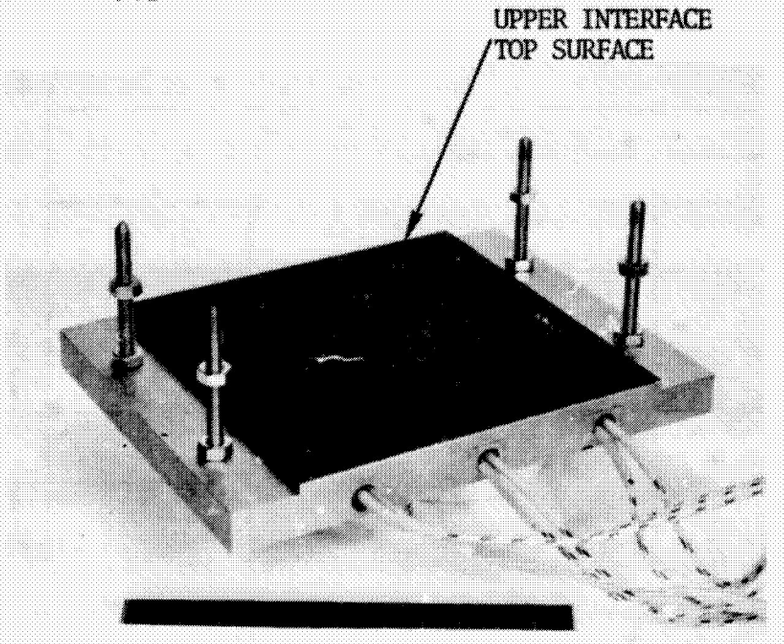

FIGURE 6 SMALL/LARGE SCALE INTERFACE DEVELOPMENT
TEST FIXTURE HEATER BLOCK (SHOWN INVERTED)

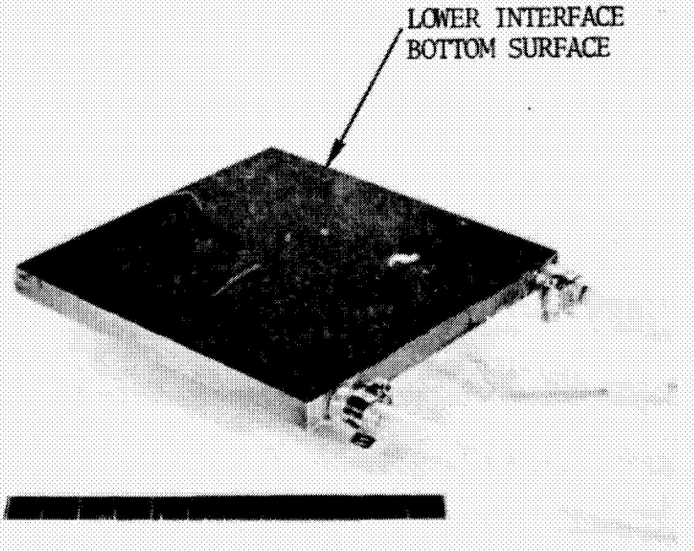

FIGURE 7 SMALL/LARGE SCALE INTERFACE DEVELOPMENT
TEST FIXTURE HEAT EXCHANGER

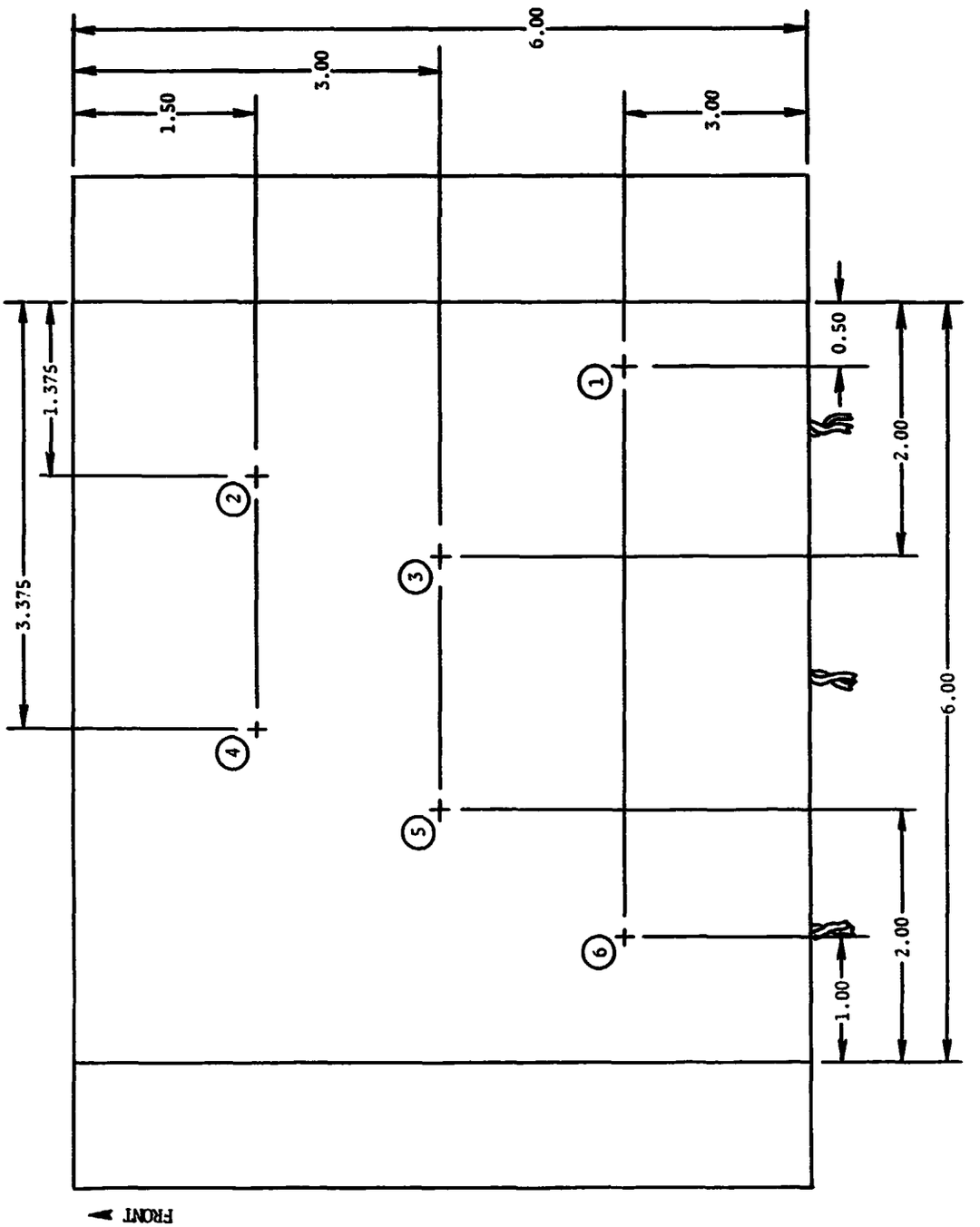

HTR TOP VIEW

FIGURE 8 SMALL/LARGE SCALE TEST HEATER BLOCK SHOWING THERMOCOUPLE LOCATIONS

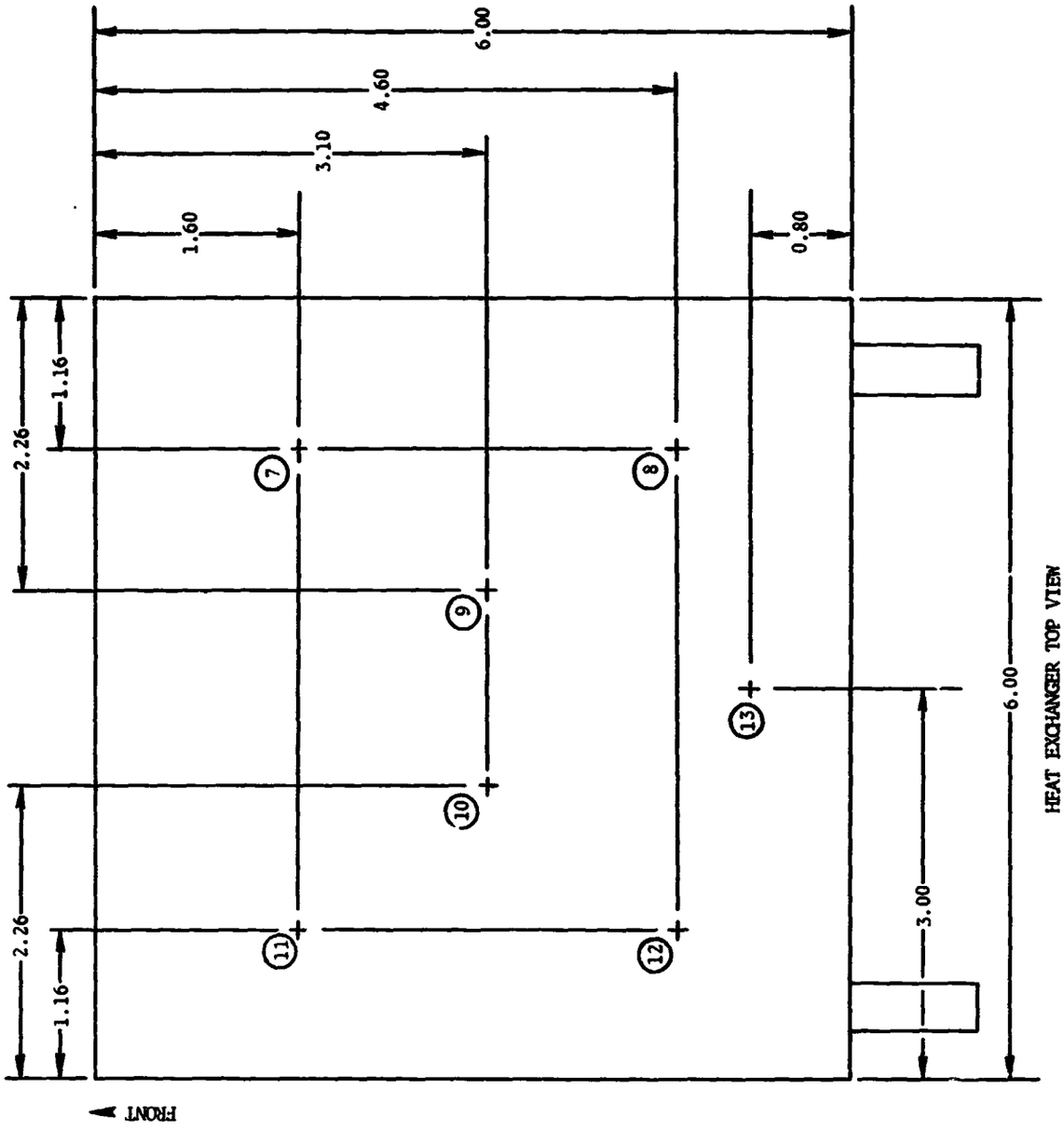

HEAT EXCHANGER TOP VIEW

FIGURE 9 SMALL/LARGE SCALE TEST HEAT EXCHANGER SHOWING THERMOCOUPLE LOCATIONS

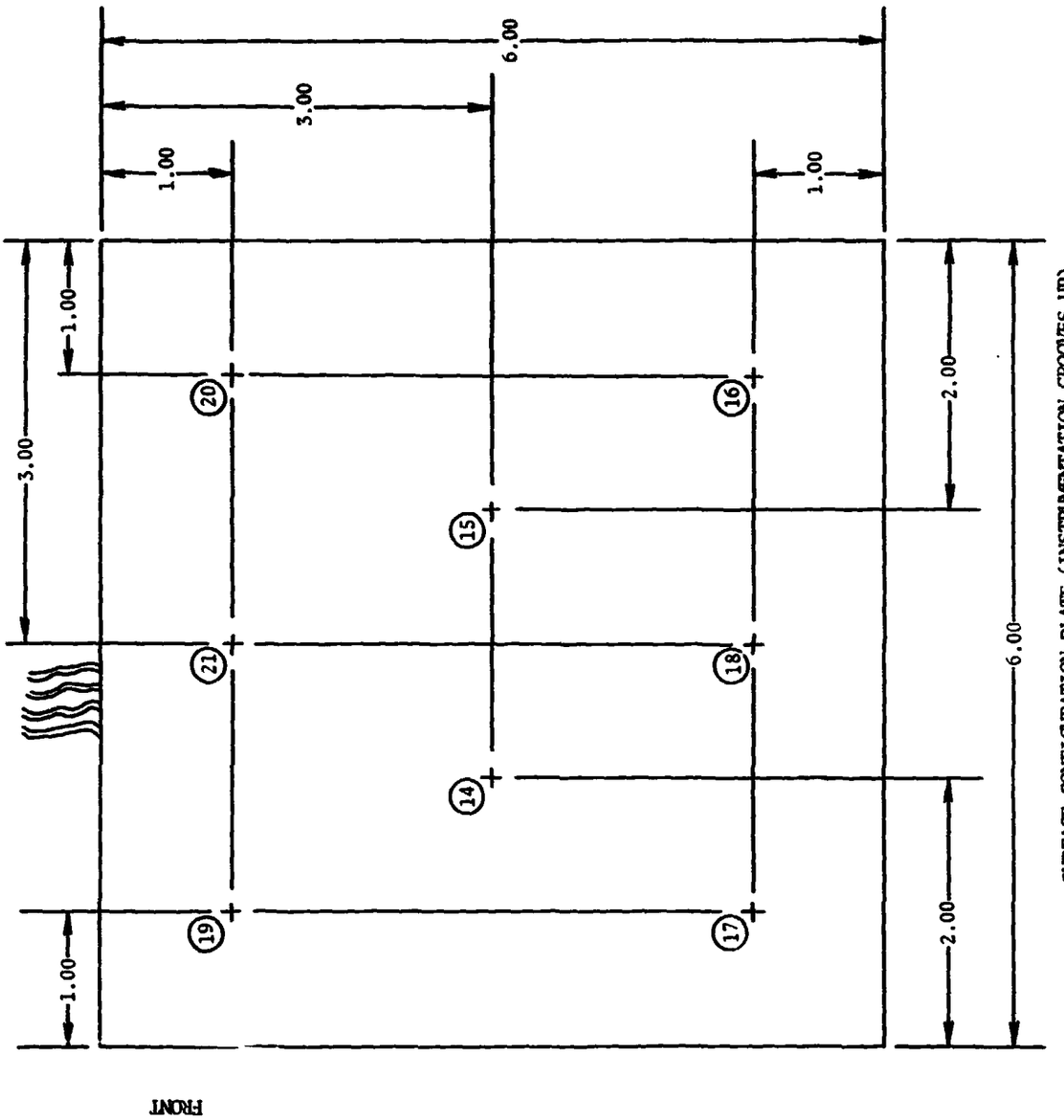

SURFACE CONFIGURATION PLATE (INSTRUMENTATION GROOVES UP)

FIGURE 10 SMALL/LARGE SCALE TEST 6X6 CONFIGURATION PLATE THERMOCUPLE LOCATIONS

FIGURE 11 6X6 CONFIGURATION PLATE - PLAIN ALUMINUM

TOP

BOTTOM

FIGURE 12 6X6 CONFIGURATION PLATE - LEAD PLATED ALUMINUM

BOTTOM

TOP

FIGURE 13 6X6 CONFIGURATION PLATE - 0.25 IN. (0.635 cm) X 0.25 IN. (0.635 cm)
SQUARE PADS - LEAD PLATED ALUMINUM

FIGURE 14 6X6 CONFIGURATION PLATE - 0.25 IN. (0.635 cm) X 0.25 IN. (0.635 cm)
ALTERNATE SQUARE PADS - LEAD PLATED ALUMINUM

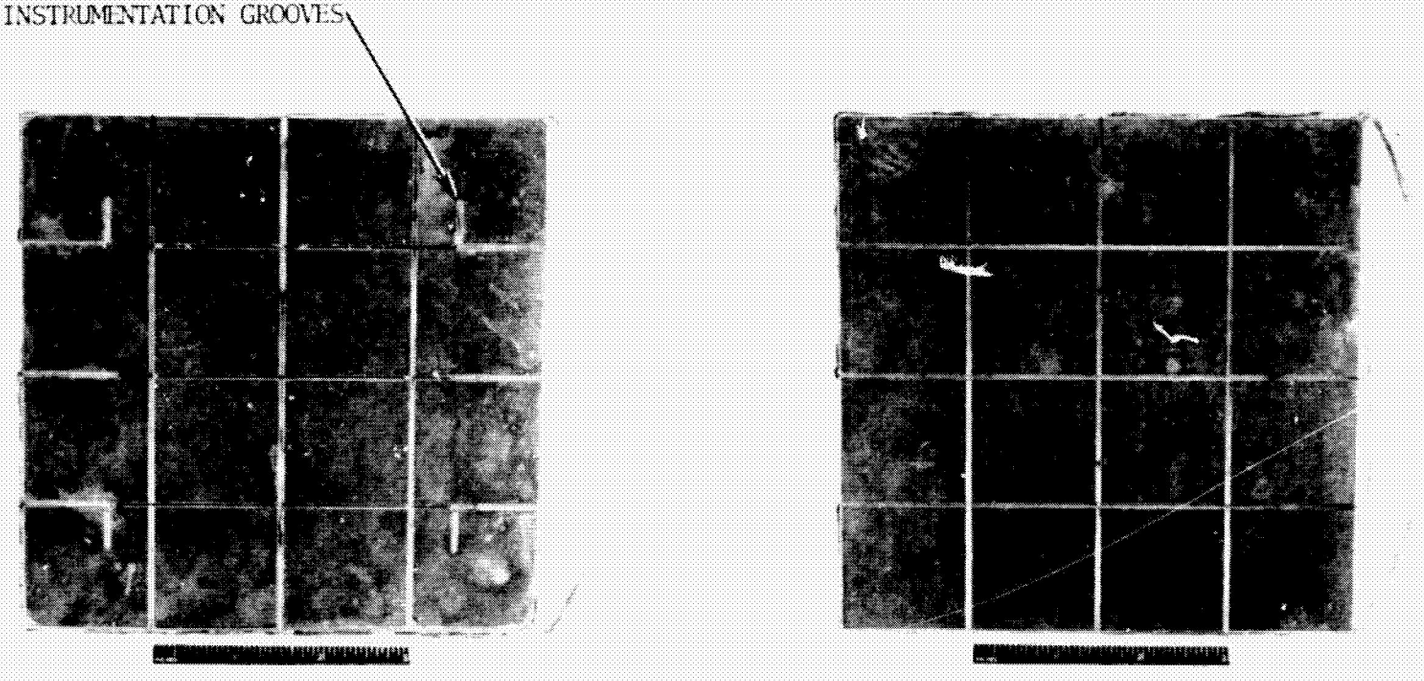

FIGURE 15 6X6 CONFIGURATION PLATE - 1.5 IN. (3.81 cm) X 1.5 IN. (3.81 cm) SQUARE PADS - LEAD PLATED ALUMINUM

BOTTOM

TOP

FIGURE 16 6X6 CONFIGURATION PLATE - 1.5 IN. (3.81 cm) X 1.5 IN. (3.81 cm)
ALTERNATE SQUARE PADS - LEAD PLATED ALUMINUM

The six configurations represented by figures 11 thru 16 were tested utilizing a preload (bladder) pressure of 8 to 30 psid (55.3 to 206.9 $kN/m^2 \Delta$). In addition, the heater block and heat exchanger surfaces were hard-coated and the configurations of figure 12 and figure 14 were retested at 8, 16, and 30 psid (55.3, 110.6, and 206.9 $kN/m^2 \Delta$). Hard-coating was used because it has superior hardness and is easy to apply uniformly.

Interface assembly was accomplished both at ambient pressure levels of 760 mm Hg (100 kN/m^2) and at vacuum conditions of less than 10^{-4} mm Hg (1.3×10^{-5} kN/m^2).

A ninth configuration, plain lead plate against aluminum, was to be tested for durability when subjected to lateral "scuffing" under pressure. This configuration was abandoned as impractical due to the extremely high force levels required to produce the lateral scuffing under preload, in the order 500 pounds (2.22 kN).

TEST DATA EVALUATION

Analytical Predictions

When two surfaces are brought together forming an interface across which heat must flow, a discontinuity in the system temperature profile (figure 17) will occur at the interface. The temperature profile within materials (1) and (2) will be a direct function of their thermal conductivities, k_1 and k_2, but the definition of the contact temperature discontinuity is not so easily described. Considerable attention to this definition has been generated since the late 1950's due to stringent aerospace requirements. In the ice pack, the contact resistance will comprise a major portion of the total system temperature drop and was the subject of considerable attention during Phase I. Although this problem could be avoided through the utilization of a one piece ice chest/LCG heat exchanger, the inherent drawbacks of that configuration (logistics, performance and potential LCG freeze-up) would produce problems with substantially higher development risk.

The actual area of the two materials in contact is a rather small fraction (possibly one to ten percent) of the projected area and is a direct function of the contact pressure or force holding the joint together and the hardness of the materials. Roughness and flatness of the two contacting surfaces result in peaks which join to form the effective heat flow area of the joint. The valleys between the peaks produce a gap which essentially insulates that portion of the heat flow path (especially in a vacuum environment). Conductance can be increased by increasing the contact pressure, which produces plastic deformation of the peaks thus increasing the effective heat flow area. Also, soft materials may be applied to the interface to deform under low load and fill the valleys providing parallel paths for heat flow. Obviously, the higher the plasticity and thermal conductivity of the interstitial material, the greater the effect.

For this design, the greatest hurdle lies in the extrapolation of reported data down to a range of contact pressure achievable by a crewman during EVA. Much data is reported at loadings above 100 psi (689.5 kN/m^2) while loadings for this effort will be 30 psi (206.86 kN/m^2) or less. Data from reference 1 are presented in figure 18 and were the basis for the following conclusions: (1)

(1) References are presented in Appendix H.

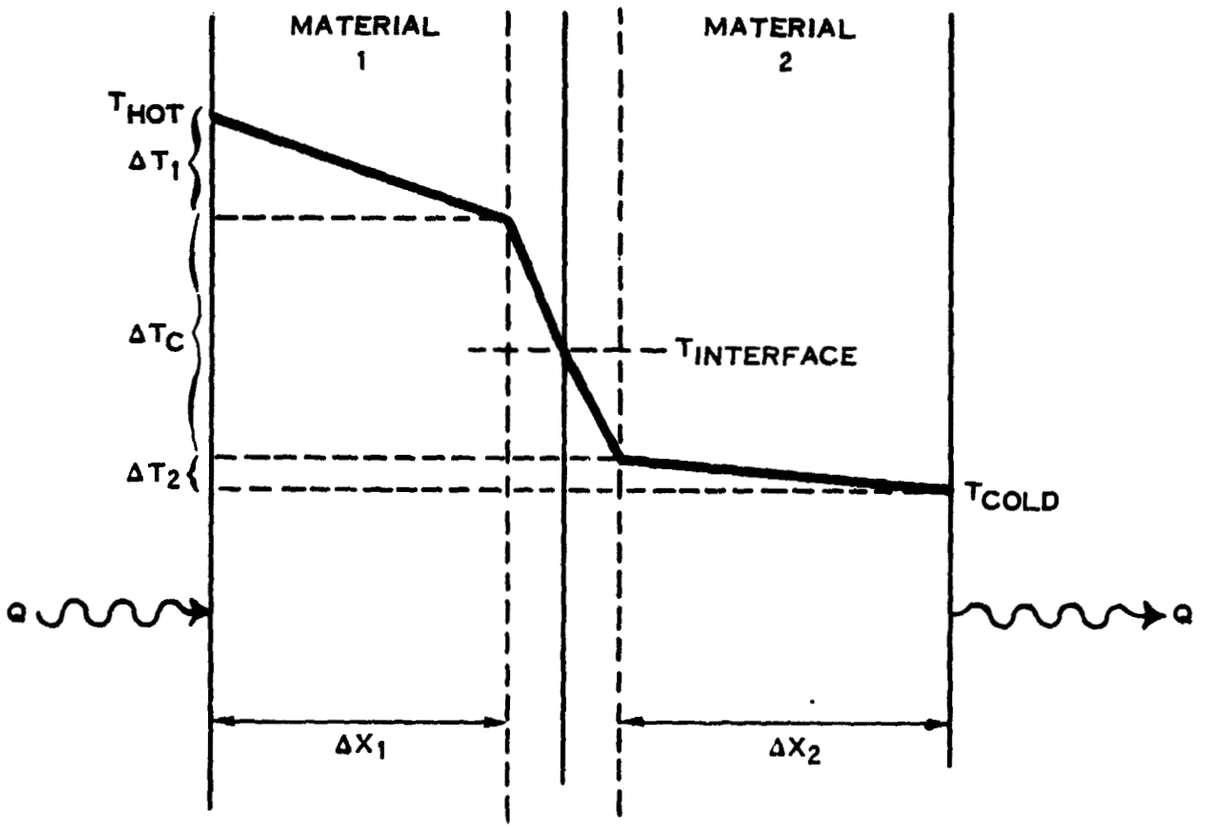

$$Q = \frac{K_1 A \Delta T_1}{\Delta X_1} = h_C A \Delta T_C = \frac{K_2 A \Delta T_2}{\Delta X_2}$$

FIGURE 17 TYPICAL TEMPERATURE PROFILE

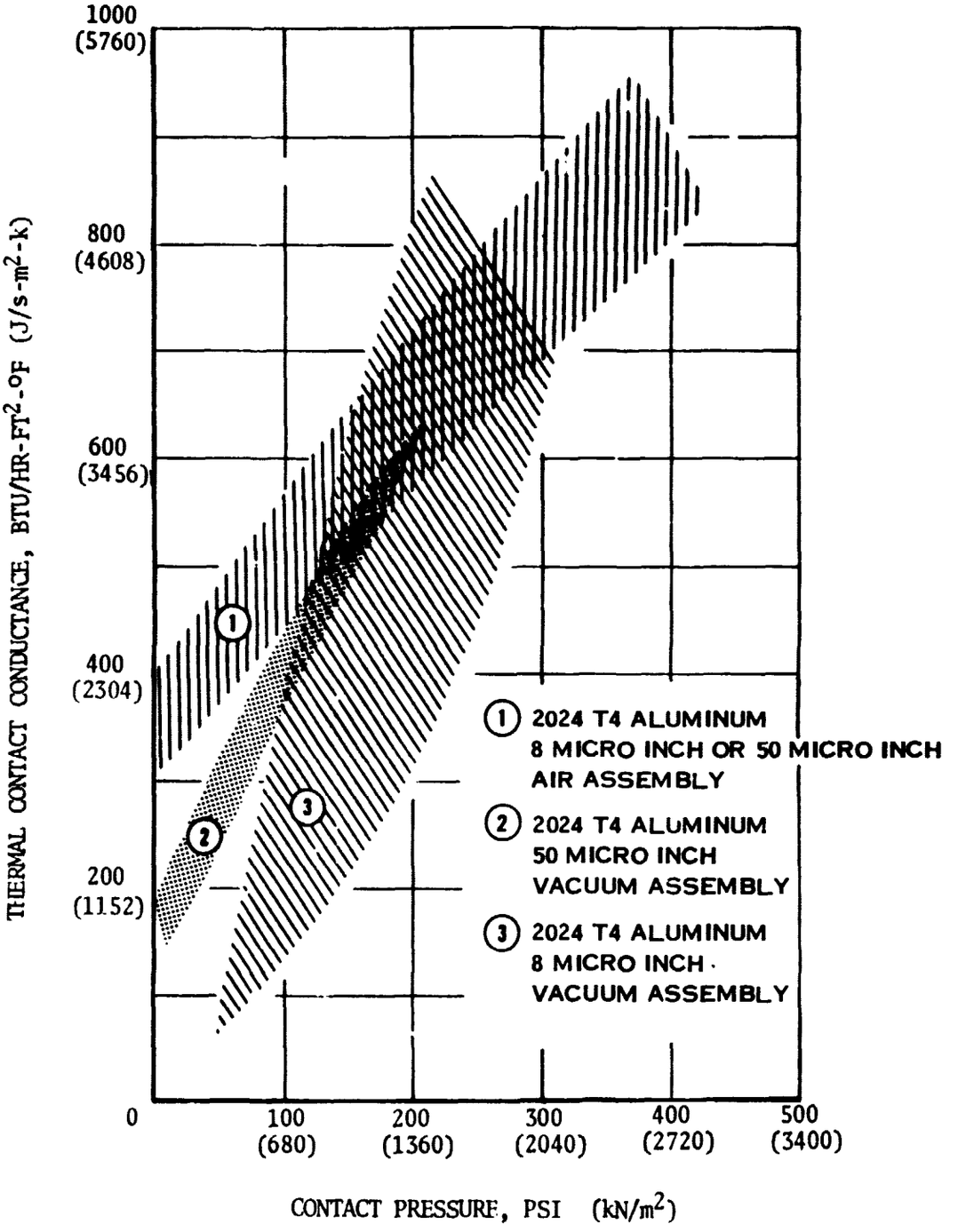

FIGURE 18 CONTACT CONDUCTANCE DATA

- Contacts assembled in a pressured environment will have substantial conductance at low applied loads as a result of gas trapped in the interface. This gas persisted in the joint throughout a one-week period during the reference 1 testing.

- Materials having a very fine finish, which are assembled in vacuum, have essentially zero conductance at zero contact pressure.

- Rougher materials, assembled in vacuum, exhibit some conductance at low contact pressures but verification of extrapolations to very low loads is required. The rate of conductance drop-off apparently is quite high in this region.

A contact conductance of 200 Btu/hr-ft^{2}oF (1152 J/s-m^2-K) was assumed for the assembly. This value was considered conservative for contacts assembled in a pressurized environment such as the lunar base or spacecraft cabin, but may be unrealistic for a vacuum assembly such as resupply during EVA.

To attack this problem and improve conductance for all modes of assembly, the inclusion of an interstitial material will be required. Data presented in reference 2 and shown in figure 19 show an order of magnitude improvement in contact conductance through the application of silicone vacuum grease and substantial improvements with indium, lead or gold. Although the grease appears to hold the highest performance potential, it poses the practical problems of contamination during assembly and excessive force requirements for disassembly. Data presented in reference 3 and shown in figure 20 substantiates the findings in reference 2 with contact pressures in the range of 20-300 psi (136-2040 kN/m^2).

The development assembly has lead plating applied to the relatively rough, approximately 32 micro-inch finish of the test specimens. A rough finish will provide the peaks necessary to load and plastically deform the lead with the intended aim of filling the valleys and voids between the two contacting surfaces.

Several other materials and applications were considered in Phase I because of their effect on contact conductance. Copper was eliminated by corrosion and storage requirements. Aluminum was disregarded because identical materials will cold weld under vacuum conditions. Although indium has a desirable effect on contact conductance, its cost is prohibitive when compared to lead. A plating procedure for the lead was deemed more applicable than leafs and foils, as leafs and foils will tear, necessitating replacement when the ice chests are removed and replaced. The lead plating is thus the most effective means of improving contact conductance by use of interstitial materials.

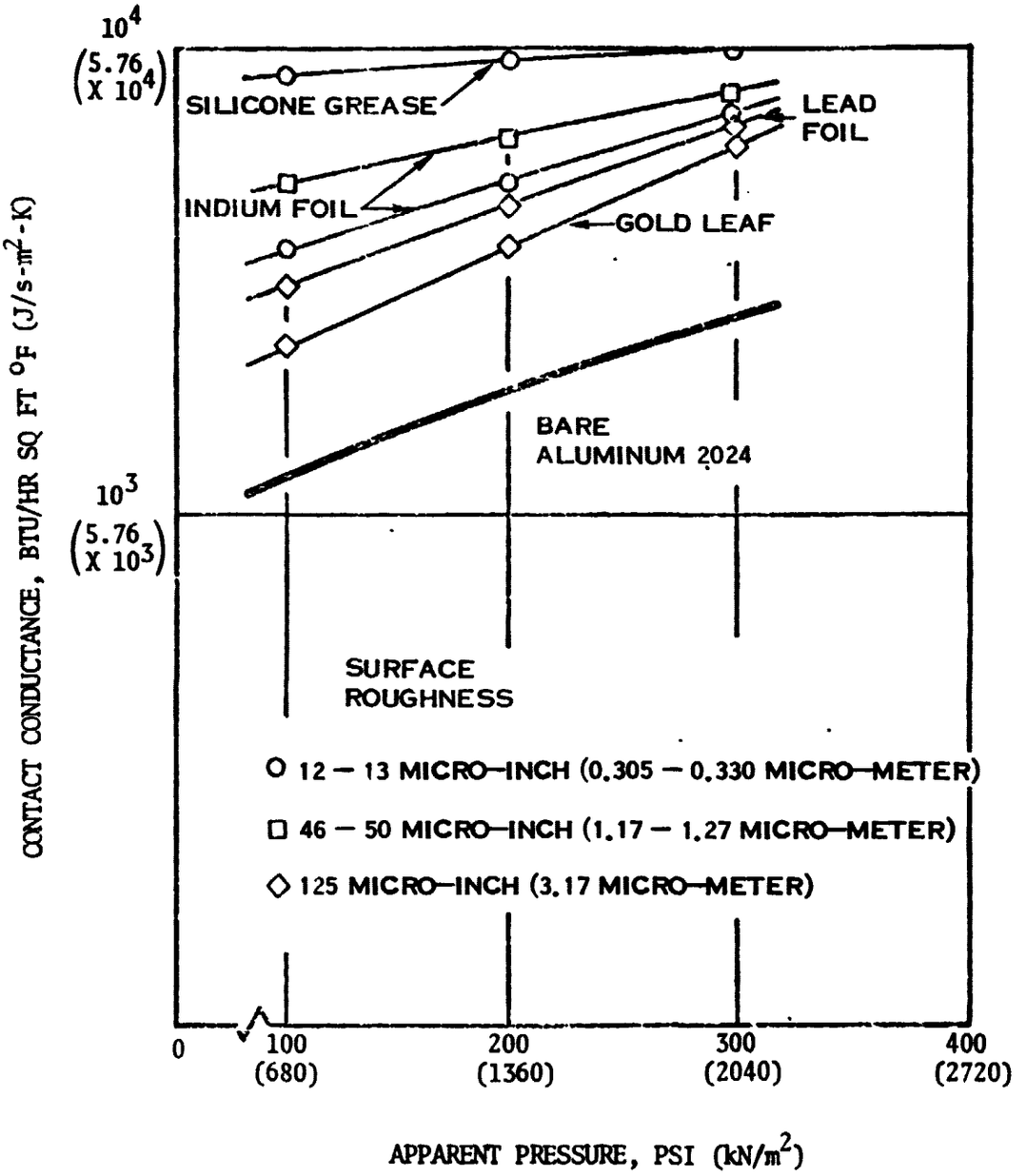

FIGURE 19 THERMAL CONTACT CONDUCTANCE OF SELECTED INTERSTITIAL MATERIALS

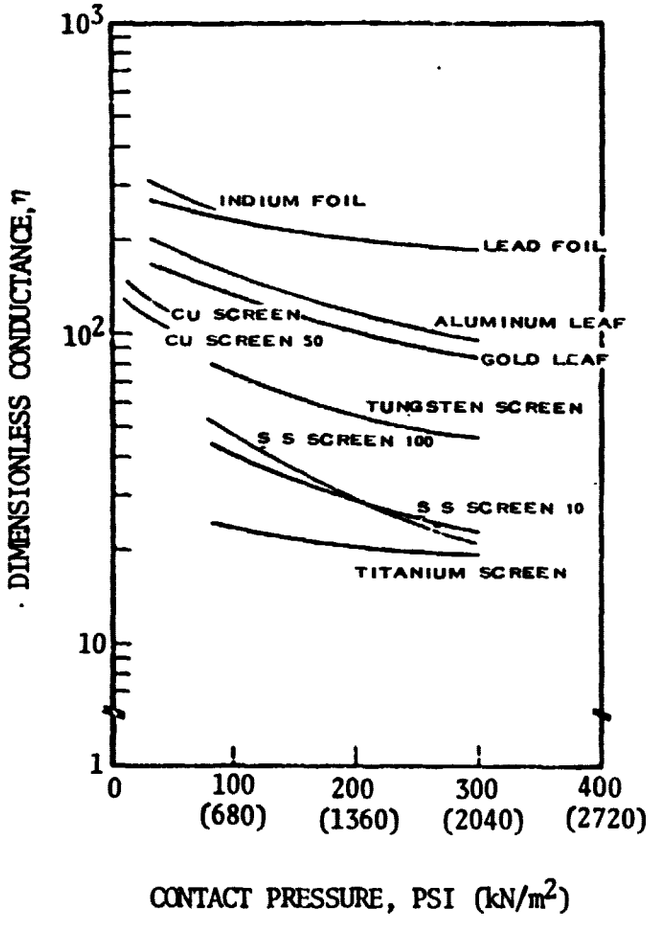

FIGURE 20 COMPARISON OF DIMENSIONLESS CONDUCTANCE FOR SELECTED METAL INTERSTITIAL MATERIALS

Prior analysis had indicated that the data of reference 3 and figure 20 would predict that the use of lead plating could increase the contact conductance by approximately 200 times - a conclusion not in keeping with the data of figure 19. Reevaluation of the data of reference 3 would indicate only a three to six-fold increase in contact conductance through the application of lead in the interface area - a level correlating directly with figure 19. Current design analysis is based on contact conductances ranging between 96 and 152 Btu/hr-ft^2-^{o}F (553 and 875 J/s-m^2-K) obtained from Phase I test results (reference 4).

Test Results

Test data acquired during the period October 9, 1973 to December 5, 1973 have been reduced to engineering design units and are presented in Table I and figures 21 and 22. The actual log sheets are reproduced as Appendix B of this report. Because the interface area is not equal for all samples (area is reduced by grooves and removed squares), two bases were utilized for data correlation. In one (figure 21), the overall apparent area of 36 in.^{2} (232 cm^2) was assumed applicable and the thermal contact conductance was derived utilizing this value. In the second (figure 22), the actual contact area was employed in the analysis and both contact conductance and pressure loading were adjusted to be representative of the interface area.

Differences in the correlations of figures 21 and 22 are most apparent for those interfaces assembled in a pressurized environment. As expected, the data correlation is substantially improved when actual contact areas are considered and derived contact coefficients and pressure loadings are representative of the conditions present at the interface.

Interestingly, this improvement does not appear for that data obtained when the interfaces are assembled in vacuum. The difference lies in the variation in slope between the two correlations. The nearly one to one slope of the vacuum assembly data produces the unique result that removal of contact area has no net effect on the relationship between loading pressure and overall thermal conductance. For example, if the contact area A_c is halved then both contact coefficient, h_c, and contact pressure, P_c, are doubled but the product h_cA_c remains a constant. This translates into the result that overall conductance will remain a constant for vacuum assembly regardless of the actual area in contact. A gross reduction in contact area, while maintaining the desired conductance could, however, produce gross irregularities in the ice melt profile resulting in secondary increases in thermal resistance. The data for bare aluminum are substantially below values interpolated for the 32 micro-inch (0.81 micro-meter) finish on the test specimens. Achieved conductances are approximately one-third those anticipated.

Hamilton Standard
DIVISION OF UNITED AIRCRAFT CORPORATION

TABLE I INTERFACE DEVELOPMENT TEST RESULTS

TEST DATE	SAMPLE CONFIGURATION	AMBIENT PRESSURE		BASED ON EXTERNAL AREA				BASED ON INTERFACE AREA			
				PRESSURE		THERMAL CONDUCTANCE		PRESSURE		THERMAL CONDUCTANCE	
		mm Hg	(kN/m^2)	psi	(kN/m^2)	Btu/hr-ft^2-°F	(J/s-m^2-K)	psi	(kN/m^2)	Btu/hr-ft^2-°F	(J/s-m^2-K)
10-9-73	5	760	100	8	54.4	388	2235	8.75	5.95	424	2442
				16	108.8	442	2546	17.5	11.9	482	2776
	1			8	54.4	280	1613	-	-	-	-
				16	108.8	338	1947	-	-	-	-
				16	108.8	344	1981	-	-	-	-
	3			8	54.4	250	1440	13.8	9.38	436	2511
				16	108.8	296	1705	27.6	18.77	516	2972
	2			8	54.4	482	2776	-	-	-	-
				16	108.8	536	3087	-	-	-	-
10-29-73		10^{-4}	$1.3X10^{-5}$	8	54.4	80.4	463	-	-	-	-
				16	108.8	112.8	650	-	-	-	-
				30	204.0	223	1284	-	-	-	-
	1			8	54.4	16.6	96	-	-	-	-
				16	108.8	23.2	134	-	-	-	-
				30	204.0	57.8	333	-	-	-	-
	3			8	54.4	46.8	270	13.8	9.38	81.2	468
				16	108.8	83.6	482	27.6	18.77	144.8	834
				30	204.0	173	996	52.0	35.36	300	1728
	5			8	54.4	37.2	214	8.75	5.95	40.4	233
				16	108.8	63.2	363	17.5	11.9	69	397
				30	204.0	128	737	32.7	22.27	136.4	786
11-2-73				8	54.4	44.8	258	8.7	5.92	48.8	281
				16	108.8	72	415	17.5	11.9	78.6	453
				30	204.0	139.2	802	32.7	22.27	151.8	874
				8	54.4	42.4	244	8.7	5.92	46.2	266
				16	108.8	78.2	450	17.5	11.9	85.4	492
				30	204.0	163	939	32.7	22.27	177.8	1024
		760	100	8	54.4	429.2	2472	8.7	5.92	468.2	2697
				16	108.8	555.8	3201	17.5	11.9	606.4	3493
11-5-73	4			8	54.4	169.6	977	27.7	18.84	587.2	3382
				16	108.8	238.2	1372	55.4	37.67	824.4	4749
		10^{-4}	$1.3X10^{-5}$	8	54.4	68	392	27.7	18.84	235.2	1355
				16	108.8	115.6	666	55.4	37.67	400	2304
				30	204.0	191	1100	103.8	70.58	661.2	3809
				8	54.4	36.6	211	27.7	18.84	126.8	730
				16	108.8	66	380	55.4	37.67	228.4	1316
				30	204.0	126.6	729	103.8	70.58	438.4	2525
11-7-73	6	760	100	8	54.4	231.6	1334	17.5	11.9	505.2	2910
				16	108.8	299.4	1725	34.9	23.73	653.2	3762
		10^{-4}	$1.3X10^{-5}$	8	54.4	51.4	296	17.5	11.9	112.4	647
				16	108.8	80.2	462	34.9	23.73	174.8	1007
				30	204.0	136.4	786	65.5	44.54	297.6	1714
				8	54.4	46.4	267	17.5	11.9	101.2	583
				16	108.8	76.4	440	34.9	23.73	166.8	961
				30	204.0	137.8	794	65.5	44.54	300.4	1730
12-5-73	8			8	54.4	35.8	206	-	-	-	-
				16	108.8	40.8	235	-	-	-	-
				30	204.0	58.6	338	-	-	-	-
	7			8	54.4	19.2	111	27.7	18.84	66.4	382
				16	108.8	27	156	55.4	37.67	93.4	538
				30	204.0	44.8	258	103.8	70.58	155	893

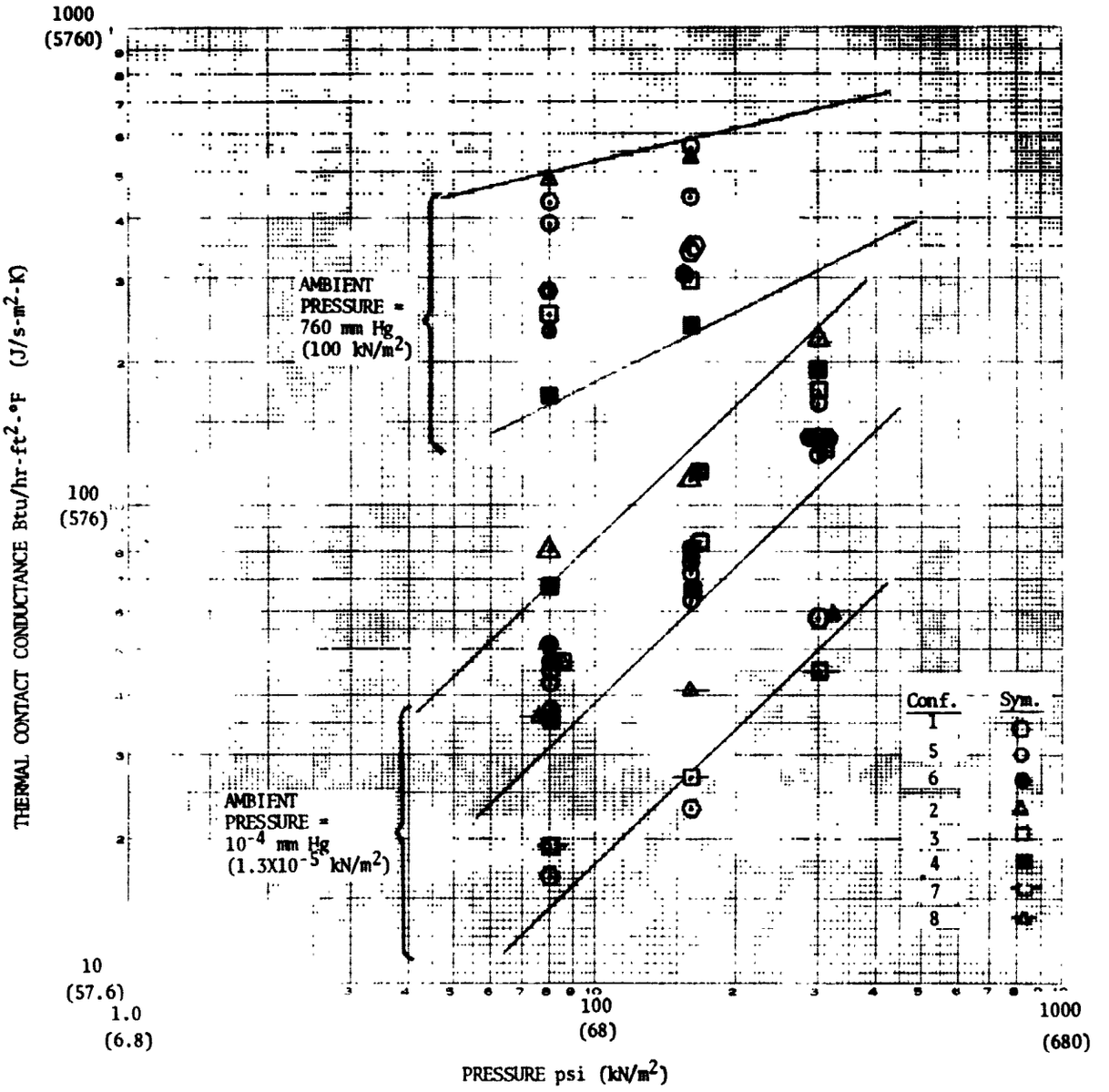

FIGURE 21 CONTACT CONDUCTANCE VS PRESSURE BASIS: APPARENT JOINT AREA

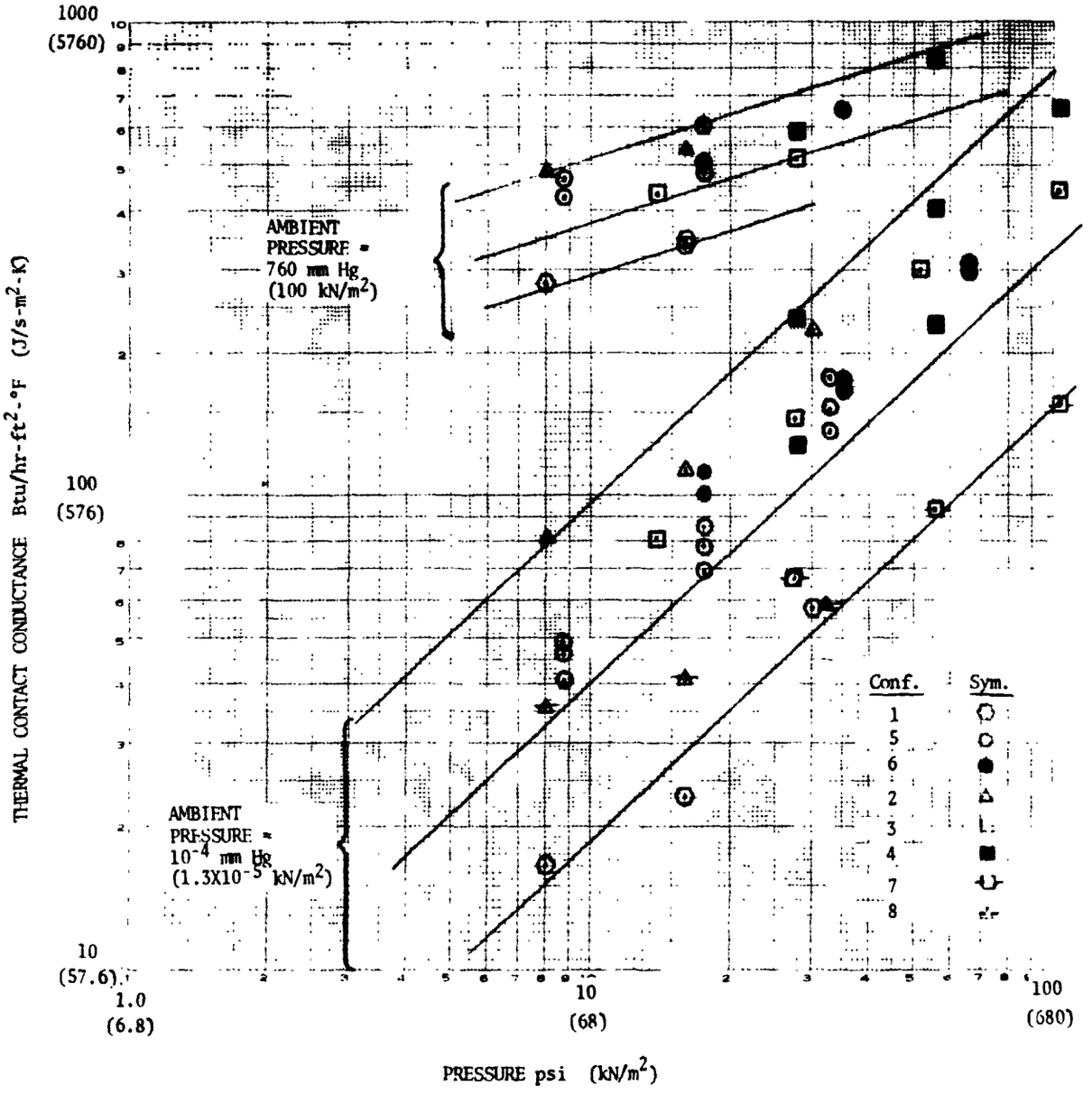

FIGURE 22 CONTACT CONDUCTANCE VS PRESSURE BASIS: ACTUAL JOINT AREA

The addition of lead plating has produced a two to five-fold increase in conductance for interfaces assembled in a vacuum. This result provides excellent correlation to the improvements predicted from the literature. Absolute values of the conductance remain at approximately one-third those presented in figure 19 and approximately one-half those achieved in Phase I testing (reference 4). This anomoly may be traced to the effect of the rigid double interface test specimens rather than the single contact semi-flexible interfaces reported in the literature and utilized in the actual ice pack design. Contact resistances derived from the test data assume that the total system resistance is attributable to the two contacts. If the actual area in contact is substantially less than anticipated and the contacting areas are not directly opposed on the test specimen then an added resistance thru the test specimen (from one contact area to another) will be present. This type of error will produce low values of contact conductance and can be avoided only by utilizing a single contact test configuration as is done in the actual prototype configuration.

Testing accomplished with the bare aluminum parts hard anodize coated (for wear resistance) produced inconclusive data. The hard coat produced a surface finish which appears smoother than the substrate - a factor which would decrease the ability to penetrate the lead coating and thus increase thermal resistance. Test results for this configuration produced results varying from those equivalent to lead at low pressures to bare aluminum at high pressure. This is exactly opposite the trend anticipated - the higher pressures should improve penetration of the lead thereby producing lower resistance.

Conclusions

The following conclusions may be derived from this test series:

1. For the limiting operating conditions for ice pack design (vacuum assembly), total interface conductance is independent of actual contact area. Configurations which remove surface area to incorporate self-cleaning effects are feasible.

2. The application of lead plating to the contact interface has produced an improvement in thermal conductance equivalent to that reported in the literature.

3. Literature values for conductance of bare aluminum junctions are approximately three times those measured in this test program. This anomoly may be due to other undefined resistances present in the test specimen - resistances which can only be eliminated thru the use of a single contact test assembly.

PRELOAD STUDY

As part of the interface development program a study was undertaken to determine the most desirable method for providing pressurization to the interface joint. The following general categories were examined and are listed in order of increasing desirability:

Electromagnetic
Permanent Magnetic
Mechanical
Pneumatic
Hydraulic

Electromagnetic

In order for an electromagnetic preload to be utilized it would be necessary to build in electromagnetic strips or coils and utilize a magnetizable surface on the mating part. Further, and more important, a continuous electric power drain would be required to maintain the preload. Therefore, this category has been eliminated from further consideration.

Permanent Magnetic

A preloading force can be generated and ungenerated by utilizing permanent magnets that can be oriented either to produce a magnetic field or to produce no field. This concept would require a magnetizable surface on the mating surface. The magnets would add approximately 25 to 30 lbs. (5.05 to 6.06 kg) to the weight of the subsystem. Further, a different method of transferring heat to or from the magnets would have to be devised. This category has been eliminated from further consideration due to the added complexities and weight.

Mechanical

Various methods for utilizing a mechanical preload were examined, including cams, ramps, and screw threads. Even though this method is potentially suitable for preloading, no method could be devised that would produce uniform preloads utilizing a practical mechanism.

Pneumatic

Pneumatic pressurization devices can be categorized into two basic types: self-contained and expendable. The device used in the Phase I portion of this contract is expendable in that it utilizes a separate gas supply for pressurization, and the gas is dumped to ambient to vent the bladder. An example of a self-contained pneumatic device is one where there is a separate accumulator into which the gas from the bladder can be pumped to relieve the bladder pressure. The primary drawback to this system is the requirement for a separate pump to transfer the compressible fluid between the bladder and the accumulator. This system is completely feasible with the pump being manually operated. The drawback lies in the fact that the fluid is compressible, thereby requiring almost complete emptying of the bladder to change the ice chest during vacuum conditions. Further, the bladder pressure is not able to self-compensate as the ambient pressure changes.

Hydraulic

A hydraulic pressurization device, to be self-contained, also requires a separate accumulator into which the bladder fluid can be transferred. However, unlike the case with the compressible fluid, only small quantities of incompressible fluid must be removed from the bladder to relieve the pressure. The accumulator can be equipped with a diaphragm and a spring, thereby automatically producing a preload pressure. To relieve the bladder pressure the accumulator diaphragm is equipped with a mechanical override that allows the operator to remove the spring force from the diaphragm, thereby unpressurizing the fluid. Furthermore, the bladder pressure is self-compensating to changes in ambient pressure since the accumulator diaphragm is referenced to ambient. This configuration is represented by the schematic shown in figure 23 and is the one incorporated into the prototype design.

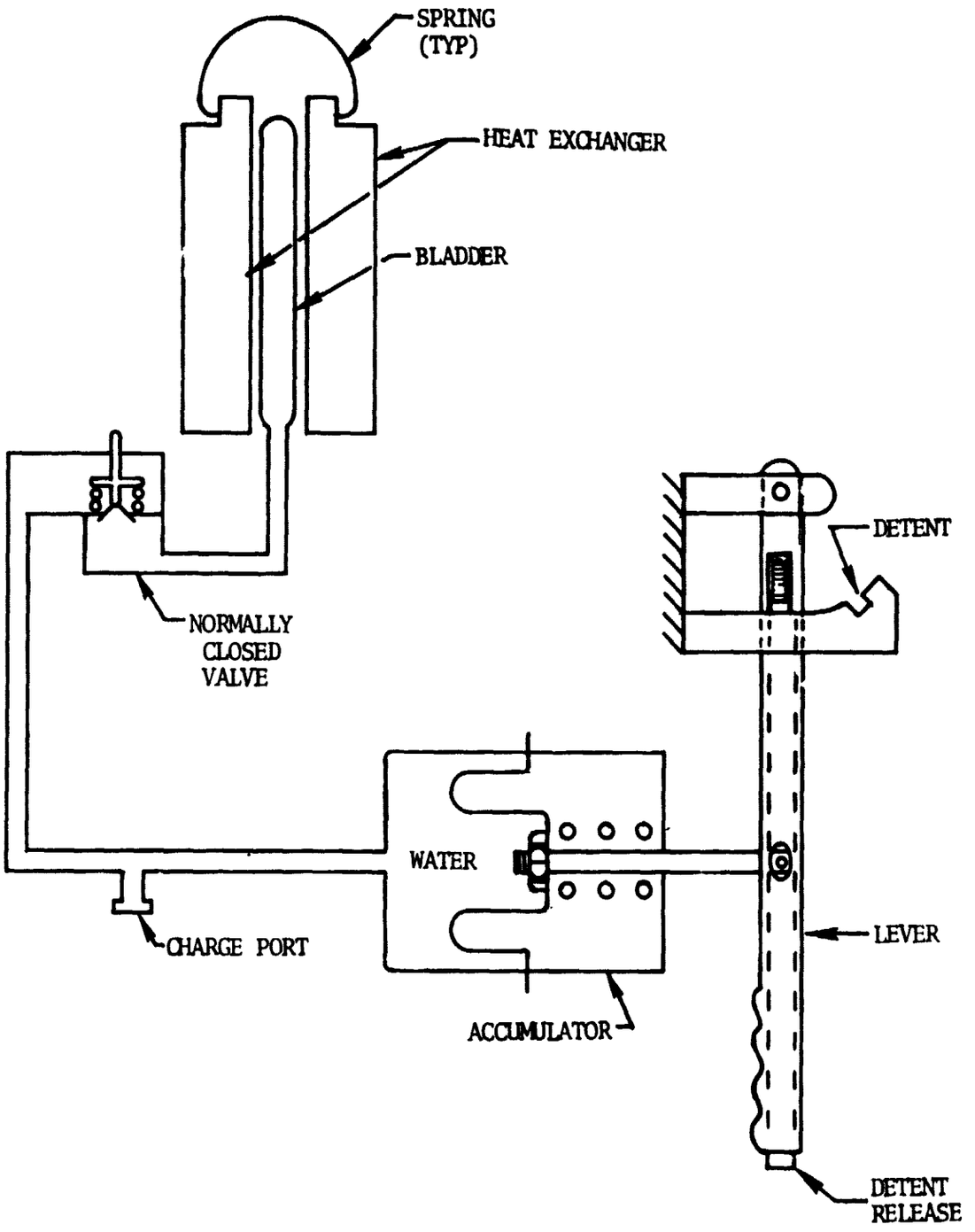

FIGURE 23 HYDRAULIC BLADDER PRESSURIZATION DEVICE

ICE PACK GEOMETRY OPTIMIZATION COMPUTER PROGRAM

The purpose of generating computer models of the Ice Pack Heat Sink Subsystem is to provide an accurate analytical tool to correlate subsystem performance test data. Normal analytical procedures are insufficient to model the melting phenomenom because of constantly varying subsystem internal resistances.

The prediction of the overall heat transfer coefficient of the Ice Pack Heat Sink Subsystem can be expressed by equation 1.

$$UA = \frac{1}{\frac{1}{h_x} + \frac{1}{h_c} + \frac{1}{h_{ice}}} \qquad (1)$$

where,

UA = overall heat transfer coefficient

h_x = conductance from LCG water to the heat exchanger

h_c = interface contact conductance between the heat exchanger and the ice chest plate

h_{ice} = conductance between the ice chest plate and the heat sink.

This overall heat transfer coefficient can then be used to determine the effectiveness of the system by use of equation 2.

$$\epsilon = f\ (UA/WCp) \qquad (2)$$

where,

ϵ = effectiveness = $\frac{\text{actual heat transfer}}{\text{maximum theoretical heat transfer}}$

W = LCG water flow rate

Cp = LCG water specific heat

However, the normal analytical procedure which considers heat exchanger effectiveness as nearly constant is complicated by the fact that the ice chest conductance, h_{ice}, varies as a function of the amount of ice that has melted. Thus, the system effectiveness will vary as a function of the total amount of energy transferred.

To simplify this predictive procedure, and also provide a means of analyzing test data, two computer models have been generated. The first model is of one-half of an ice chest cell. This model is used to determine the conductance from the heat exchanger plate surface to the liquid/ice melt interface as a function of the amount of ice which has melted. The model utilizes a generalized heat transfer program which was developed several years ago at United Aircraft Research Laboratory and subsequently expanded and refined at Hamilton Standard in late 1972.

The resultant conductance from the above model is then used as input to the second model, which consists of the full size Ice Pack Heat Sink Subsystem. This model uses a special Ice Chest Computer program recently developed at HSD. Both of these models are discussed in detail below.

Ice Cell Melt Model

Since each ice cell is symmetrical about the cell and fin centerlines, a one-half cell model is adequate to determine the melting characteristics of the ice. The ice melt model therefore consists of one-half of one ice cell over a full cell length.

The nodal break-down of the melt model is presented in figure 24. The ice and half-fin portion of the cell is divided into 10 nodes. 10 nodes is sufficient to determine an accurate melt characteristic while also keeping computer execution time within reasonable limits.

In the generalized heat transfer program, each node is assigned a thermal mass equivalent to the mass of the node times its specific heat. To model the heat of fusion of each ice mode, a dimensionless temperature dependent thermal mass multiplier is used. This multiplier is determined from equation 3.

$$\text{Multiplier} = \frac{\dot{m}_{ice}\, h}{\dot{m}_{ice}\, Cp_{ice}\, \Delta T} \qquad (3)$$

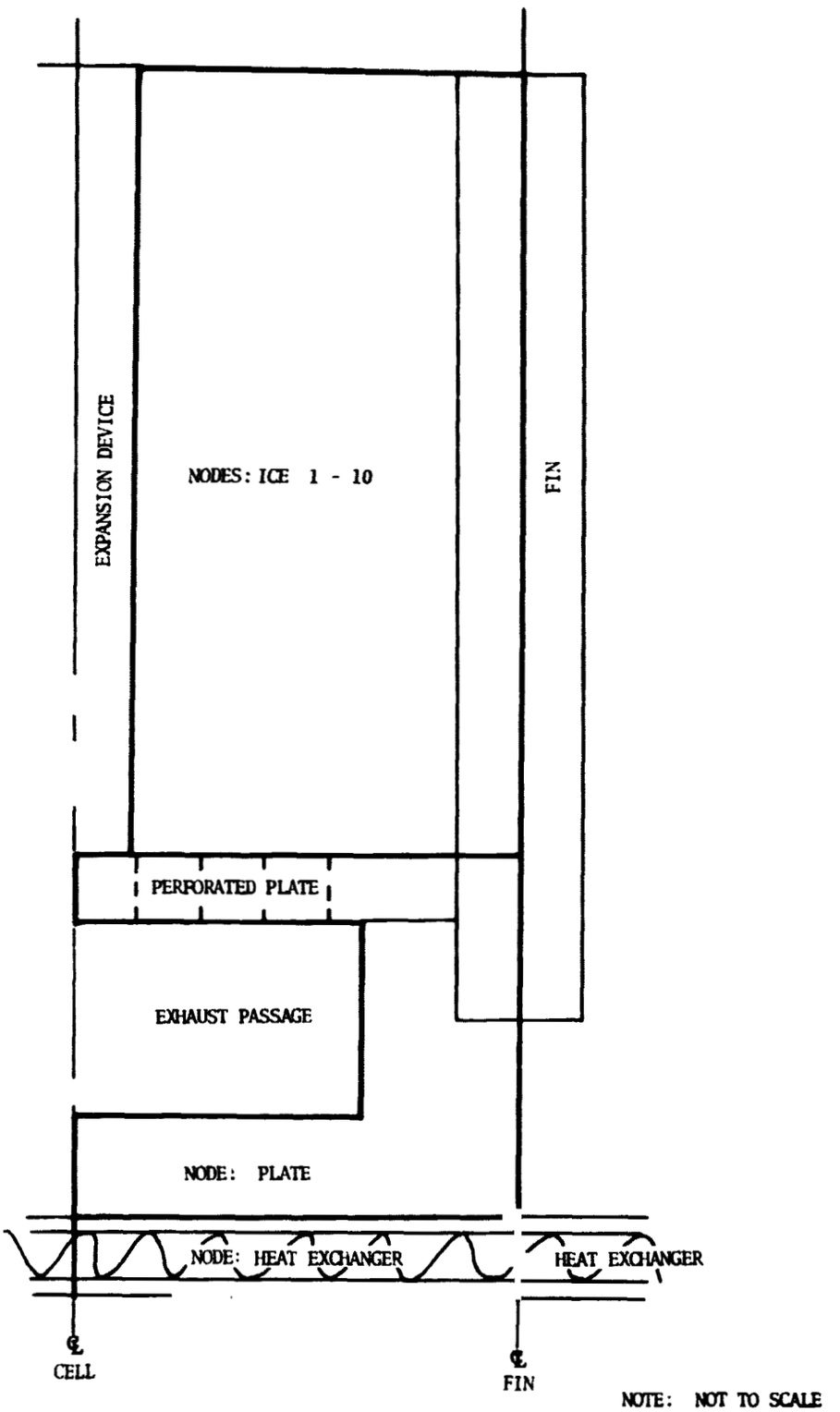

FIGURE 24 NODAL BREAKDOWN HALF CELL MODEL

where,

m = mass

h = heat of fusion

Cp = specific heat

T = temperature range of melt

The actual physical melting process occurs at 32°F (273.16K). However, it is impossible to model the melt process as an instantaneous step function with H-179 because not enough heat can be absorbed by the model node as the computer process moves forward in time. The model thus assumes that the ice melting process occurs over a range of 31°F to 33°F (272.60K to 273.72K). This insures that the proper amount of heat is absorbed by each ice node to model the heat of fusion.

Within the computer model, each node is connected by a conductance. In the connection between nodes HX and PLATE (see figure 24), the conductance used was an assumed minimum contact conductance of 96 Btu/hr-ft^2-°F (544.3 J/s-m^2-K) which was determined from Ice Pack Heat Sink Subsystem development testing conducted at HSD from February to March 1973.

Several heat loads were then impressed on the node, HX, to simulate Ice Pack Heat Sink Subsystem loads of 475, 2000, and 4000 Btu/hr (139.3, 586.7, 1173 J/s). The resultant conductances from node PLATE to the ice/liquid interface were then plotted as figure 25.

From figure 25, it can be seen that the computer model ice cell conductance is approximately equal for Ice Pack Heat Sink Subsystem loads of 475, 2000, and 4000 Btu/hr (139.3, 586.7, 1173 J/s). For use as input in the full system computer model the ice cell conductance will therefore be assumed to be independent of the heat load.

Also depicted on figure 25 are the analytical calculations of ice cell conductance for the present design. These values are approximately one-half of the analytical calculations presented in reference 5 for the ice cell conductance. The difference between the two sets of analytical calculations is caused by differences in geometry between the two units and by use of a more accurate thermal conductivity of the metal for the analytical ice conductance calculations of the present design.

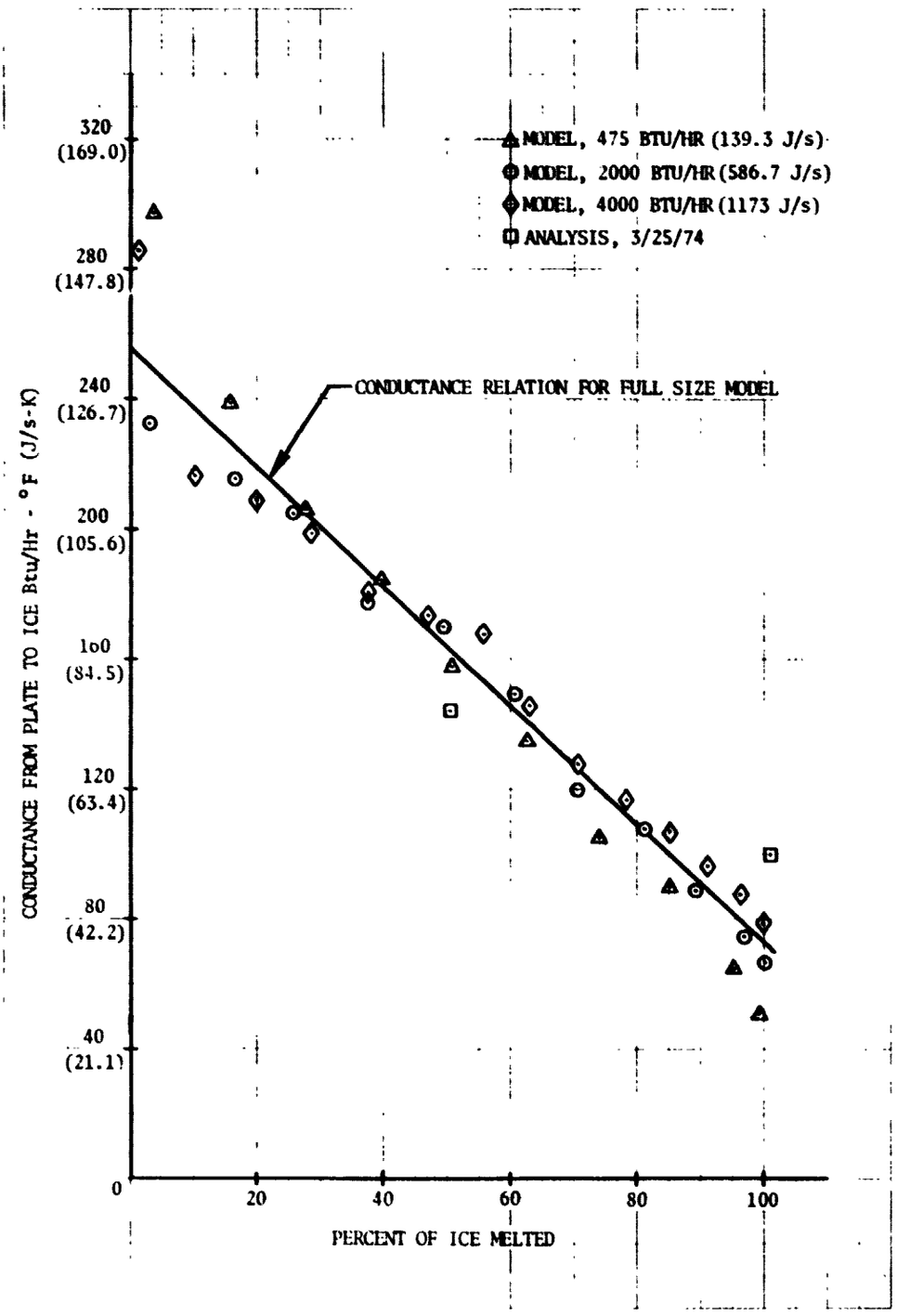

FIGURE 25 ICE CELL CONDUCTANCE DURING MELT PROCESS

Comparing the analytical calculations of the present system with the results of the computer model, a difference in slope can be noted. This discrepancy is to be expected as the computer model treats the melt process and multi-dimensional heat transfer more accurately than analytical approximations. This difference is discussed in detail in Appendix C.

The conductance results of this ice cell melt model are now used in the full Ice Pack Heat Sink Subsystem model described below.

Full Size Ice Pack Heat Sink Subsystem Model

A computer program was recently developed to model the full size Ice Pack Heat Sink Subsystem thermal performance. A new program was necessary because the generalized heat transfer program used with the melt model cannot handle conductance as a function of the total heat input to a node.

Since the LCG water traverses a path consisting of two single passage four pass heat exchangers connected in series, the model is set up into eight major segments (see figure 26) with each major segment consisting of one full pass of the LCG water through the heat exchanger. Each major segment is then subdivided into four nodes (see figure 27) to simulate the LCG water; heat exchanger; ice cell plate and supports; and the ice cell itself. As can be seen from figure 27, each LCG pass width encompasses five ice cells and fins.

Each node is assigned an appropriate thermal mass, as discussed in the melt model section. However, this model becomes more complex than the melt model when determining node connector values.

Each LCG water node is connected to the appropriate heat exchanger node by heat transfer coefficients determined from heat exchanger theory. The values of this transfer coefficient as a function of LCG water flow rate in the heat exchanger is presented in figure 28. This curve was generated from data in reference 6.

Each heat exchanger node is connected to the adjacent plate node by the same contact conductance described previously.

The plate node is then connected to the ice cell node by the ice cell conductance determined from the ice cell melt model that was presented as figure 25. During the computing process, the temperature of the ice cell node is maintained at 32°F until enough heat has been added to the node to completely melt the ice and the connection from the ice

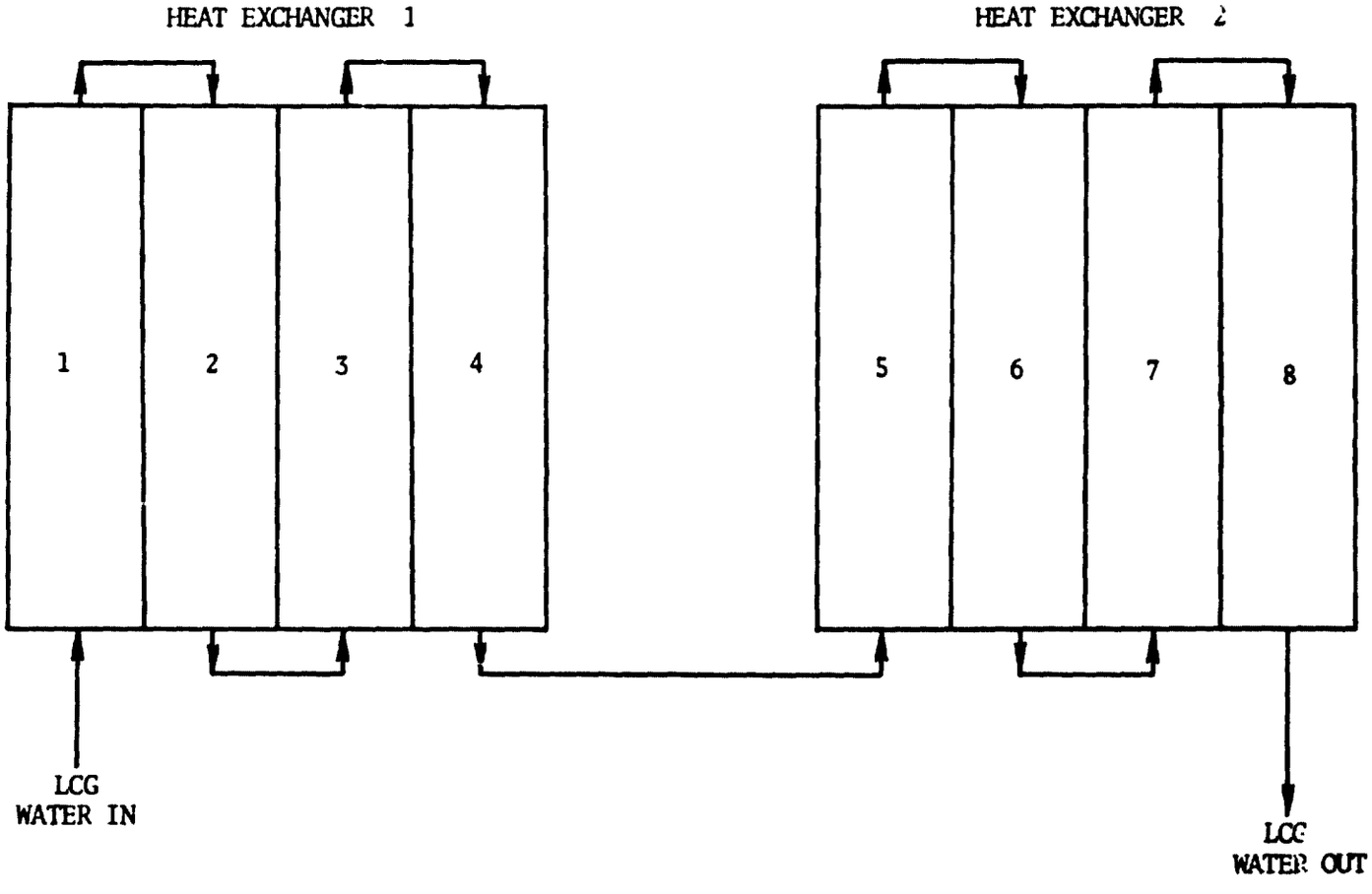

NOTE: NOT TO SCALE

FIGURE 26 FULL SIZE ICE PACK HEAT SINK SUBSYSTEM
MAJOR MODEL SEGMENTS

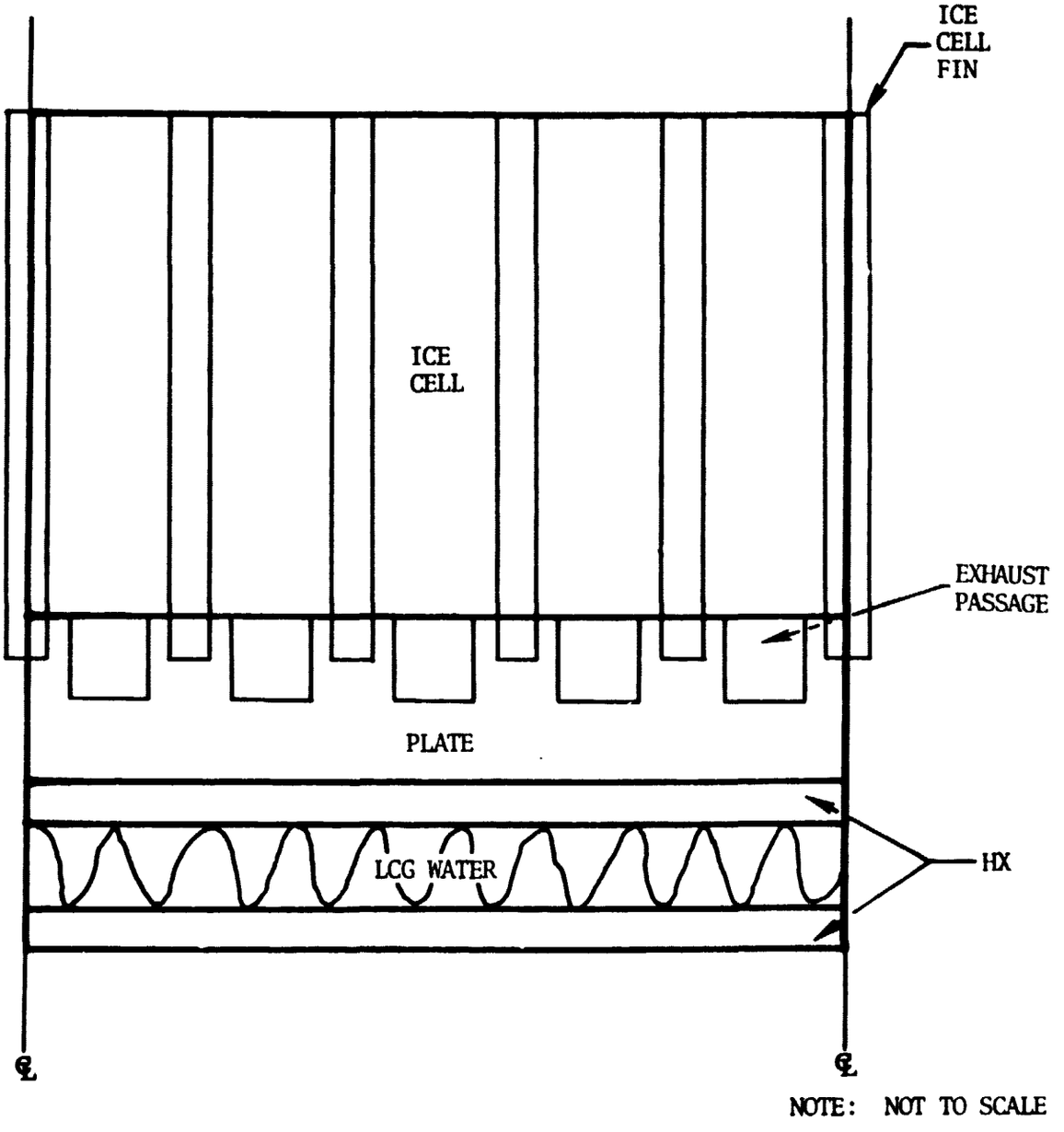

FIGURE 27 FULL SIZE ICE PACK HEAT SINK SUBSYSTEM
NODES OF MAJOR SEGMENTS

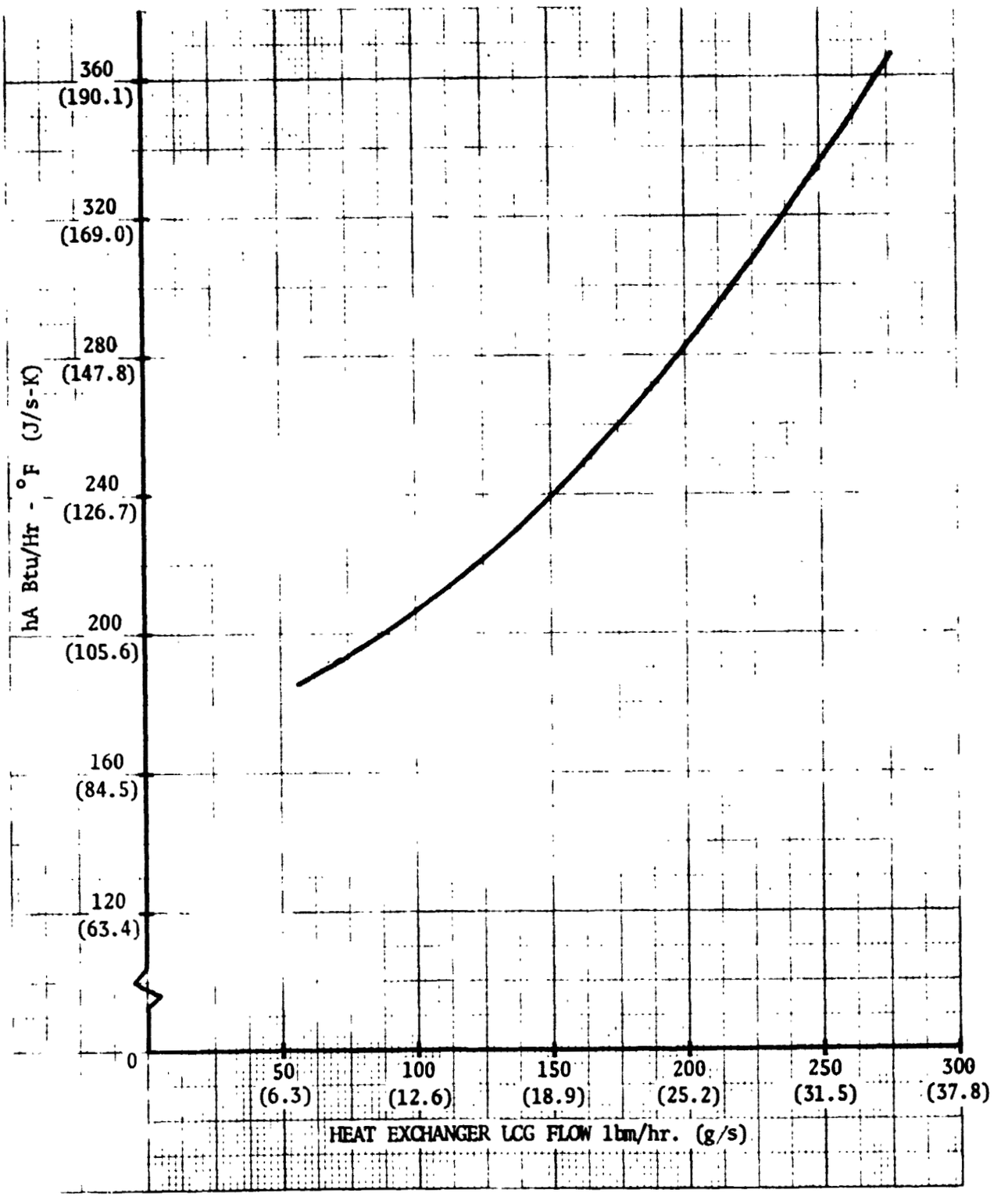

FIGURE 28 ESTIMATED HEAT EXCHANGER COEFFICIENTS

cell to the plate is calculated anew during each interaction as a function of the percentage of ice melted. This relation (determined from figure 25) can be expressed as

$$C = 255 - 184 \left(\frac{\text{percent melted}}{100}\right) \qquad (4)$$

where

C is in units of Btu/hr-^{o}F (1.89 J/s-K).

Furthermore, sideways connections (i.e., from major segment 2 to major segment 3, etc., from figure 26) are used for the heat exchanger, plate, and ice cell nodes. These values are all straight conductance terms, $kA/\Delta x$. Each water node also conducts heat to each subsequent downstream water node with a connection equivalent to the LCG water weight flow times the specific heat of water.

Computer runs of this model indicate correlation greater than 98% between analytical predictions of the time to melt all the ice and computer model calculations of the time to melt. A sample print-out of this model is contained in Appendix D.

Results

By using the ice cell conductance relations of figure 25, the full size Ice Pack Heat Sink Subsystem model was run for LCG water flow rates of 120, 180, and 240 lbm/hr (15.1, 22.7, and 30.2 g/s). The conductance from the LCG water to the heat exchanger was calculated by use of figure 27 with a segment primary area (Ap) of 0.158 ft^2 (0.0147 m^2). The contact conductance between the heat exchanger and plate nodes was assumed to be 96 Btu/hr-ft^2-^{o}F (544.3 J/s-m^2-K). The effectiveness of the Ice Pack Heat Sink Subsystem was then calculated by use of equation 5 at various ice cell percentage melt points.

$$\epsilon = \frac{T_{in} - T_{out}}{T_{in} - m\, P_{ice}} \qquad (5)$$

where

ϵ = effectiveness

T_{in} = LCG water inlet temperature

T_{out} = LCG water outlet temperature (segment 8)

$m\ p_{ice}$ = Melting point of ice

The results of this computer/analytical procedure are presented in figure 29. From figure 29, the dependence of the overall thermal performance upon the amount of ice that has melted is readily apparent.

With the use of the computer models, this type of prediction can be made for various LCG water flow rates and various contact conductances. Each computer run also requires an input of the LCG water inlet temperature and the amount of time that the melt process is to cover. In this manner, it will be possible to compare predicted performance with Ice Pack Heat Sink Subsystem test data by actually inputting the test conditions into the computer model.

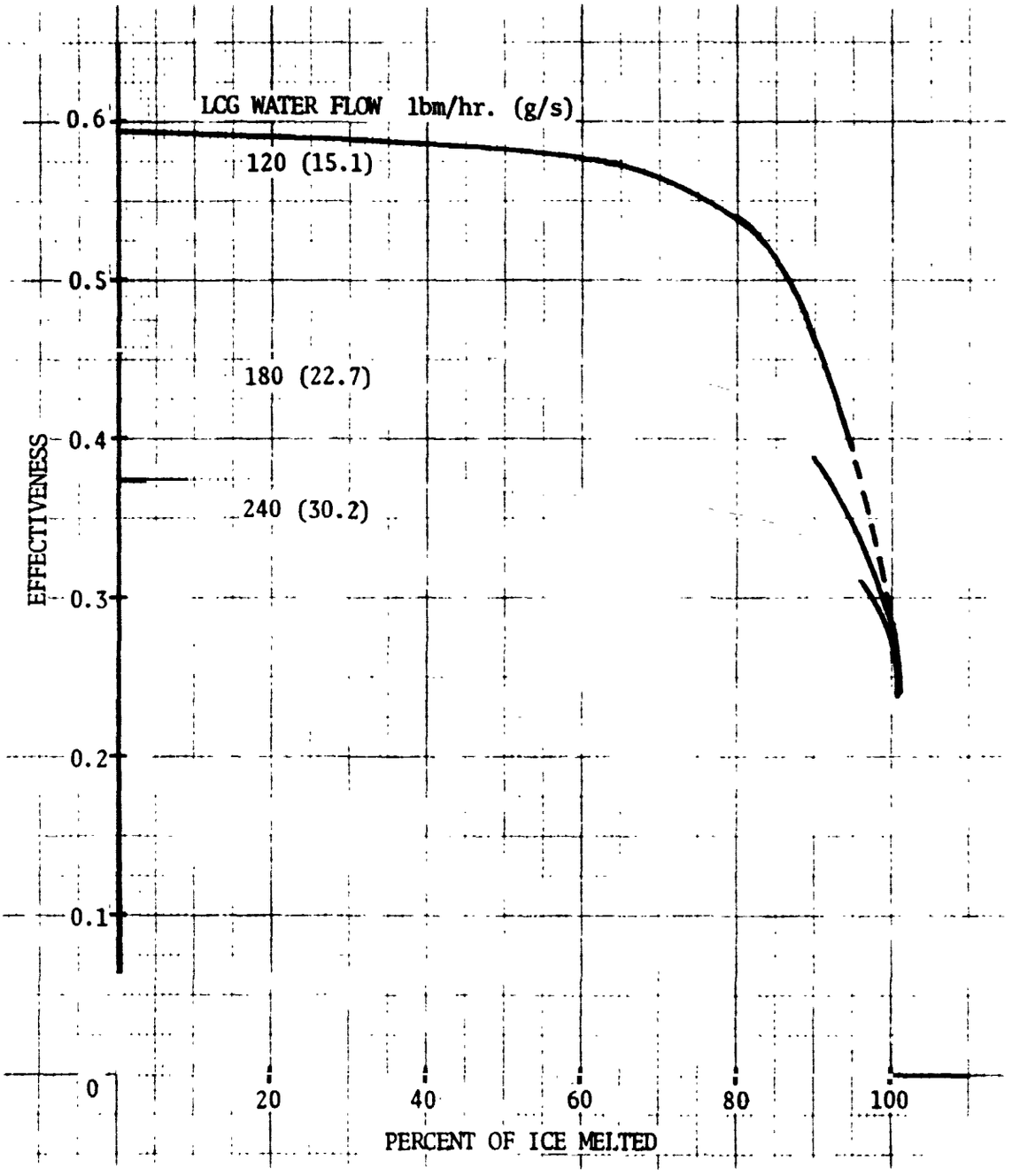

FIGURE 29 COMPUTED THERMAL PERFORMANCE - OVERALL EFFECTIVENESS AS A FUNCTION OF AMOUNT OF ICE MELTED

PROTOTYPE DESIGN, FABRICATION AND ACCEPTANCE TEST

DESIGN AND FABRICATION

Based on the results of the Interface Development effort as well as on the experience gained in the laboratory model development program (NAS 2-7011 Phase I), a prototype system has been designed, fabricated and acceptance tested. Two prototype ice chests were designed and fabricated: one with and one without the requirement that the ice chest function as a water boiler for emergency cooling. A heat exchanger and mounting assembly has been designed and fabricated to be capable of mating with each of the ice chests developed in this task.

The prototype hardware was designed to meet the following requirements:

Ice pack water weight:	approximately 4.75 kg (10.45 lb)
Maximum heat rejection rate:	2000 Btu/hr (2130 kJ/hr)
Average heat rejection rate:	1500 Btu/hr (1600 kJ/hr)
Minimum heat rejection rate:	750 Btu/hr (800 kJ/hr)
LCG coolant flow rate:	0.48-0.53 gpm (108-120 kg/hr)
Ice chest #1:	normal mode, no emergency mode
Ice chest #2 (Boiler):	normal mode, emergency mode

The internal configuration of the ice chest and boiler is identical to that developed during Phase I of this effort and is documented in reference 4.

The prototype hardware consists of the following assemblies:

Boiler Assembly	SVSK 88482-500, Rev. C
Ice Chest Assembly	SVSK 88482-600, Rev. B
Mounting Assembly and Harnesses	SVSK 87308-100, Rev. B

A functional schematic of the prototype system is shown in figure 30.

Appendix E contains a complete set of prototype hardware parts lists.

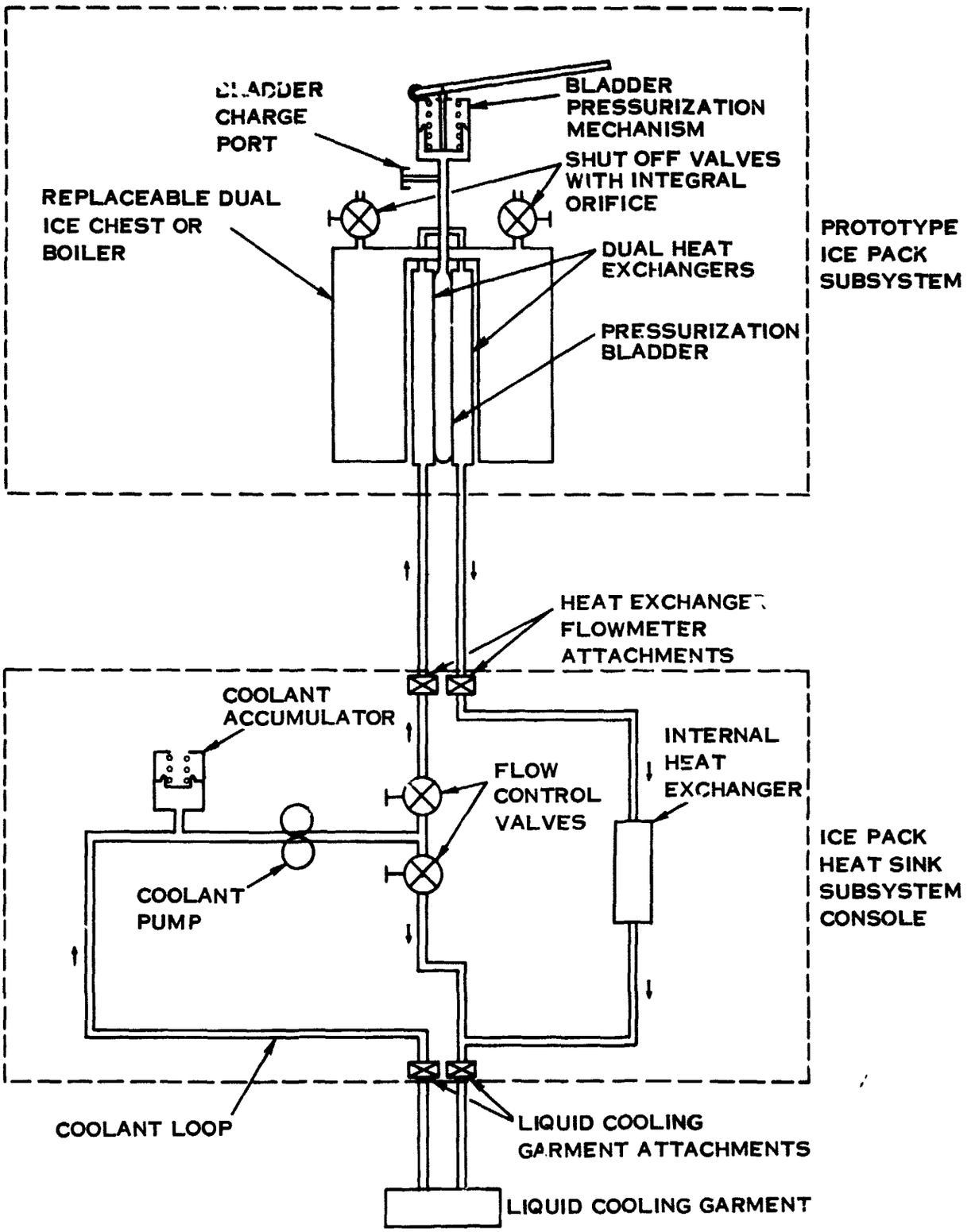

FIGURE 30 ICE PACK FUNCTIONAL SCHEMATIC

Boiler Assembly

Figure 31 illustrates a view of the boiler assembly with the cover removed and prior to installation of the wicks and expansion compensation assemblies.

Figure 32 shows the boiler assembly with the wicks and expansion compensation assemblies installed.

Figure 33 shows the boiler assembly completely assembled.

Ice Chest Assembly

Figure 34 is a view of the heat transfer surface of the ice chest assembly.

Figures 35 and 36 show the ice chest assembly completely assembled.

Mounting Assembly and Harnesses

Figures 37 and 38 show frontal views of the completely assembled mounting assembly.

Figure 39 shows a side view and figure 40 shows a bottom view.

Figure 41 is a rear view of the mounting assembly showing the mounting rings for the harnesses (not shown).

Figure 42 shows the mounting assembly with a boiler assembly installed.

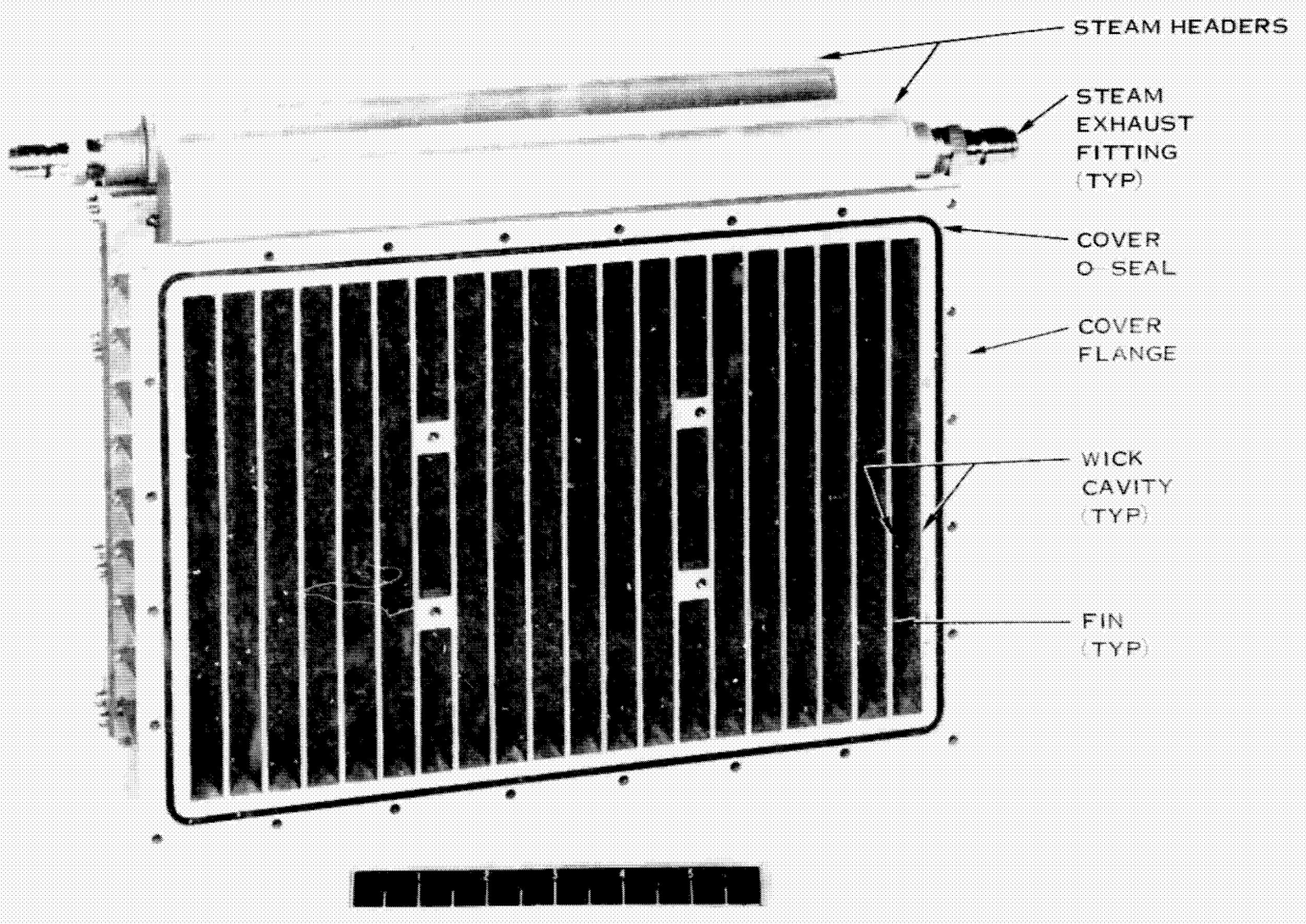

FIGURE 31. BOILER PRIOR TO WICK INSTALLATION

Hamilton Standard

FIGURE 32. BOILER WITH WICK ASSEMBLIES INSTALLED

FIGURE 33. BOILER ASSEMBLY

FIGURE 34. ICE CHEST HEAT TRANSFER SURFACE

Hamilton Standard U A

FIGURE 35. ICE CHEST ASSEMBLY — SIDE VIEW

FIGURE 36. ICE CHEST ASSEMBLY – BOTTOM VIEW

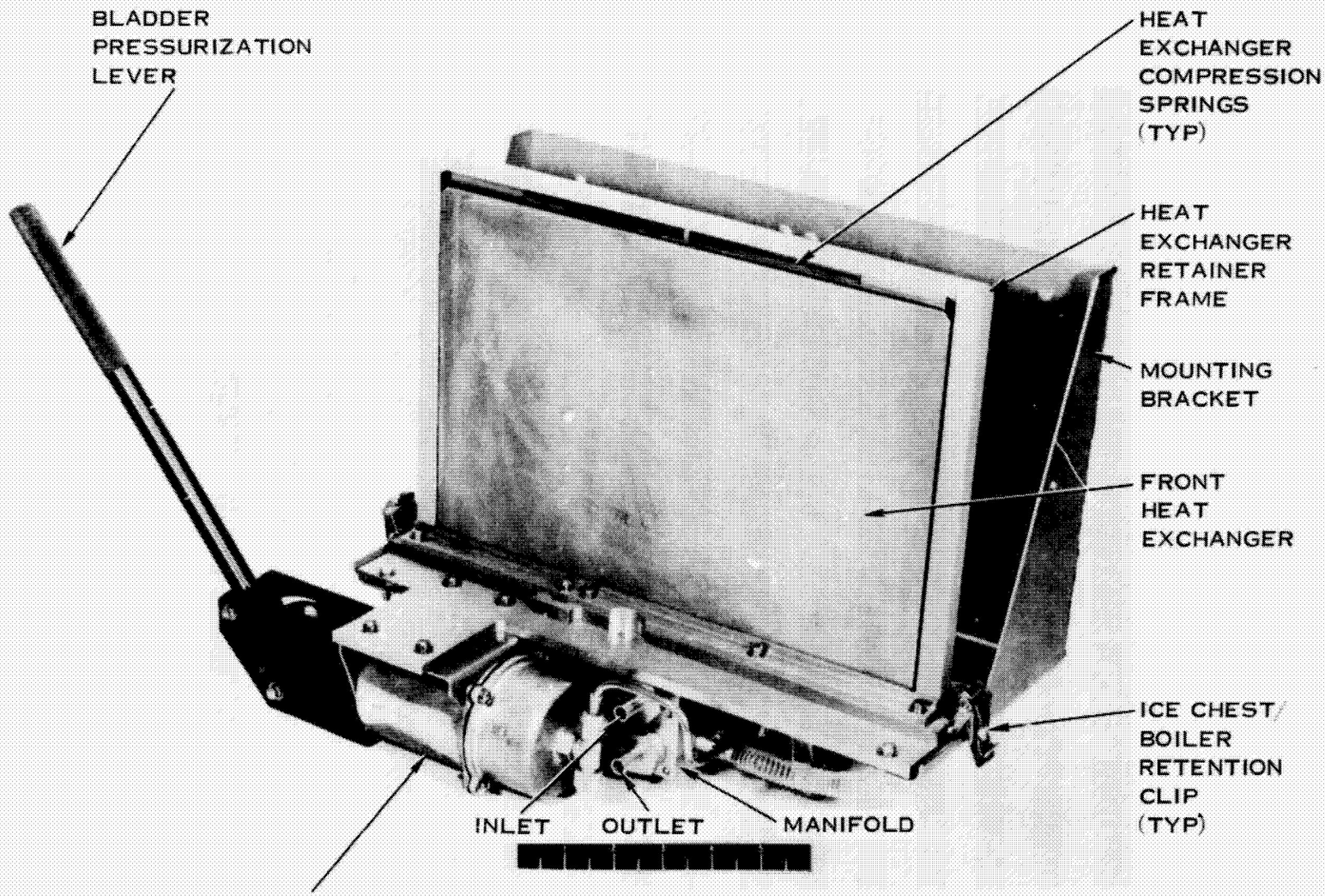

FIGURE 37. MOUNTING ASSEMBLY

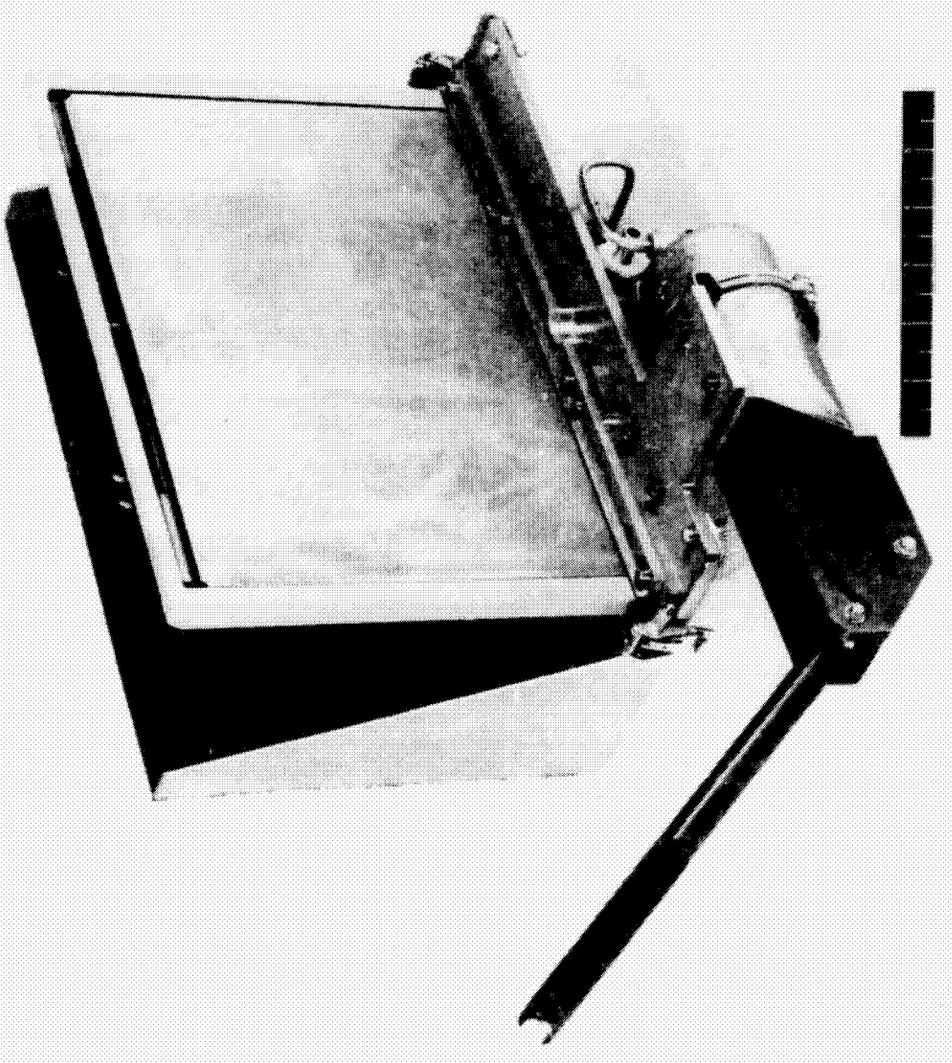

FIGURE 38. MOUNTING ASSEMBLY

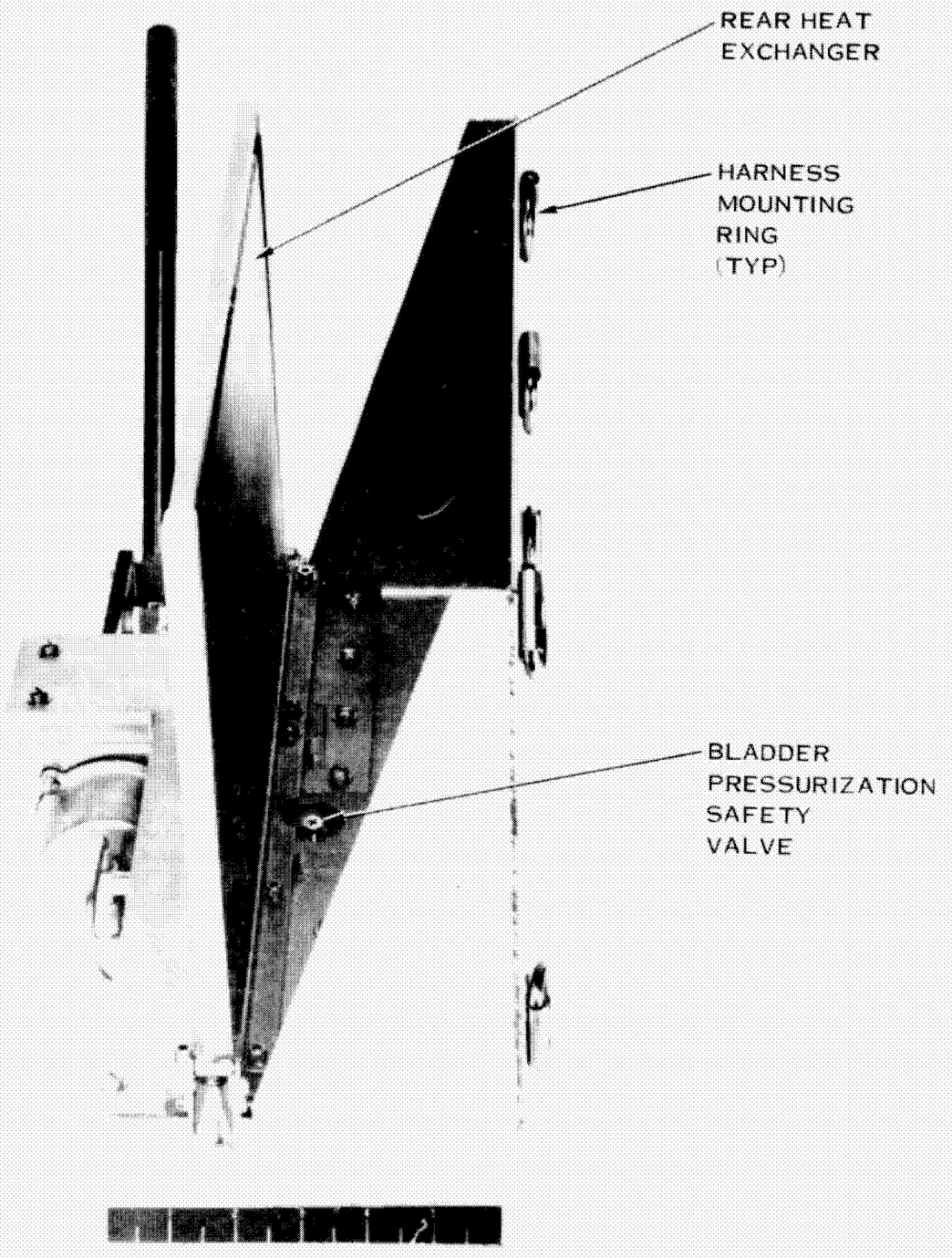

FIGURE 39. MOUNTING ASSEMBLY SIDE VIEW

FIGURE 40. MOUNTING ASSEMBLY BOTTOM VIEW

FIGURE 41. MOUNTING ASSEMBLY — REAR VIEW

Hamilton Standard
DIVISION OF UNITED AIRCRAFT CORPORATION

FIGURE 42. MOUNTING ASSEMBLY WITH BOILER ASSEMBLY INSTALLED

ACCEPTANCE TEST

Performance requirements for this subsystem consist of providing a heat sink for the LCG coolant [coolant flow rate is 240 lbs H_2O/hr (1814 g H_2O/min)] for one hour at a 1500 Btu/hr (1600 kilojoules/hr) heat rejection rate and with an LCG inlet temperature compatible to astronaut comfort.

Test Summary

Two configurations of the ice chest were tested, one a pure ice chest and the second an ice chest with emergency capability to operate in a water boiler mode. Test runs are summarized in Table II. Tests completed during the series have confirmed the adequacy of the design. A Performance Test Plan is included in this plan as Appendix F. The actual log sheets are reproduced as Appendix G.

Test Results

Figure 43 presents the test results as heat exchanger effectiveness, ϵ vs fraction of ice melted. All the data are consistent except for the ice chest test at 1500 Btu/hr (1600 kilojoules/hr) which exhibited thermal sink exhaustion at approximately 80% of nominal capacity. This anomoly has been explained as an incomplete ice freeze at the beginning of the run, with subsequent loss of heat sink capacity. This explanation is consistent with all the remaining data obtained during this series and would produce excellent correlation if the questionable data were transposed to the right by a constant increment of 20 to 30 percent of the ice melt fraction.

Several inflections are noted in the test data plots, primarily in the runs at 1500 Btu/hr (1600 kilojoules/hr). These discontinuities reflect changes in the flow rate thru the ice chest heat exchanger and are to be expected since overall effectiveness is reduced as flow rate increases.

Unit effectiveness vs heat exchanger flow rate at the point of zero ice melt is important since this is also the system effectiveness in the emergency boiler mode. These data, taken from the six ice melt tests, are shown in figure 44 and are compared to analytical predictions. The results are excellent and deviate from analytical predictions only in the high effectiveness or low flow regime. This result is not unusual in that the heat exchanger flow passages are designed to meet performance and pressure drop for the high flow case and flow maldistribution can be expected when flow rates are reduced by an order of magnitude. Unit performance at the low flows is substantially above system requirements.

TABLE II ICE CHEST TEST RUNS

Test Date	Log Sheet No.	Configuration		Heat Sink Mode		Heat Rate	
		Ice Chest	Ice Chest, Boiler	Melt	Boiler	Btu/hr	(kJ/hr)
10-1-74	10509	X		X		1500	(1600)
10-2-74	10510 10511	X		X		750	(800)
10-2-74	10512		X	X		2000	(2130)
10-3-74	10516		X	X		1500	(1600)
10-3-74	10517		X		X	750	(800)
10-3-74	10518	X		X		2000	(2130)
10-4-74	10520 10521		X	X		750	(800)
10-4-74	10522		X		X	1500/ 2000	(1600/ 2130)

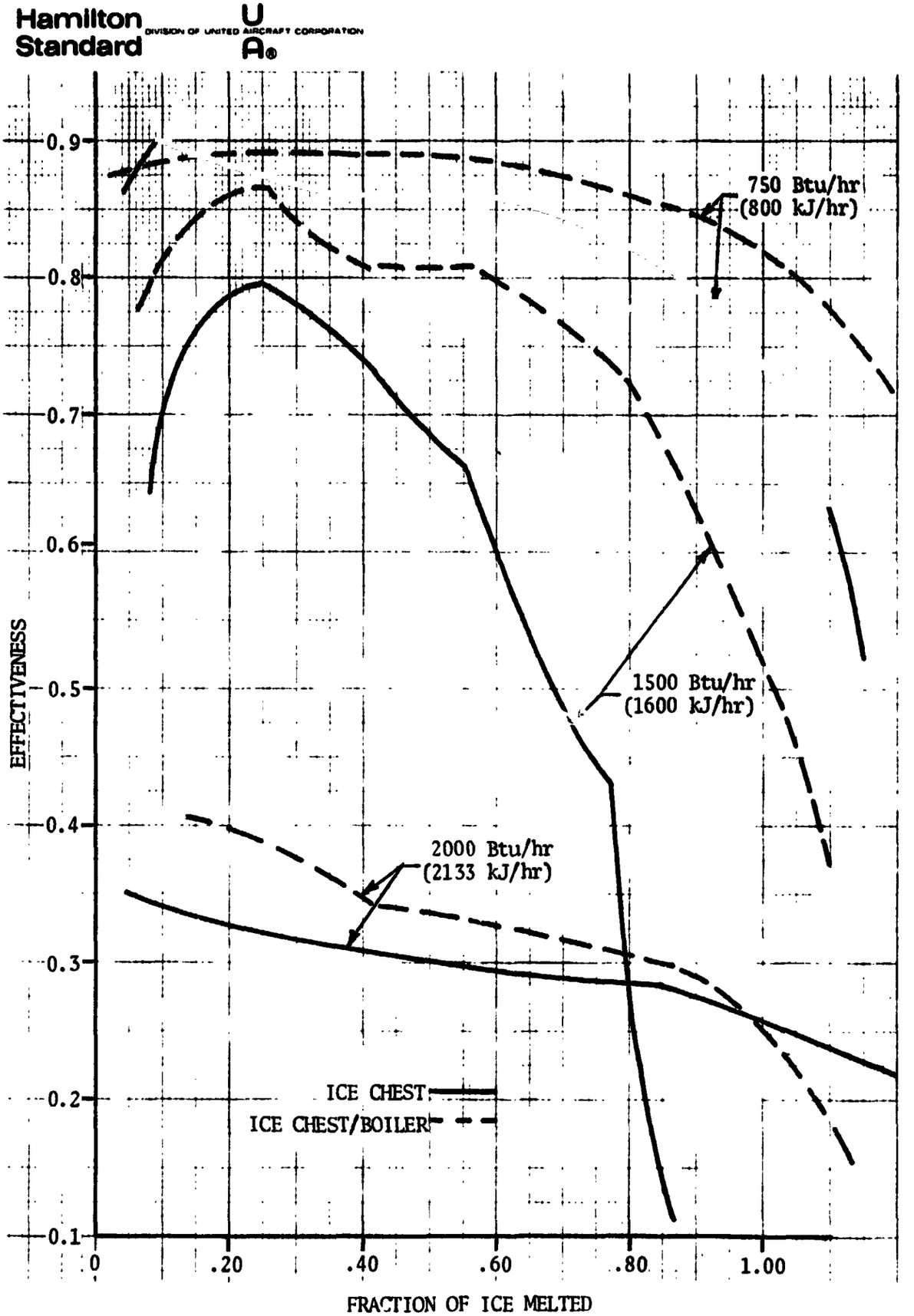

FIGURE 43 ICE CHEST ACCEPTANCE TEST RESULTS

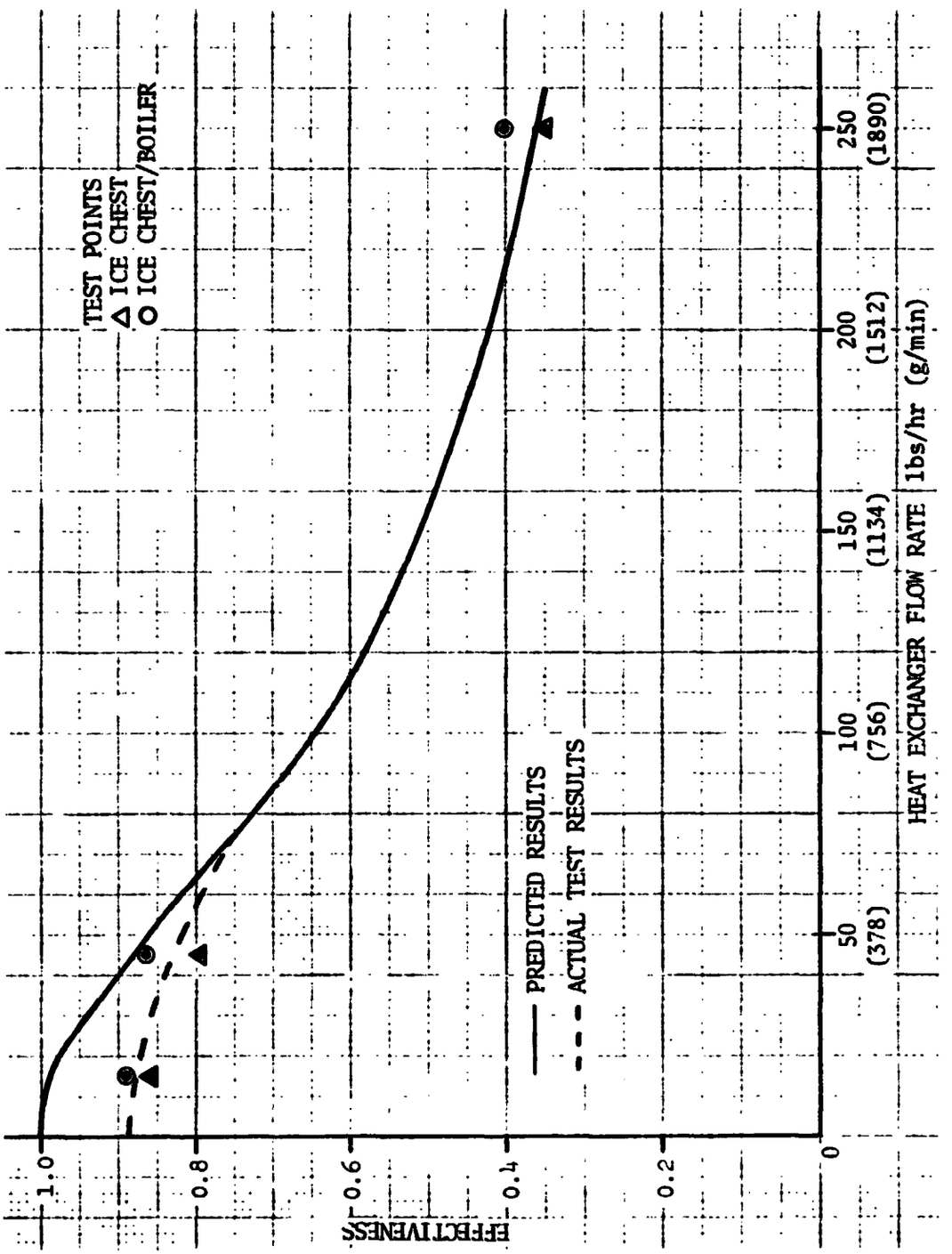

FIGURE 44 EFFECTIVENESS VS HEAT EXCHANGER FLOW RATE AT THE POINT OF ZERO ICE MELT

ANALYTICAL CORRELATION

Math model correlation has been established and has been utilized to create a simple procedure to schedule ice chest water flow as a function of heating rate, inlet water temperature and fraction of ice melted.

Ice Melt

A math model of the ice chest/water boiler was presented in reference 7 and has been utilized to correlate the data of Table II. Within the heat sink subsystem the three areas that are considered in the resistance to thermal transfer are:

1) Heat exchanger resistance.
2) Contact resistance between the ice module and the heat exchanger.
3) Resistance between the contact interface and the ice melt boundary.

The first two resistance should be constant within any one test while the third will increase as the ice/water boundary recedes from the aluminum containment. Overall system resistance between the LCG water and the melting ice will therefore increase with run time and can be described as a decrease in component effectiveness with run time or fraction of ice melted. This characteristic is evident from the data of figure 43. Comparison to the analytical predictions of reference 7 is, however, not precise. The reduction in effectiveness forecast with the original model was not as severe as experienced in test. This was corrected when the ice cell conductance during the melt process was modified from a linear decrease between 255 and 71 Btu/hr-^{o}F (490 and 136 kilojoules/hr-K) to a linear decrease between 255 and 0 Btu/hr-^{o}F (490 and 0 kilojoules/hr-K). Original predictions of contact conductance, 96 Btu/hr-^{o}F (184 kilojoules/hr-K), and heat exchanger conductance (figure 5 of reference 7) were confirmed by this test series as evidenced by the data of figure 44. Revised math model results are presented in figure 45 and incorporate corrections for flow maldistribution at flows below 75 lbs. H_2O/hr (567 g H_2O/min.). The same data without the flow maldistribution corrections is shown in figure 46.

Boiling Mode

In the boiling mode the total ice chest thermal resistance includes only those values attributed to the heat exchanger, the interface contact and the resistance between the interface and the boiling water. This total is identical to the ice chest value at the point of zero ice melt.

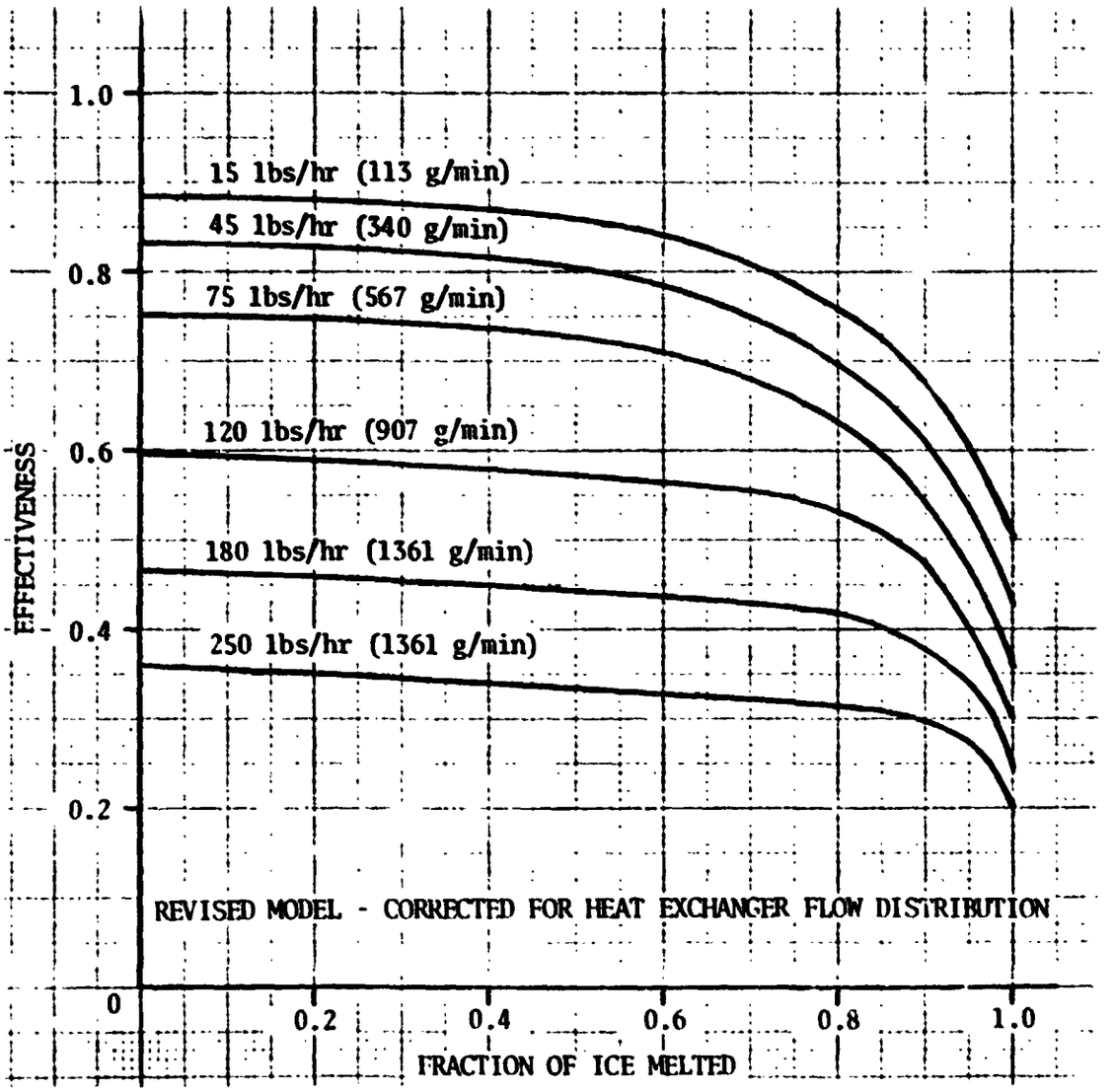

FIGURE 45 PREDICTED ICE CHEST PERFORMANCE

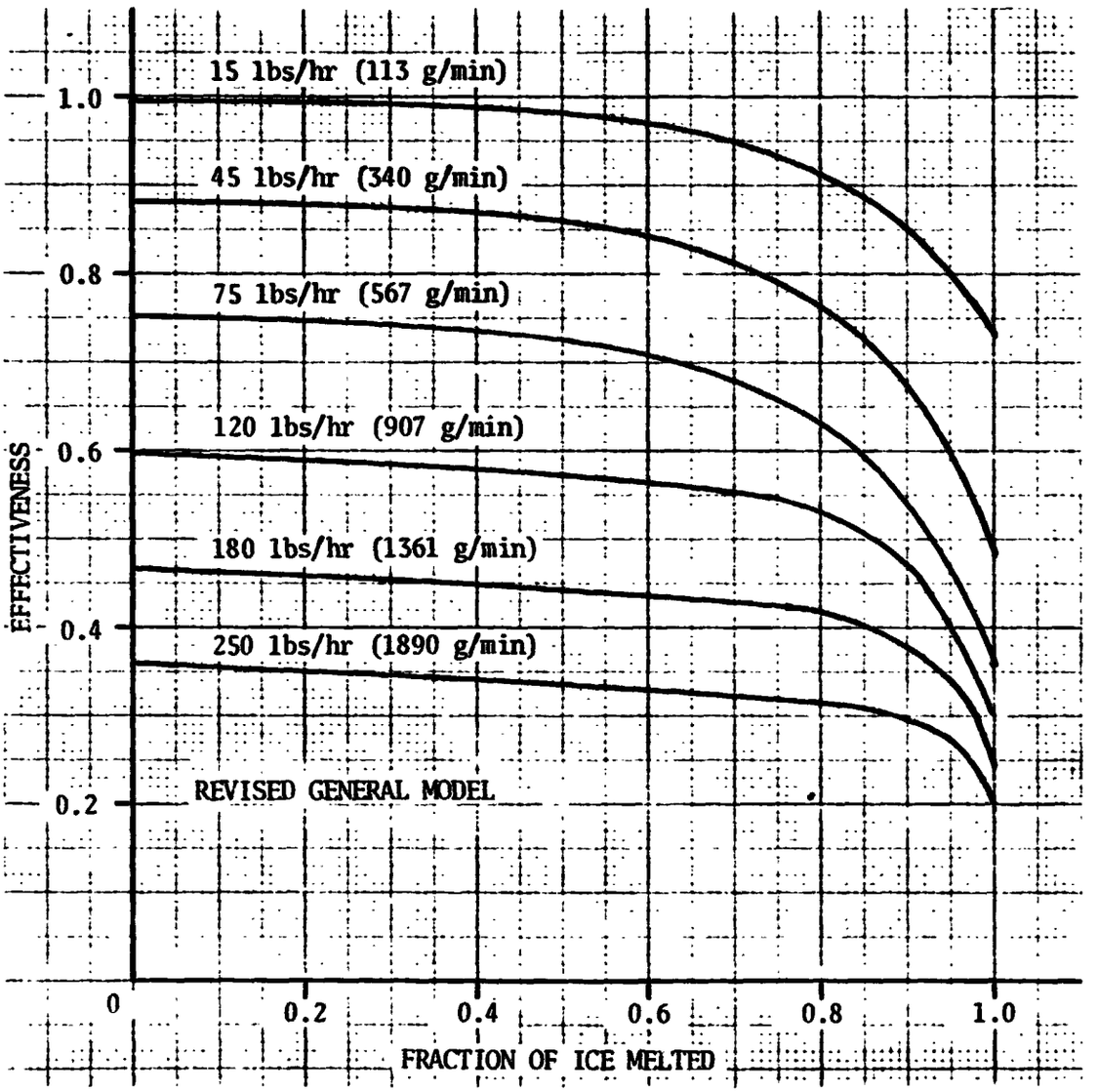

FIGURE 46 PREDICTED ICE CHEST PERFORMANCE

Utilizing the data of figure 44, the approximate heat sink temperature experienced in test can be calculated as follows:

$$\epsilon = \frac{T_{in} - T_{out}}{T_{in} - T_{sink}}$$

or,

$$T_{sink} = T_{in} - \frac{(T_{in} - T_{out})}{\epsilon}$$

For heat loads ranging from 750 to 2100 Btu/hr (800 to 2237 kilojoules/hr), heat sink or water boiling temperature in test has been estimated as 4C ± 1.0°F (4.4 ± 0.5°C). This is approximately 10°F (5.5°C) below the values predicted during component design. This anomoly has been traced to the intentional omission of the steam vent orifice in the assembly. Instead of the desired orifice restriction diameter of 0.381 inches (9.7 mm), a 0.47 inch (11.9 mm) diameter restriction was present in the exhaust fitting. This difference in diameter would permit the saturation pressure to seek a level of 0.25 inch Hg (846 N/m^2) [40°F (4.4°C) dew point] rather than the predicted 0.37 inch Hg (1252 N/m^2) [50.5°F (10.3°C) dew point] at heat loads of 1000 Btu/hr (1067 kilojoules/hr) per orifice (there is one orifice in the vent line from each ice chest or two per system). Back pressure provided by this fitting will reduce to 0.186 in. Hg (629 N/m^2) at a heat load of 750 Btu/hr (800 kilojoules/hr) and provide a heat sink of 32.8°F (0.4°C).

Mission Performance Prediction

Results of the math model and the test results have been combined to provide a procedure to enable prediction of ice chest operating conditions throughout its mission life. The working chart is presented in figure 47 and is utilized as follows:

$$Q = \dot{W}cp\ (T_{in} - T_{out})$$

and,

$$\epsilon = \frac{T_{in} - T_{out}}{T_{in} - T_{sink}}$$

Hamilton Standard
DIVISION OF UNITED AIRCRAFT CORPORATION

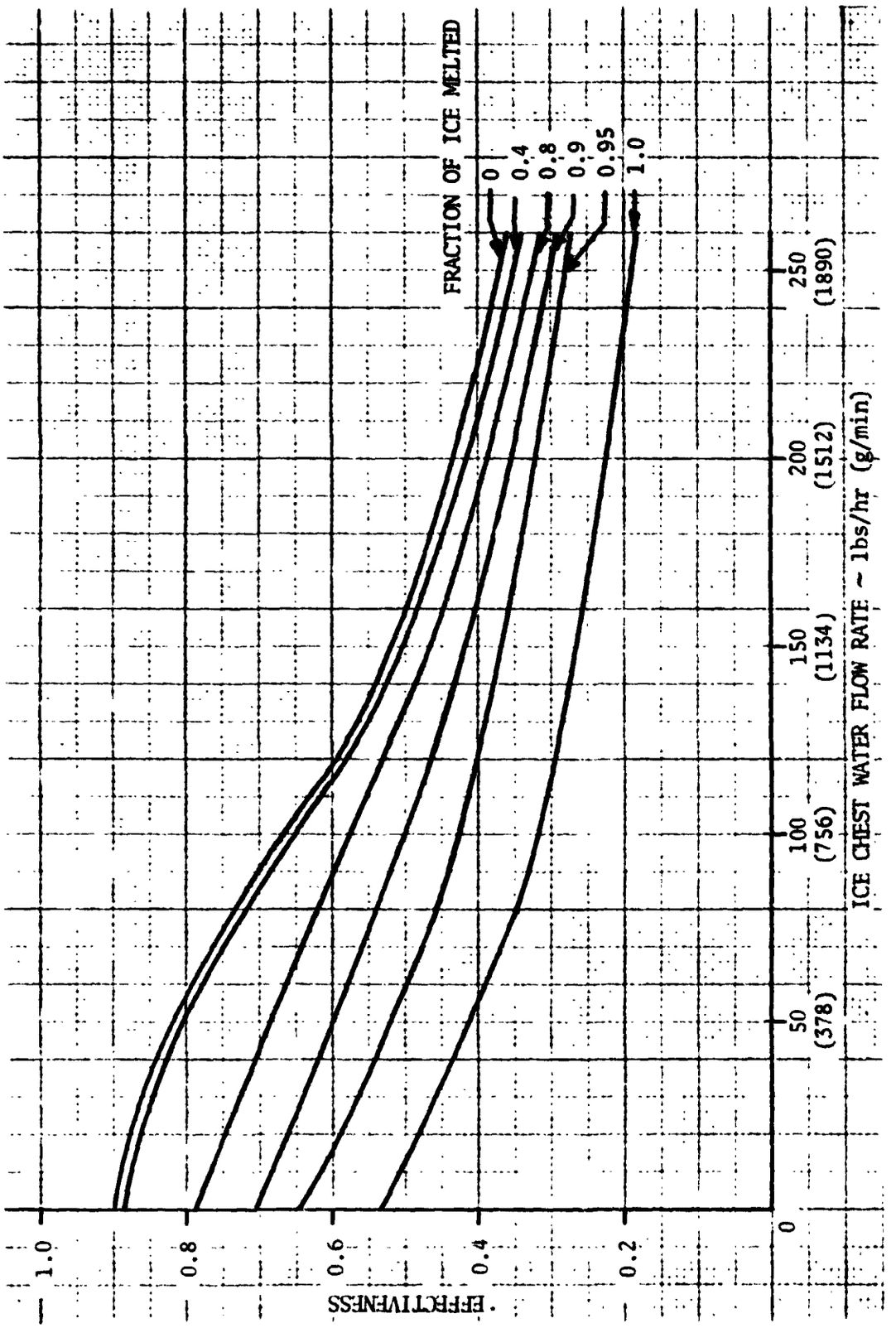

FIGURE 47 WORKING CHART FOR ICE CHEST PERFORMANCE PREDICTIONS

where,

Q = heat load, Btu/hr
$\dot{W}$ = ice chest water flow, lb/hr
cp = water heat capacity 1.0 Btu/lb°F
ϵ = ice chest effectiveness, dimensionless
T_{in} = ice chest water inlet temperature, °F
T_{out} = ice chest water outlet temperature, °F
T_{sink} = ice chest sink temperature = 32°F

Rearranging,

$$\dot{W}\epsilon = \frac{Q}{T_{in} - 32}$$

Now for any given heat load and water inlet temperature, ice chest water flow may be determined as a function of unit effectiveness. This relationship is shown in figure 48 for a heat load of 1500 Btu/hr (1600 kilojoules/hr) at a water inlet temperature of 56°F (286.5K) and for one of 70°F (294.3K). The plot is used as follows:

What is the ice chest flow rate 45 min. into a run at 1500 Btu/hr with a water inlet temperature of 56°F?

$$\text{Fraction of ice melted} = \frac{(\text{heat load})\ (\text{run time})}{(\text{wt. Ice})\ (\text{latent heat of fusion})}$$

$$= \frac{(1500\ \text{Btu/hr})\ (45/60\ \text{hours})}{(10.45\ \text{lbs.})\ (144\ \text{Btu/lb})}$$

$$= 0.75$$

Working off the 56°F inlet temperature isotherm (figure 48), the intersection at 0.75 fraction of ice melted indicates unit effectiveness will be 0.56 and a water flow rate of 112 lb/hr is proper. Similarly, at 70°F inlet temperature the proper flow would be 60 lbs/hr at 45 minutes.

This procedure may now be followed thru an entire preplanned mission to provide prior knowledge of operating conditions.

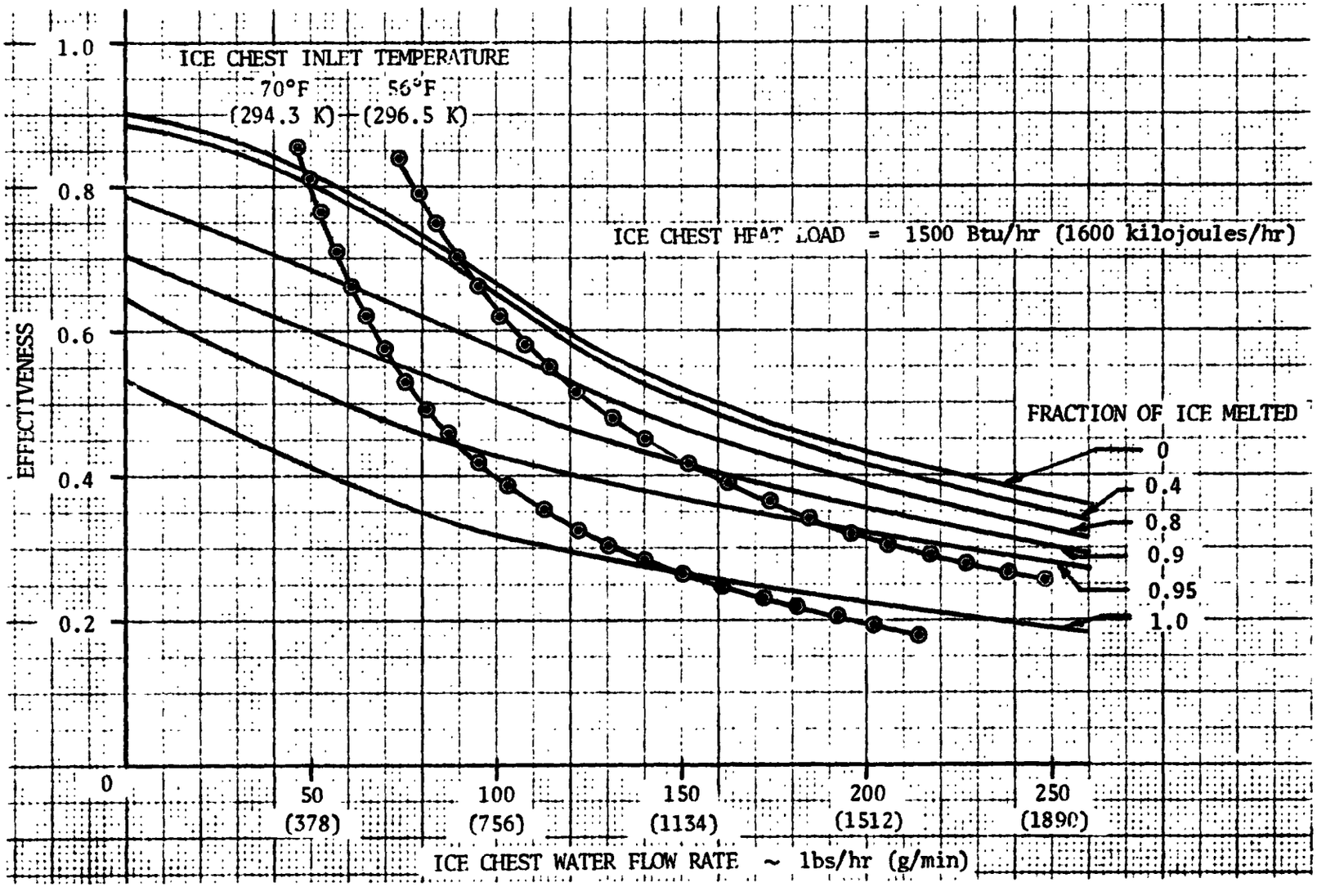

FIGURE 48 WORKING CHART SAMPLE USE

THERMAL STORAGE MATERIALS EVALUATION

ANALYTICAL INVESTIGATION

Introduction

This portion of the study has consisted principally of a literature search and analysis of available data on various thermal storage materials that were candidates for use in thermal storage systems.

The overall target of this analytical investigation was the doubling of the cooling capacity per unit weight of the heat sink material over that provided by water ice, while maintaining a low volume change and a density equal to or greater than that of water ice. Other target criteria for candidate materials were as follows:

1. Materials must be regenerable.
2. Primary concern is heat absorption per unit weight.
3. Thermal conductivity must be at least 0.3 BTU/hr-ft°F (0.52 W/mK).
4. Heat absorption and rejection temperatures should be within 18°F (10 K).
5. Vapor pressure of material should be less than 1000 psia (680 kN/m^2 abs).
6. Material must be safe to handle under operational conditions.
7. A non-corroding container must be possible.
8. Material must be non-explosive.
9. Material should have no toxic effects down to 20 ppm concentration.
10. Material must be non-radioactive.

None of the literature sources revealed any compounds that would simultaneously meet all of the acceptance criteria targeted for the thermal storage material. The work performed in this analytical investigation has resulted in establishing techniques for predicting classes of molecules which may have large heats of fusion.

The processes considered in the literature search and subjected to analysis were:

heat if fusion;
heat of solution plus heat of fusion; and
solid-solid transitions.

Literature Search

The initial program of study by the United Aircraft Research Laboratories has comprised a canvass of eight major sets of abstracts of chemical literature plus seven major sources of data for heats of fusion of chemical compounds. The search included study of references to thermal storage systems as well as to compounds with high heats of fusion. The sources searched are listed below along with the earliest year searched. In all cases, the search was carried through October 1973.

Chemical Abstracts (1937)
International Aerospace Abstracts (1961)
Scientific and Technical Aerospace Reports (1963)
Metals Abstracts (1968)
Nuclear Science Abstracts (1948)
Physics Abstracts (1950)
Engineering Index (1962)
Applied Science & Technology Index (1958)

In addition, the following data compilations were searched for suitable materials with higher heats of fusion than water:

Handbook of Tables for Applied Engineering Science - p. 398-403
Circular 500 - Bureau of Standards
Bulletin 393 - Bureau of Mines
Physical Properties of Chemical Compounds - R. R. Dreisbach - Amercian Chemical Society
International Critical Tables - Vol. III, p. 131-134

Results of the following two searches conducted by NASA and the Defense Department were also reviewed:

NASA Literature Search #23680 - Heat of Fusion
Defense Documentation Center - Compounds with Heat of Fusion Greater Than Ice

One review article was found on the subject of heat storage (Ref. 8) at low temperature and others (Refs 9-16) were found which described materials unsuited to the present application, but which included design data which might be found useful in overall system design.

Table III lists the heats of fusion and melting temperatures of the fifty materials that were found to have heats of fusion per gram greater than ice. Of the compounds on this list, there are only five that melt below 392°F (473 K), and only one, hydrazine (Ref. 17), that melts in the required temperature range. The small improvement over ice (19%) makes hydrazine unattractive because of its toxicity and corrosive properties.

TABLE III

COMPOUNDS WITH HIGHER HEAT OF FUSION THAN WATER

Material	Formula	Melting Point		ΔH_f	
		°C	(K)	cal/gm	(J/g)
Magnesium oxide	MgO	2800	(3073)	460	(1925)
Beryllium oxide	BeO	2547	(2820)	680	(2846)
Boron	B	2170	(2443)	490	(2051)
Aluminum oxide	Al_2O_3	2045	(2318)	260	(1088)
Magnesium silicate	$MgSiO_3$	1525	(1798)	146	(611)
Silicon	Si	1400	(1673)	431	(1804)
Cobalt silicide	$CoSi_3$	1306	(1579)	238	(996)
Beryllium	Be	1280	(1553)	250	(1046)
Calcium borate	$CaOB_2O_3$	1162	(1435)	141	(590)
Magnesium silicide	Mg_2Si	1106	(1379)	270	(1130)
Sodium fluoride	NaF	995	(1268)	180	(753)
Lithium fluoride	LiF	850	(1123)	250	(1046)
Sodium chloride	NaCl	800	(1073)	116	(485)
Vanadium oxide	VaO	2077	(2350)	224	(937)
Aluminum	Al	660	(933)	96	(401)
Magnesium	Mg	650	(923)	89	(372)
Lithium	Li	180	(453)	150	(627)
Carbon dioxide	CO_2	-109.5	(163.5)	137	(573)
Barium oxide	BaO	1923	(2196)	93	(389)
Calcium carbonate	$CaCO_3$	1282	(1555)	126	(527)
Calcium metasilicate	$CaSiO_3$	1512	(1785)	115	(481)
Calcium oxide	CaO	2707	(2980)	218	(912)
Copper oxide	Cu_2O	1230	(1503)	94	(393)
Germanium	Ge	959	(1232)	114	(477)
Iron oxide	FeO	1380	(1653)	107	(447)
Iron oxide	Fe_3O_4	1596	(1869)	142	(594)
Lithium hydroxide	LiOH	462	(735)	103	(431)
Lithium nitrate	$LiNO_3$	250	(523)	88	(368)
Magnesium fluoride	MgF_2	1221	(1494)	95	(397)
Manganese oxide	MnO	1784	(2057)	183	(766)
Manganese oxide	Mn_3O_4	1590	(1863)	170	(711)
Nickel chloride	$NiCl_2$	1030	(1303)	143	(598)
Potassium fluoride	KF	875	(1148)	112	(468)

TABLE III (continued)

Material	Formula	Melting Point		ΔH_f	
		°C	(K)	cal/gm	(J/g)
Sodium borate	$NaBO_2$	966	(1239)	135	(565)
Sodium cyanide	NaCN	562	(835)	89	(372)
Strontium oxide	SrO	2430	(2703)	161	(673)
Tantalum pentoxide	Ta_2O_5	1877	(2150)	109	(456)
Thorium dioxide	ThO_2	2592	(2865)	1102	(4612)
Titanium	Ti	1800	(2073)	104	(435)
Titanium dioxide	TiO_2	1825	(2098)	143	(598)
Titanium oxide	TiO	991	(1264)	219	(916)
Yttrium oxide	Y_2O_3	2227	(2500)	111	(464)
Zinc sulfide	ZnS	1745	(2018)	93	(389)
Zirconium oxide	ZrO_2	2715	(2988)	169	(707)
Hydrazine	N_2H_4	-2	(271)	95	(397)
Lithium hydride	LiH	686	(959)	1110	(4646)
Ammonium carbamate	$NH_2CO_2NH_4$	145	(418)	165	(690)
Ammonium hydrogen fluoride	NH_4HF_2	125	(398)	275	(1151)
Lithium aluminum fluoride	Li_3AlF_6	785	(1058)	147	(615)
Potassium aluminum fluoride	K_3AlF_6	1020	(1293)	173	(724)

Although the governing criterion for selecting the compounds listed in Table III has been a large heat of fusion per gram of material, it might be useful to consider one material that was found to have a larger heat of fusion than water on a volume basis. Gallium (Ref. 18) is such an element, melting at 84°F (307 K) with a heat of fusion of 19 cal/gm (80 J/g) having a solid density of 5.9 g/cm^3 and a liquid density of 6.1 g/cm^3. Taking an average density of 6 g/cm^3, gallium has a heat absorption capability of 114 cal/cm^3 (480 J/cm^3) which is a 43% improvement over ice on a volume basis. Further advantages of gallium are its low toxicity and its high thermal conductivity. Although heat absorption per unit weight of gallium is only one-fourth that of ice the volumetric improvement might permit advantageous trade-offs for certain applications, particularly where complex regeneration systems may lower the overall effectiveness of materials with a higher intrinsic heat of fusion per unit of weight. Although no further work in this direction was done under this program, such trade-off studies may prove profitable in the future.

A number of references concerning heat storage applications to solar energy (Refs 19-24) at higher temperatures were found, which report design features which might have some value in the design of lower temperature heat storage hardware. However, no use was made of these references in the present study and they are reported for completeness only.

Various methods for the estimation of heats of fusion were found (Refs. 25-35) with the method of Turkdogan and Pearson, (Ref. 35) described later, as the most useful.

Heat of Fusion of Pure Materials

Thermodynamic Consideration

The molar heat of fusion is related to the melting point and to the molar entropy of fusion (Ref. 36) through the expression:

$$\Delta H_f = T_f \Delta S_f$$

where T_f is the melting temperature in degrees absolute at one atmosphere pressure. Thus, a high molar heat of fusion may result from either a high melting temperature or a high molar entropy increase on melting. Since the melting temperatures of compounds to be considered in this study are restricted to the range of approximately 23 to 149°F (268 to 338 K), the candidates with the highest molar entropy of fusion will be expected to result in the highest molar heat of fusion.

The molar increase in entropy that occurs upon the melting of a solid is given by the Boltzmann expression (Ref. 37),

$$\Delta S_f = R \ln \frac{W_L}{W_S}$$

where W_L and W_S are the number of states possible in the liquid phase and in the solid phase respectively, and R is the gas constant. The entropy of the liquid phase is always greater than that of the solid phase because of the additional degrees of freedom or number of states that are possible. These additional states arise from four principal sources. First, the positional entropy increase is the result of the loss of long distance order that existed in the crystal. Second, additional modes of vibration and rotation may be possible in the liquid state and if these states do not also occur in the crystal, a large entropy increase can occur on melting. Third, the more varied orientation possible for large assymetric molecules in the liquid state can cause an entropy increase. Finally, for large linear molecules such as n-butane, the extra configurations possible in the liquid state that are not possible in the closely packed solid, will cause an entropy increase on melting. Thus a large molar entropy increase is likely to be associated with large, multi-atom molecules that have rigid, restricted solid structures. Since there is a weight consideration for space applications, a large entropy change per mole must be accompanied, for purposes of this study, by a low molecular weight in order to insure that the entropy change, and thus the heat absorbed, on a per gram basis will be large.

Prediction of Promising Compounds

The preceding considerations were used to formulate a list of compounds (Table VI) which might have high heats of fusion. In establishing this list, the first step was the tabulation of positive radicals shown in Table IV primarily from the first three periods of the Periodic Table. The only multi-atom radical in the list is NH_4^+. For this type of radical, the mean atomic weight is defined as the radical's molecular weight divided by the number of atoms in the radical. For single atom radicals, the mean atomic weight is identical to the radical's molecular weight.

A similar list (Table V) was made of negative radicals and their mean atomic weights were calculated. A listing was then made of compounds which could be formed from the positive and negative radicals with the lowest mean atomic weights (Table VI).

It is interesting to note that many compounds on this list are known to have large heats of fusion. These are water, ammonium carbamate, ammonia, lithium hydroxide, lithium hydride and hydrazine. There are other compounds on the list that have suitable melting points for which no heat of fusion data is available. These are lithium acetate, ammonium biacetate, and hydroxylamine. There are other compounds on the list for which melting point data are not available. The three compounds with suitable melting points all have estimated heats of fusion that are higher than ice.

Estimate of Heat of Fusion

The method of Turkdogan and Pearson (Ref. 35) allows the heat of fusion to be calculated from melting point, molecular weight and number of atoms present in the molecule. For this calculation, first ΔT is determined from:

$$\Delta T = T_f - 298$$

where T_f is the melting point in °K. Then, L_f/T_f is determined from a plot of L_f/T_f vs ΔT according to the following empirical list of data:

ΔT	L_f/T_f
0	1.9
300	2.5
700	3.0
1200	3.2

where L_f = cal/mean gram atom. The mean gram atomic weight is the molecular weight divided by the number of atoms. In Table VII the experimentally

TABLE IV

POSITIVE RADICALS

Radical	Name	# Atoms	Radical Molecular Weight	Mean Atomic Weight
Li^{+}	lithium	1	6.9	6.9
Na^{+}	sodium	1	23	23
NH_4^{+}	ammonium	5	18	3.6
H^{+}	hydrogen	1	1	1
Be^{++}	beryllium	1	9	9
B^{+++}	boron	1	10.8	10.8
C^{++++}	carbon	1	12	12
Mg^{++}	magnesium	1	24.3	24.3
Al^{+++}	aluminum	1	27	27
Si^{++++}	silicon	1	28	28
P^{++++}	phosphorous	1	31	31
S^{++++}	sulfur	1	32	32

TABLE V

NEGATIVE RADICALS

Radical	Name	# Atoms	Radical Molecular Weight	Mean Atomic Weight
$C_2H_3O_2^-$	acetate	7	59	8.4
$H(C_2H_3O_2)_2^-$	hydrogen acetate	15	119	7.9
Cl^-	chloride	1	35.5	35.5
$AsO_2^=$	arsenite	3	107	35.7
N_3^-	azide	3	42	14
$B_5O_8^-$	pentaborate	13	182	14
BO_3^-	peroxyborate	4	58.8	14.7
$B_4O_7^=$	tetraborate	11	155.2	14.1
BrO_3^-	bromate	4	128	32
Br^-	bromide	1	80	80
$NH_2CO_2^-$	carbamate	6	60	10
$CO_3^=$	carbonate	4	61	15.25
HCO_3^-	hydrogen carbonate	5	62	12.2
CLO_3^-	chlorate	4	83.5	20.9
CLO_4^-	perchlorate	5	99.5	19.9
$CrO_4^=$	chromate	5	116	23.2
$Cr_2O_7^=$	dichromate	9	216	24
$CrO_8^=$	peroxychromate	9	180	20
OCN^-	cyanate	3	42	14
CN^-	cyanide	2	26	13
BF_4^-	fluoborate	5	86.8	17.3
PF_6^-	fluophosphate	7	145	20.7
F^-	fluoride	1	19	19
HF_2^-	hydrogen fluoride	3	39	13
CHO_2^-	formate	4	45	11.25
NO_3^-	nitrate	4	62	15.5
NO_2^-	nitrite	3	46	15.3
$C_2O_4^=$	oxalate	6	88	14.7
$H_2P_2O_6^=$	hypophosphate	10	160	16
$AsO_4^=$	arsenate	5	139	27.8

TABLE V (continued)

Radical	Name	# Atoms	Radical Molecular Weight	Mean Atomic Weight
$HPO_4^=$	orthophosphate	6	96	16
$H_2PO_4^-$	orthophosphate	7	97	14
$H_2PO_2^-$	hypophosphite	6	65	13
$H_2PO_3^-$	orthophosphite	6	81	13.5
$NH_2SO_3^-$	sulfamate	7	98	12.6
$SO_4^=$	sulfate	5	96	19.2
HSO_4^-	bisulfate	6	97	16.2
$S_2O_8^=$	peroxydisulfate	10	192	19.2
$S^=$	sulfide	1	30	30
HS^-	hydrosulfide	2	31	15.5
$SO_3^=$	sulfite	4	78	19.5
HSO_3^-	bisulfite	5	79	15.8
SCN^-	thiocyanate	3	56	18.7
NH_2^-	amide	3	16	5.3
$B_2H_6^=$	diborane	8	27.6	3.5
$B_5H_9^=$	pentaborane	14	63	4.5
$BeF_4^=$	fluoberyllate	5	85	17
$SiF_6^=$	fluosilicate	7	142	20.3
H^-	hydride	1	1	1
$MnO_4^=$	manganate	5	119	24
$HC_2O_4^-$	hydrogenoxalate	7	89	12.7
$O^=$	oxide	1	16	16
AlH_4^-	Aluminum Hydride	5	31	6.2
OH^-	hydroxide	2	17	8.5
I^-	iodide	1	127	127

TABLE VI

COMPOUNDS WITH LOW MEAN ATOMIC WEIGHT

Compound	Name	Molecular Weight	# Atoms	Mean Atomic Weight	Melting Point		ΔH_f	
					°C	(K)	cal/gm	(J/g)
$HC_2H_3O_2$	Acetic acid	60	8	7.5	16	(290)	45	(187)
$LiC_2H_3O_2$	Lithium acetate	66	8	8.3	70	(343)	82 Est	(343)
$NH_4C_2H_3O_2$	Ammonium acetate	77	12	6.4	114	(387)		
$Be(C_2H_3O_2)$	Beryllium acetate	127	15	8.5	300	(573)		
$LiH(C_2H_3O_2)_2$	Lithium bi-acetate	127	16	7.9				
$NH_4H(C_2H_3O_2)_2$	Ammonium bi-acetate	137	22	6.2	66	(339)	107 Est	(448)
$Be(H[C_2H_3O_2]_2)_3$	Beryllium bi-acetate	366	46	8.0				
$LiNH_2CO_2$	Lithium carbamate	67	7	9.6				
$NH_4NH_2CO_2$	Ammonium carbamate	78	7	11.1	145	(418)	165	(690)
$Be(NH_2CO)_2$	Beryllium carbamate	129	3	9.9				
H_2O	Water	18	3	6	0	(273)	80	(333)
LiOH	Lithium hydroxide	24	3	8	421	(694)	208	(871)
NH_3	Ammonia	17	4	4.3	-78	(195)	108	(452)
$Be(OH)_2$	Beryllium hydroxide	43	5	8.6	decomposes			
$LiNH_2$	Lithium amide	23	4	5.8	380	(653)		
$Be(NH_2)_2$	Beryllium amide	41	7	5.9				
LiH	Lithium hydride	8	2	4	686	(959)	1110	(4650)
BeH_2	Beryllium hydride	11	3	3.7	125	(398)		
N_2H_4	Hydrazine	32	6	5.3	-2	(271)	95	(398)
Li	Lithium	6.9	1	6.9	179	(452)	158	(662)
NH_2OH	Hydroxylamine	33	5	6.6	33	(306)	88 Est	(368)

TABLE VII

COMPARISON OF EXPERIMENTAL AND CALCULATED
VALUES OF THE HEAT OF FUSION OF SELECTED COMPOUNDS

Compound	T_f K	ΔT	L_f/T_f	L_f cal/gm Atom	Mole Wt # Atoms	ΔH_f Calc Cal/gm	Calc (J/g)	Exp. Cal/gm	Exp. (J/g)
LiOH	694	446	2.5	1730	8	216	(904)	208	(871)
LiF	1121	873	3.0	3370	13	259	(1084)	240	(1003)
LiH	959	711	3.0	2050	4	720	(3010)	1110	(4650)
$NH_2CO_2NH_4$	418	170	2.3	962	7.1	136	(569)	165	(691)
NH_4HF_2	398	150	2.26	835	7.1	126	(528)	275	(1150)
N_2H_4	271	-27	1.9	520	5.3	98	(410)	95	(376)
H_2O	273	-25	1.9	518	6	86.3	(362)	79	(331)

determined values for heats of fusion of selected compounds are compared with values calculated by the method of Turkdogan and Pearson.

Although the inaccuracy of the method for estimating heats of fusion in this set of comparisons ranges from 4% to about 54%, it should be noted that those cases for which the theory predicts too high a value for the heat of fusion are in error by less than 10% while the large errors occur in underestimating the value of heat of fusion. It would thus appear that use of this estimating technique will in general give a reasonably accurate or conservative result. This method was therefore used to estimate the heats of fusion of lithium acetate, ammonium biacetate and hydroxylamine as listed in Table VI. The estimated heats of fusion for each of these compounds is somewhat higher than that of ice.

Supplementary Compound Selection

The preceding paragraphs have emphasized the desirability for searching the literature especially for compounds with low mean atomic weights and this activity has constituted the major portion of its search. In addition, compounds that were known to melt in the proper range were screened for high heat of fusion that might occur due to unforeseen anomalous effects. Those compounds for which no heat of fusion data were available are listed in Table VIII, inspite of their relatively high mean atomic weights. Measurement of heat of fusion of such compounds would be desirable.

TABLE VIII

SELECTED COMPOUNDS MELTING IN THE HEAT SINK TEMPERATURE RANGE

Compound	Molecular Weight	#Atom	Mean Atomic Weight	Melting Point °C	Melting Point (K)
N_2S_5	188	7	27	10	(283)
$POCl_2Br$	198	5	39.6	13	(286)
$POClBr_2$	242.5	5	48.5	30	(303)
PI_3	412	4	103	61.5	(334.5)
$PSBr_3$	303	5	60.6	38	(311)

Eutectic Mixtures

A eutectic mixture acts as pure(or single) material in that it has a well defined melting point and its freezing and melting temperatures are the same. Table IX contains a list of mixtures that form eutectics with melting points in the proper temperature range for this study. Since some of the pure components in this list have large heats of fusion but do not have suitable melting temperature, the formation of a eutectic melting in the desired range could result in a material having both a large heat absorbing capacity and a satisfactory melting temperature.

In addition to the mixtures shown in Table IX the thermodynamics of two other systems appears promising. The eutectic mixtures possible in one of these - the ammonium fluoride system - are indicated in Table X.

Ammonium bifluoride is a white translucent solid available at about $1/lb as white flakes. It is used in industy for metal pickling and cleaning, glass frosting, oil well acidizing, building cleaning, and removal of iron stains from textiles. This compound has a heat of fusion over three times that of ice (Ref. 38) but its melting point is outside the target temperature range. However, some of the eutectic mixtures shown do have suitable melting points, and perhaps they retain a high heat of fusion also.

The compound ammonium carbamate ($NH_2CO_2NH_4$), melting at 145°C (418 K), has a heat of fusion of 165 cal/gm (690 J/g) (Ref. 39). This compound may form eutectic mixtures with water or ammonia that have suitable melting points, although the literature search has failed to discover them.

TABLE IX

MOLTEN SALT EUTECTIC MIXTURES WITH LOW MELTING POINTS

Salt System	Melting Point	
	°C	(K)
$SnBr_4$-SnI_4	19.4	(292)
$AlBr_3$-$SnBr_4$	20	(293)
$AsBr_3$-PBr_5	23.5	(296.5)
$AlBr_3$-$AsBr_3$	25.5	(298.5)
$SbBr_3$-$SnBr_4$	27	(300)
$Ca(NO_3)_2$-$Na(NO_3)$-NH_4NO_3	42	(315)
$Ca(NO_3)_2$-NH_4NO_3	44	(317)
$LiNO_3$-$N_2H_4 \cdot HNO_3$	25	(298)
$LiNO_3$-$AgNO_3$-NH_4NO_3	52	(325)
$GaCl_3$-NH_4Cl	58	(331)

TABLE X

MELTING POINTS AND HEATS OF
FUSION FOR THE AMMONIUM FLUORIDE SYSTEM

Eutectic	Melting Point °C	Melting Point (K)	ΔH_f Cal/gm	ΔH_f (J/g)	Density g/cm^3
NH_4F	230	(503)			
NH_4F-NH_4HF_2	109	(383)			
NH_4HF_2	125	(398)	275	(1150)	1.5
NH_4HF_2-$NH_4H_3F_4$	-6	(267)			
$NH_4H_3F_4$	23	(296)	49	(205)	
$NH_4H_3F_4$-$NH_4H_5F_6$	-14	(259)			
$NH_4H_5F_6$	-8	(265)			

Systems Combining Heat of Fusion and Heat of Solution

Some solids dissolve in water with the absorption of large amounts of heat. Table XI shows those salts with known values for heat of solution above 71.7 cal/gm (300 J/g). In this case, as in the fusion process, entropy is increased because of the destruction of the ordered arrangement of molecules in the solid state, and the formation of new arrangements having a greater degree of randomness than the original. The dissolution of the solid requires that the lattice energy be overcome, as it is in fusion with thermal energy. This energy is supplied by the solvent through solute-solvent interactions. The formation of these solute-solvent structures is an ordering process and therefore results in the evolution of heat. The relative magnitude of the randomization of the solid molecules by dispersion and the ordering by solvation will determine if the overall process will absorb or release heat. In addition, the order that exists in the solvent is disrupted by the addition of solute and this contributes an endothermic effect to the total.

The magnitude of these effects depends in a complex manner upon the size of the solute particles and their charge, as well as the degree of order that existed in the solid. Hydrated salts, compared to their anhydrous counterparts always have a large endothermic heat of solution due to the elimination of entropy decreasing solvent ordering. A procedure for obtaining a large heat absorption from a salt-water system could involve the melting of water at 32°F (273 K), followed by dissolving the salt in the water to obtain added heat absorption from the heat of solution. The regeneration of these salt-water mixtures may be accomplished by nothing more complicated than a slow cooling to precipitate out the salt-hydrate, then further cooling to freeze the water. The regeneration step when carried out under zero gravity conditions may result in a more uniform, dispersed mixture of hydrate and ice and therefore a more uniform and reproducible heat absorption capacity.

Table XI shows that only a few compounds are known to have a heat of solution greater than the heat of fusion of water, 80 cal/gm (333 J/g). It is necessary to exceed this value, since otherwise the salt could simply be replaced by more water to obtain the same absorption capacity. The salt must also have a high solubility in water in order to use as little water as possible, and not diminish the overall effect of the large heat of solution. The table shows that potassium thiocyanate has the largest heat of solution, and a very large solubility in water. This compound is soluble in water to the extent of 1 mole of solute (97 g) to 3 moles of water (54 g). The heat of solution is 126 cal/gm (528 J/g) of solute. However, if the weight of water needed is considered then it is 81 cal/gm (339 J/g) of water-salt mixture.

TABLE XI

COMPOUNDS WITH HEATS OF SOLUTION
APPROXIMATING THE HEAT OF FUSION OF WATER

Name	Formula	ΔH		Solubility at 32°F (273 K) gm/100 ml ($g/100\mu m^3$) H_2O
		Cal/gm	(J/g)	
ammonium acid carbonate	NH_4HCO_3	84.6	(354)	11.9
ammonium chloride	NH_4Cl	76.5	(320)	29.7
ammonium cyanide	NH_4CN	98.7	(413)	
ammonium nitrate	NH_4NO_3	79.1	(331)	118.3
ammonium nitrite	NH_4NO_2	74.3	(311)	
ammonium oxalate hydrate	$(NH_4)_2C_2O_4 \cdot H_2O$	81.0	(339)	
ammonium thiocyanate	NH_4CNS	74.6	(312)	128
boric acid	H_3BO_3	87.5	(366)	1.95
potassium chlorate	$KClO_3$	83.7	(350)	7.1
potassium acid fluoride	KHF_2	76.5	(320)	41 (21°F)
potassium nitrate	KNO_3	83.9	(351)	13.3
potassium acid oxalate	KHC_2O_4	74.8	(313)	2.5
potassium tetraoxalate	$KHC_2O_4 \cdot H_2C_2O_4$	72.4	(303)	1.8 (13°F)
potassium thiocyanate	KCNS	126	(528)	177.2
rubidium thiocyanate	RbCNS	100	(419)	
sodium cyanate	NaCNO	72.9	(305)	
sodium cyanide hydrate	$NaCN \cdot 2H_2O$	90.3	(378)	
sodium acid oxalate hydrate	$NaHC_2O_4 \cdot H_2O$	73.6	(308)	1.7

The heat of fusion allows ice to adsorb 80 cal/gm (333 J/g) of ice or 28.5 cal/gm (119 J/g) of ice-salt mixture. This brings the total to 109.5 cal/gm (458 J/g) of ice salt mixture which is a 30% improvement over the use of ice alone. Thus, a powdered salt and ice mixture is placed in the heat exchange vessel, the ice melting and absorbing heat, then the salt dissolving in the water to absorb more heat.

It is well known (Ref. 36) that the heat of solution is concentration-dependent, and the values given in the literature for potassium thiocyanate and other salts are for the infinite dilution case. The heat of solution is measured at several successively smaller concentrations until the heat of solution per gram of solute no longer changes with concentration. This value is taken as the heat of solution at infinite dilution, and is very useful for theoretical comparisons of salts in a single solvent, since it contains no perturbations due to solute-solute interactions. However, for heat sink applications, concentrations of salt near the saturation point must be used to gain maximum advantage from the process. Therefore, if KCNS, for example, is added to water to make a saturated solution, the first salt added absorbs an amount of heat essentially equal to that for the solute dissolving in pure water, whereas the last KCNS is added to a solution that is highly concentrated. It is impossible to predict how much smaller the total heat of solution will be because the concentration at which solute-solute interactions begin to be important cannot be predicted. There will be a concentration before the saturation point is reached at which further additions of solute will no longer be justified due to the decreased heat of solution. The data necessary to make the various trade-offs are accessible only by experiment.

Solid-Solid Transitions

These transitions typically are not associated with large entropy changes, and therefore do not have large heat absorbing capability. The increase in degrees of freedom from one solid form to another, does not have the same potential for large effects as does the transition from solid to liquid. The Bureau of Standards Table in Circular 500 lists 18 solid-solid transitions in the temperature range from 230°F (268 K) to 149°F (333 K). These have heats of transition ranging from 0.5 cal/gm (2.1 J/g) to 43.5 cal/gm (182 J/g) and pressures up to 5×10^6 mm Hg (667 MN/m^2) are necessary.

Solid-solid transitions are important only in that some solids undergo premelting transitions where some entropy changes take place before the solid undergoes fusion.

The solids with transitions close to their melting points were checked for high combination transition-fusion heat absorption and none were found.

Conclusions

The results of a literature search for a material or process with a heat absorption capability greater than ice, 80 cal/gm (333 J/g), lead to the following conclusions:

1. There is no data reported in the available literature that defines a suitable candidate thermal storage material which offers a substantial improvement over ice in heat absorption capability per unit weight in the temperature range 23 to 149°F (268 to 338 K).

2. There are several pure materials, and several eutectic mixtures melting in the proper range, that offer promise of higher heat absorption capability than water-ice but for which no data is currently available.

3. A combination of two heat absorption processes, the melting of water-ice, followed by dissolving a salt in water, may be able to supply a heat absorption 30% greater per unit weight than that obtained from the use of water-ice alone.

There appear to be no other phase changes or processes described in the available literature which will equal or even approach the heat absorption currently available from heat of fusion in the temperature and pressure ranges of interest.

In the following section the heat of fusion has been experimentally determined for certain compounds that appear to offer a good possibility of having substantially higher values than water-ice.

The heat absorbing capability of a combination of two heat absorbing processes - heat of fusion of water-ice followed by heat of solution of salt in water, and methods for the regeneration of the water-salt mixture to achieve ice-salt separation are investigated.

EXPERIMENTAL INVESTIGATION

Introduction

The analytical portion of the study, comprising a canvass of eight major sets of abstracts of chemical literature plus three major sources of data for heats of fusion of chemical compounds, did not reveal any compounds that would simultaneously meet all of the acceptance criteria targeted for an improved thermal storage material. The survey did, however, reveal certain areas where acquisition of experimental information which was not available might provide a way to significantly increase the present heat storage capability. One of these areas was the use of the heat absorption available from dissolution of salts in melting water-ice. The study revealed that an extremely soluble salt capable of dissolving in water with a heat absorption greater than 80 cal/gm (333 J/g), the value for the heat of fusion of water-ice, would upgrade the heat sink absorption capability. For example, a salt with a heat of solution of 120 cal/gm (500 J/g) that dissolved to the extent of 100g of salt to 100g of water would result in 25 percent more heat absorption over the use of an equivalent amount of water-ice. It was expected from the literature search of the previous portion that there were salts which fit the dual criteria of high heat of solution and high solubility.

In addition to the combined heat of fustion-heat of solution absorption process of a salt and water-ice, an investigation was undertaken to explore the possibility of using fused salt eutectic mixtures that melt in or near the temperature range -5 to 65°C (268 to 338K). Also, compounds that seemed to satisfy certain common characteristics of materials with high heats of fusion -- that is, low molecular weight, high number of atoms and rigid solid structure -- were investigated.

Experimental Methods

Two experimental techniques for measuring heat absorption were used in this study. First, a Beckman Model DSC-1 differential scanning cal rimeter was used for measurements of the heat of fusion of single compounds and eutectics. Second, a Paar rotating bomb calorimeter was used for the measurement of heat of solution and regeneration experiments. This section describes the operation of these instruments and the procedures used to obtain the data in the following sections. It was the intent throughout this work to adhere to the techniques required to achieve a level of accuracy necessary to determine if the heat absorption of the compound or process was significantly greater than that of water-ice. Emphasis was placed on verification of concepts, evaluation of a larger number of candidate materials, and identification of most promising candidate materials for development and application rather than an achievement of high precision in measurement for a small number of materials.

The Beckman Differential Scanning Calorimeter

The operation of the Differential Scanning Calorimeter (DSC) is based on the temperature control of two miniature sample holders, one for the sample and one for a reference located in the sample holder assembly (see Fig. 49). The system consists of two separate control loops, the first for average temperature control and the second for differential temperature control. In the average temperature loop the electronic programmer provides an electrical signal proportional to the temperature desired. This signal is compared to the average signal from platinum resistance thermometers permanently embedded in the sample and reference holders. When this feedback signal calls for heat, both reference and sample holder are brought up to the proper temperature together.

In the differential temperature control loop, signals representing the sample and reference temperatures measured by platinum resistance thermometers are fed to a circuit which determines whether the reference or sample temperature is greater. This error signal will cause a heater output sufficient to equalize the temperature of sample and reference. A signal relating the difference in heater power between sample and reference is fed to a recorder. The integral of the resulting signal is the internal energy change, and the direction of the signal indicates whether the process occurring in the sample chamber is endothermic or exothermic.

For the series of runs whose results are reported here, a standard composed of 5.81 mg of Indium metal was run in the sample holder while the reference holder was empty. The resulting endothermic peak occurring at 152°C (425K) was integrated by tracing the peak and weighing the tracing paper.

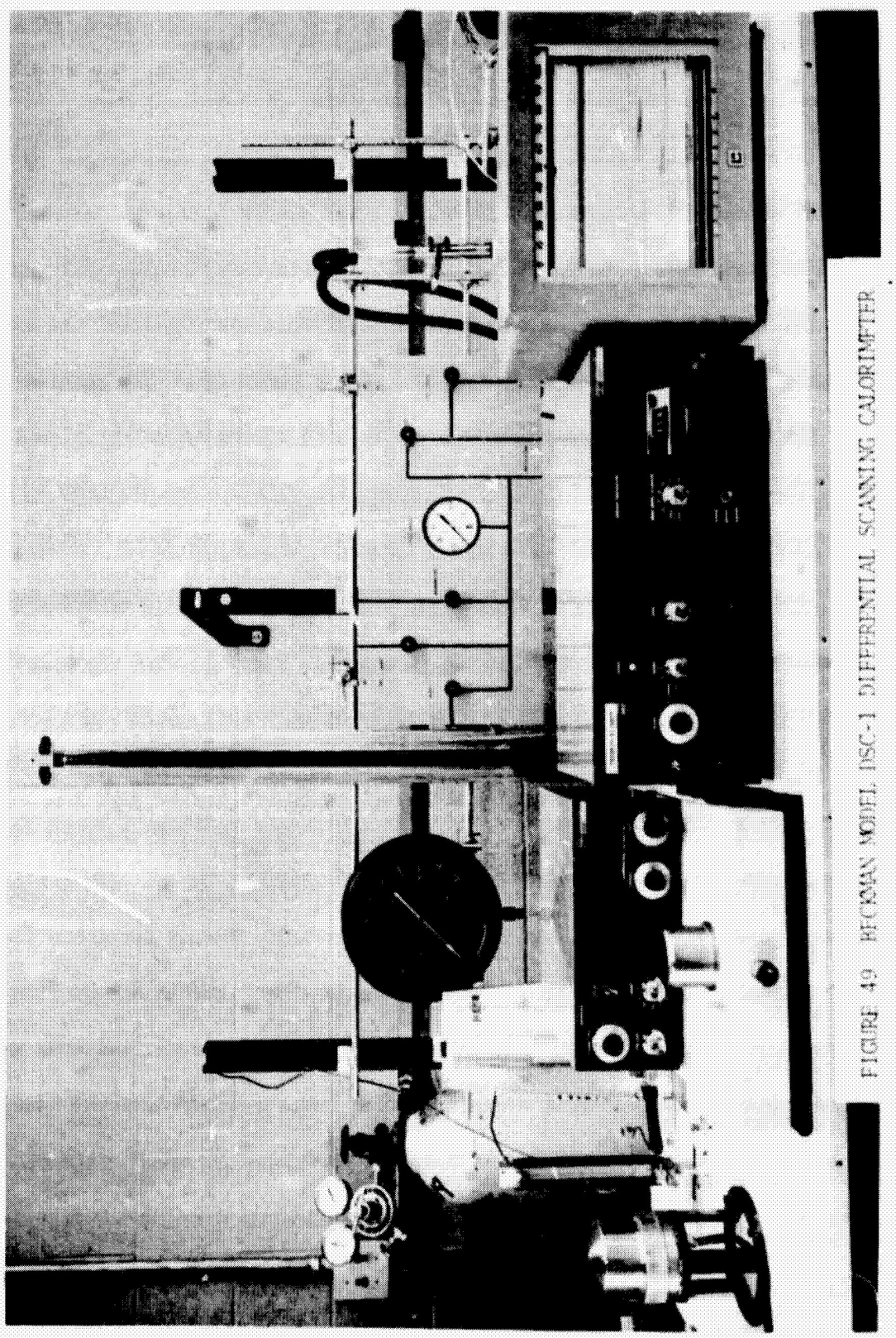

FIGURE 49 BECKMAN MODEL 1SC-1 DIFFERENTIAL SCANNING CALORIMETER

This calibration procedure was repeated each day the DSC was run. The samples were run as the standard was, with the reference pan empty, at a temperature scan rate of 10K/minute. Each run was repeated at least once, and five samples of each material were prepared. Therefore, each heat of fusion is the result of at least ten determinations.

For those samples whose melting points were close to room temperature, a dewar attachment allowing the cooling of the sample holder to below ambient temperatures was used. The dewar filled with liquid nitrogen enabled runs to start at about 30K below the expected melting point.

The eutectic samples were made up in a dry box since many of the components are hygroscopic. The sample containers and covers are made of aluminum and were weighed before being placed in the dry box. After the samples were placed in the containers they were sealed with a crimping device and removed from the dry box for weighing. The samples used varied in weight from 5 to 40 mg. Materials that are not hygroscopic were prepared in a fume hood.

The Rotating Bomb Calorimeter

The apparatus consists of a stainless steel, platinum lined combustion bomb, calorimeter, thermometric system, power input measuring system and liquid nitrogen cooling system. The calorimeter schematic is shown in Fig. 50 and a photograph of the apparatus is shown in Fig. 51. The bomb may be rotated inside the calorimeter and thus is suited to measurements of heats of solution and mixing. The bomb has an internal volume of 331.8 ml (Paar Instrument Co. Catalogue No. 1004), teflon head gasket and valve packing and a Kel-F valve seat. In the present work the valves were kept closed during all measurements. All internal parts of the bomb are plated with 10% iridium-platinum. A platinum crucible containing the sample salt was mounted in an offset gimbal so that the bomb can be set at a 45° angle for filling. About 35 grams of salt can be accommodated in the crucible. The calorimeter can surrounding the bomb contained about 2 liters of a 50-50 by volume methyl alcohol-water mixture that freezes at -100°C (173K). During operation the bomb was completely immersed in this liquid which was kept at a known level for all runs by weighing the calorimeter can and contents before each run on a 5 kg capacity Seko 140 series balance. The calorimeter can also contains a stirrer, rotating mechanism, platinum resistance thermometer, and a 75 watt heater. The stirrer is operated at a constant 450 rpm using a belt drive from a synchronous motor. The rotation mechanism operates from a synchronous motor through a drive gear at a constant 10 rpm.

The thermometric system includes a platinum resistance thermometer of the flat calorimetric type (Leeds & Northrup type 8160B), a G-2 Mueller bridge (Leeds & Northrup type 8069B), and a high sensitivity galvonometer (Leeds &

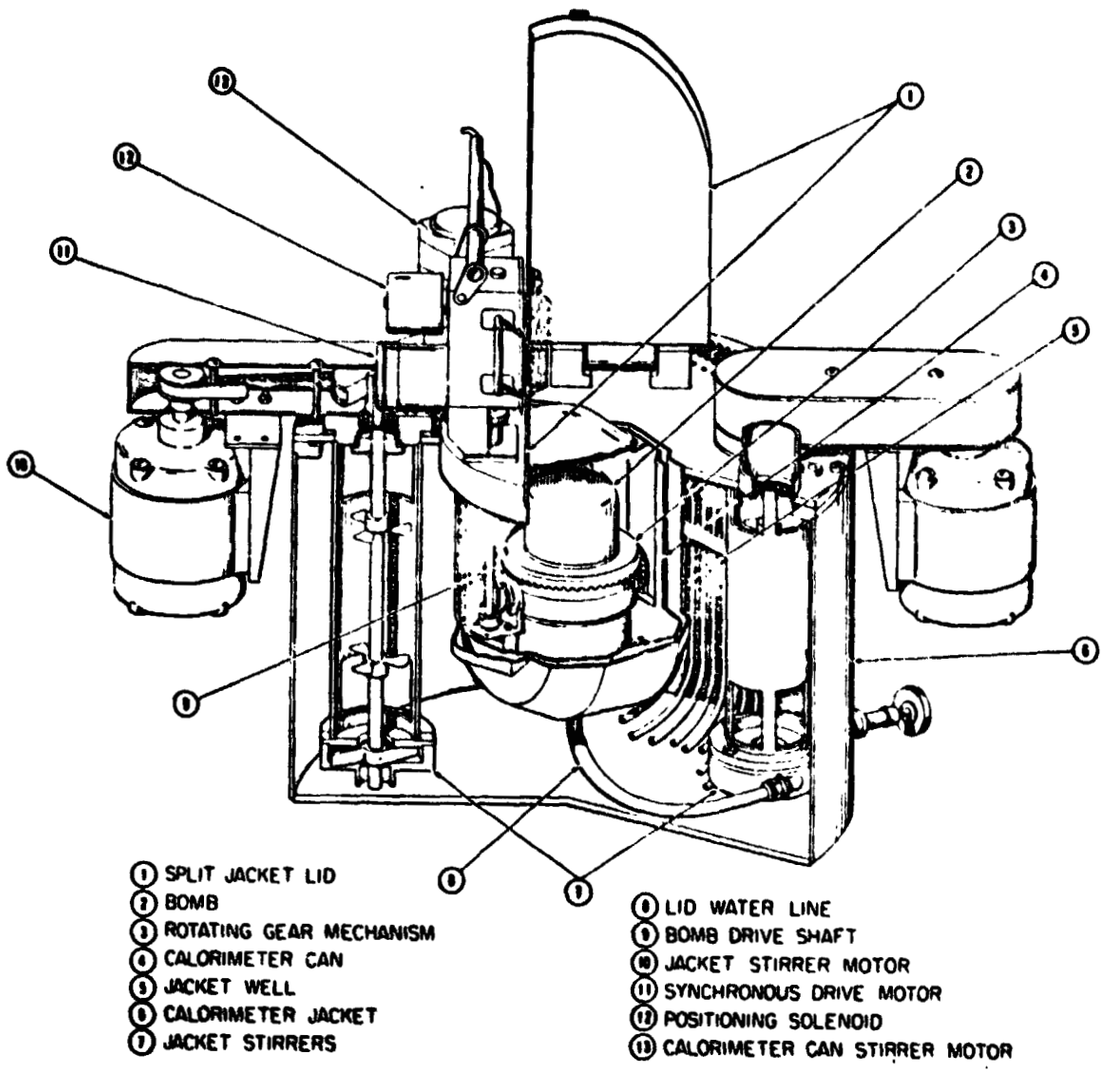

FIGURE 50 SCHEMATIC OF ROTATING BOMB CALORIMETER

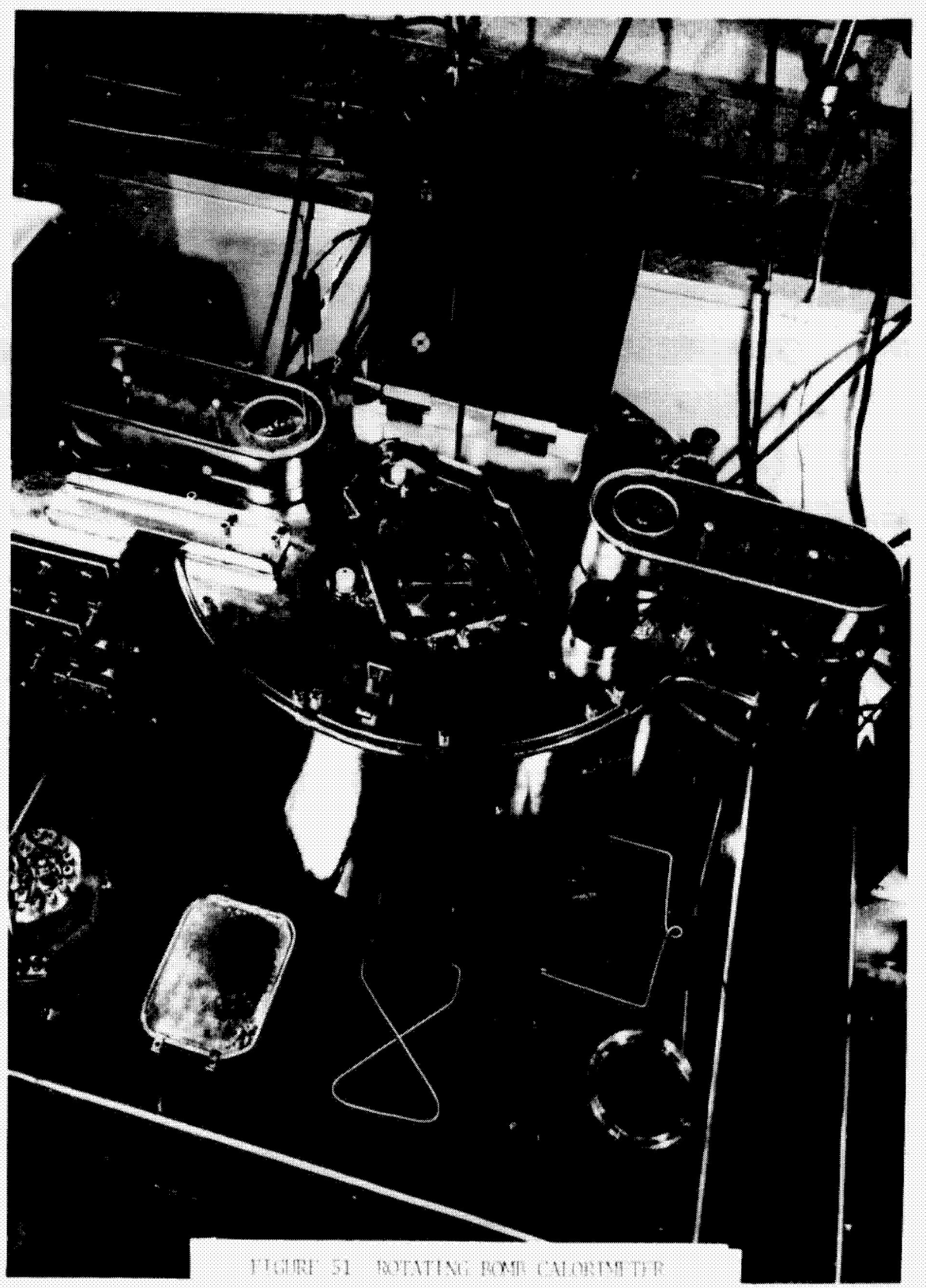

FIGURE 51 ROTATING BOMB CALORIMETER

Northrup type HS2284d). The galvonometer is mounted on a Julius suspension and the light beam is projected vertically over a path of two meters. The thermometer was certified by L&N in April 1974 and the bridge was certified in 1962. Both the thermometer and bridge are periodically checked using a triple point cell and standard resistor. The sensitivity of this system is .001K/mm of galvonometer movement.

The calorimeter can is surrounded by a jacket containing 10 gallons ($3.785 \times 10^{-2} M^3$) of fluid that completely enclosed it on all sides (see Fig. 50). A 50% by volume methyl alcohol-water mixture was used in this jacket in such a way as to minimize the heat flow to or from the calorimeter can. By adjusting the jacket fluid temperature to within 1K of the calorimeter can temperature, the calorimeter was effectively under adiabatic conditions. A liquid nitrogen cooling system permitted operation at jacket temperatures below 0°C. This system consisted of a 50 liter dewar, a high pressure nitrogen bottle to pressurize the system, insulated polyflow tubing and a copper tube suspended near the bottom of the jacket fluid. By forcing LN_2 through this system it was possible to reduce the jacket temperature from 20°C (293K) to -15°C (258K) in one hour. After the run had begun the jacket temperature was regulated manually by short bursts of LN_2 or by activation of heaters located within the jacket fluid.

The temperature of the calorimeter fluid in the can was lowered to the starting temperature for a run by the use of dry ice lumps, about one pound being sufficient to lower the temperature of the calorimeter fluid to -15°C (258K). The temperature of the filled bomb was lowered by placing the bomb itself in a styrofoam chest surrounded by dry ice. The bomb was then placed in the calorimeter and allowed to come to temperature equilibrium with it. If this temperature was satisfactory for the run desired, then the jacket temperature was adjusted to within one degree of the temperature of the calorimeter can whose value was monitored every two minutes as the run proceeded.

A cartridge heater immersed in the calorimeter fluid was used to raise the temperature of the bomb, its contents and the calorimeter can and fluid to a temperature above that of the melting point of the water-ice or salt-ice mixture used in the bomb. The amount of electrical energy in watts applied to the calorimeter was monitored with the use of a Weston wattmeter Model 432. The energy balance is:

$$\text{Electrical Energy in (J)} = \Delta T \, (C_{cal} + C_{bomb} + C_{fluid}) + \text{heat absorbed} \quad (1)$$

where C_{cal}, C_{bomb}, and C_{fluid} represents the heat capacity of the calorimeter can, the bomb and its contents, and the calorimeter fluid respectively, in J/K and ΔT is the temperature rise of the calorimeter. When the electrical energy applied to the calorimeter is not equal to the temperature rise term,

then the difference represents a heat absorption process that is occurring in the bomb.

Calibration and Checkout of Bomb Calorimeter Technique

In order to test the validity of equation (1) the experiments whose results are reported in Table XII were carried out. In these experiments there was no heat absorption process occurring in the bomb and consequently the electrical energy input should have been exactly equal to the temperature rise term. For convenience of notation, the temperature rise term, ΔT ($C_{cal} + C_{bomb} + C_{fluid}$) has been designated "Energy out" .

TABLE XII

HEAT BALANCE TESTS ON ROTATING BOMB CALORIMETER

Run #	Electrical Energy In Joules	ΔT K	C_{TOTAL} J/K	Energy Out Joules	% Difference
1	108,000	7.60	14,340	108,983	.9
2	72,000	5.15	14,342	73,861	2.6
3	108,000	9.00	11,829	106,462	1.4
4	72,000	5.95	11,822	70,340	1.5
5	108,000	9.50	11,758	111,700	3.4
6	72,000	6.15	11,764	72,350	.5

In runs 1-6 shown in Table XII, the bomb contained 100g of water and the temperature was varied from about +5°C (278K) to +15°C (288K). Equation (1) was used to calculate the energy output from the specific heat capacity of the calorimeter can, C_{cal}, the bomb, C_{bomb} and the calorimeter fluid, C_{fluid}. Thus, the C_{TOTAL} in Table I was calculated from:

$$C_{TOTAL} = C_{cal} \cdot W_{cal} + C_{bomb} \cdot W_{bomb} + C_{fluid} \cdot W_{fluid} \qquad (2)$$

where W_{can}, W_{bomb} and W_{fluid} are the weights of the calorimeter can, bomb, and fluid, respectively. Water was used as the calorimeter fluid in runs 1 and 2 and in runs 3-6 a 50-50 by volume mixture of methanol and water was used. This difference accounts for the change in C_{TOTAL} after the second run. The average difference between the electrical energy input and the energy output as measured by the temperature rise was 1.6%.

The heat of solution measurements described in the next section were made in the same way as were the experiments leading to the results of Table XII. Rotation was started to mix the salt and water after a stable temperature

had been reached. During the dissolution, the temperature of the calorimeter dropped by a few tenths of a degree. When the temperature was again stabilized the heater in the calorimeter was turned on for 60 seconds at 60 watts to inject 3600 Joules of energy. The temperature rise caused by this energy served to calibrate each run and was fairly sensitive to the amount of calorimeter fluid present. The figure calculated from the heat capacity of the calorimeter and the amount of calorimeter fluid used in the heat of solution runs was 12,150 Joules/K.

At this point in the experimental program several runs were made using 100 ml of water in the bomb and starting at sub-freezing temperatures in order to determine the heat of fusion of water-ice as a calibration check on the calorimeter procedure. The results of these tests are shown in Table XIII.

The electrical input from the cartridge heater ranged from 30 to 60 watts, with on-times from 60 to 100 minutes. The temperature changes ranged from about 6 degrees to almost 19 degrees. The average value obtained for the heat of fusion is 78.7 cal/gm (329 J/g) which is 1.3% below the literature value of 79.8 cal/gm (333.5 J/g). The standard deviation of these runs is 3.8 cal/gm (15 J/g). The largest uncertainty in evaluating the heat of fusion is in the determination of C_{TOTAL} which is defined as:

$$C_{TOTAL} = C_{bomb} + C_{calorimeter} + C_{fluid} \qquad (3)$$

The first two terms on the right in (3) are invariant and since the bomb and calorimeter are nearly all stainless steel and their combined weight is 7,976g, the total heat capacity for bomb and calorimeter can be calculated. Using a c_p (specific heat capacity at constant pressure) of 445 J/kg-K (Ref. 40).

$$C_{bomb} + C_{calorimeter} = 3549 \text{ J/K} \qquad (4)$$

In the runs of Table XIII, the bomb contained 100g of water at 4,180 J/kg-K for a total of 418 J/K which must be added to the value from Eq. (4) to give a total of 3967 J/K. The third term C_{fluid} is very sensitive to the amount of alcohol-water mixture in the calorimeter can. Those runs that exhibited a C_{TOTAL} that was low, were run with less calorimeter fluid than those showing a high C_{TOTAL}. The average amount of fluid used was 2245 cm^3, and this varied by about -125 to +400 cm^3. The C_{TOTAL} calculated from c_p for the alcohol-water mixture of 3550 J/kg-K is 11,500 J/K, when 2122 gms of fluid is used.

The experimental determination of C_{TOTAL} was made in two ways. First the initial slope of a plot of electrical energy input versus temperature rise was determined. Secondly, at the end of the run, when it was certain that no more phase changes would be taking place, a known small amount of electrical energy was injected and the subsequent temperature rise measured from the

difference between the equilibrium temperatures before and after the heater was activated. Both of these methods gave C_{TOTAL} ranging from 10,500 J/K to 13,000 J/K, depending on how much calorimeter fluid was present.

TABLE XIII

HEAT OF FUSION OF WATER-ICE

Run #	Electrical Energy In Joules	ΔT K	C_{TOTAL} J/K	Energy Out Joules	ΔH_{H_2O} Cal/gm	(J/g)
1	108,720	6.85	11,060	75,761	78.8	(330)
2	108,000	6.70	11,060	74,102	81.1	(339)
3	108,360	6.80	11,060	75,208	79.3	(332)
4	158,400	9.70	12,900	125,712	78.2	(327)
5	115,200	6.23	12,900	80,367	83.3	(348)
6	172,800	10.89	12,900	140,481	77.3	(323)
7	233,179	17.189	11,500	197,674	84.9	(355)
8	220,884	16.494	11,500	189,681	74.6	(312)
9	246,015	18.608	11,500	213,992	76.6	(320)
10	220,020	16.260	11,500	186,990	78.9	(330)
11	220,158	16.249	11,500	186,864	79.7	(333)
12	212,552	15.926	11,500	183,149	70.3	(294)
13	235,179	17.590	11,500	202,285	78.7	(329)

Measurements of Heats of Fusion

Heats of Fusion for Selected Compounds

The compounds for which heats of fusion were measured as part of this program are listed in Table XIV. This list was supplemented by selection of additional compounds known to melt in the proper range for space suit applications since on occasion anomolous effects have resulted in occurrence of unexpectedly large heats of fusion. All of the heats of fusion reported in Table XIV are the average of at least four runs.

TABLE XIV

HEAT OF FUSION OF SELECTED COMPOUNDS

Compound	Melting Point (literature) °C	(K)	Molecular Weight/ # of Atoms	ΔH_f Cal/gm	(J/g)
heptadecanol	54	(327)	4.7	60	(250)
octadecyl acetate	29	(302)	5.0	38	(159)
acetophenone	19	(292)	7.1	32	(134)
1-Naphthyl acetate	44	(317)	7.8	28	(117)
trimethyl pentandiol	46	(319)	5.2	45	(188)
trilaurin	45	(318)	5.4	56	(234)
dicyclohexyl adipate	34	(307)	6.0	36	(150)
benzofuroxan	69	(342)	9.1	30.4	(127)
benzhydrol	67	(340)	7.1	30.6	(128)
arachidic acid	74	(347)	5.0	57.9	(242)
didecyl sebacate	28	(301)	5.2	35.8	(150)
adiponitrile	1	(274)	6.8	44.8	(187)
dibutyl tartrate	18	(291)	6.6	2.7	(11)
bix-2 ethoxy ethyl sebacate	-2	(271)	6.0	31.5	(132)
didodecylamine	44	(317)	4.2	52.7	(220)
bicyclohexyl	3	(276)	4.8	21.6	(90)
butyl carbamate	53	(326)	6.2	45.9	(192)
2 amino 2 methoxy propanol			5.8	27.3	(114)
3 amino 1 propanol	10	(283)	5.4	50.1	(209)
1 amino 2 propanol	-2	(271)	5.4	28.4	(119)
pentamethyl benzene			5.5	5.12	(21)
tert butyl isothiocyanate	8	(281)	7.2	31.2	(130)
2,4-di-tert-pentylphenol	25	(298)		24	(102)
2,5-dimethoxytoluene	19	(292)	6.6	17	(71)
α,α-dimethylbenzyl alcohol	19	(292)	6.2	23	(95)
α,α-dimethylphenethyl alcohol	22	(295)	6.0	14	(56)
diacetyl	-6	(267)	7.2	28	(117)
dimethyl adipate	9	(282)	6.7	52	(216)
piperazine hydrate	42	(315)	8.8	64	(268)
1-tetradecanol	35	(308)	4.8	45	(189)
pivalic acid	32	(305)	6.0	36	(148)
1-pentadecanol	41	(314)	4.8	66	(275)
1-phenoxy-2-propanol	13	(286)	6.6	10	(42)
1,4-butanediol	15	(288)	5.6	43	(181)
lithium acetate	70	(343)	8.3	67	(278)
ammonium bifluoride	126	(399)	7.1	73	(306)
lithium biacetate			7.9	32	(135)

The compounds tested exhibited heats of fusion ranging from ~ 3 cal/gm (11 J/g) to 73 cal/gm (306 J/g), compared to the values for water-ice of 79.8 cal/gm (333.5 J/g). The table also includes the value of the molecular weight divided by the number of atoms for each compound. The compounds for which this value is low, between 4.2 and 5.4, exhibited an average heat of fusion of 46 cal/gm (192 J/g) and those compounds for which this value is high, between 6.0 and 9.1, exhibited an average heat of fusion of 29 cal/gm (121 J/g). The standard deviation for each of these means is 13 cal/gm (54 J/g) and a "t" statistical test shows that, at the 99 percent confidence level, the two means are different. Although compounds that have low molecular weight and larger numbers of atoms do have higher specific heats of fusion, none was found that exceeded the value of water-ice.

The heat of fusion of NH_4HF_2, ammonium bifluoride is given in a Russian paper (Ref. 38) as 275 cal/gm (1150 J/g), a figure more than three times that for water-ice. Because this material melts at a temperature beyond the backpack coolant range, 126°C, (399 K), we would have to form mixtures with hydrogen fluoride which are known to form eutectics with lower melting temperatures. However, as the value in the table shows, we could not reproduce the Russian work, and the material was consequently dropped from further consideration. Lithium acetate showed a heat of fusion of 67 cal/gm (278 J/g) only on the first run through the DSC, subsequently failing to freeze when the temperature was brought down. Apparently meling is accompanied by decomposition. Lithium biacetate made by evaporation from a water solution of the acetate and acetic acid exhibited the same behavior. Attempts to run ammonium biacetate did not result in reproducible results, probably because of decomposition on melting.

The compound ammonium carbamate is reported (Ref. 39) to have a heat of fusion of 165 cal/gm (690 J/g) with a melting point of 145°C (418 K). It was hoped that eutectic mixtures using this compound could be found to bring the melting temperature below 70°C (343 K). However, it was not possible to determine the heat of fusion of ammonium carbamate on the DSC. The problem may be that of sealing the sample pans so that higher pressures can be attained. It is probable that many of the compounds for which measurements were made would exhibit high heats of fusion only in sealed systems at higher than atmospheric pressure.

Heats of Fusion for Eutectic Salt Mixtures

Table XV lists the results obtained on 8 molten salt eutectics ranging in melting points from 3.5°C (276.5 K) to 70°C (343 K). These mixtures were found to have very low heats of fusion, well blow the range of interest.

TABLE XV

HEAT OF FUSION OF SOME MOLTEN SALT EUTECTIC MIXTURES

Salt System	Melting Point (Literature)		ΔH_f	
	°C	(K)	Cal/gm	(J/g)
$LiNO_3$-$AgNO_3$-NH_4NO_3	52	(325)	7.45	(31.1)
$SbBr_3$-$SnBr_4$	27	(300)	6.96	(29.1)
$SnBr_4$-SnI_4	19.4	(292.4)	5.21	(21.8)
$AlBr_3$-$SnBr_4$	20	(293)	5.74	(24.0)
$AlBr_3$-$AsBr_3$	25.5	(298.5)	1.65	(6.9)
$AsBr_3$-$SnBr_4$	3.5	(276.5)	8.62	(36.0)
$AsBr_3$-PBr_5	23.5	(296.5)	5.3	(22.2)
$LiNO_3$-$NaNO_3$-KNO_3	70	(343)	1.2	(5.02)

Measurements of Heats of Solution

Some solids dissolve in water with the absorption of large amounts of heat. The combination of any solid and liquid will absorb heat if a pre-existing ordered arrangement of particles gives way to a new formation that contains less order than the original. The solid during dissolution, as in the melting process, undergoes an entropy increase because of the destruction of the ordered arrangement of molecules in the solid state, and the formation of arrangements having a greater degree of randomness than the original. The energy necessary to disperse the solid throughout the liquid is essentially the same as the energy necessary to melt the solid, namely, the lattice energy. In the dissolution process, the energy to overcome the lattice forces does not come from thermal energy as in melting, but in solvent-solute interactions. The dissolution process actually consists of three separate processes: 1) the destruction of the lattice; 2) the formation of solute-solvent structures; and 3) disruption of the solvent structure. The first process results in an absorption of heat and a large increase in entropy from the dispersion of the particles making up the crystal lattice. The second process reduces entropy and releases heat since structures of more or less permanency are formed. The third process increases entropy since the solute modifies the hydrogen bonded solvent-solvent interaction occurring among the water molecules. This effect is smaller than the first two, and for our limited purposes here, can be ignored. Therefore, the total heat of solution q_{mx} can be represented as (Ref. 36, p.412),

$$q_{mx} = U_{mx} - (W_m^+ + W_x^-) \qquad (7)$$

where the term U_{mx} is the lattice energy of the solid mx and the term in the parenthesis is the hydration energy. We can see from equation (7) that the heat of solution will be a maximum for salts that have large lattice energies and low hydration energies. However, if the lattice energy is too large, the compounds will not dissolve in the solvent at all. Small hydration energy will be favored by ions with low charge density (large size) and a charge of unity. Hydrated salts, compared to their anhydrous counterparts always have a larger endothermic or smaller exothermic heat of solution due to the elimination of the entropy decrease which accompanies solvent-solute structure formation.

When a large amount of solute is added to a solvent, the heat of solution per gram of salt added is not the same as when a small amount of solute is added. The reason for this is that the first amount of solute added sees an essentially pure solvent, while the last solute added sees a concentrated solution. The differential heat of solution is the heat evolved or absorbed when no change of concentration takes place, in other words, the "instantaneous" heat of solution at a particular concentration. The integral heat of solution

which is the one of interest in the present application is the total heat absorbed or evolved when an amount of salt is dissolved up to the saturation point. The heats of solution given here are the integral heats as measured in the bomb calorimeter and represent the heat absorption to be expected in practical application.

Table XVI shows the heat of solution of potassium thiocyanate (KCNS).

TABLE XVI

INTEGRAL HEAT OF SOLUTION, ΔH_s, OF KCNS

Concentration g KCNS/100g H_2O	ΔH_s		NBS Circ. 500	
	cal/gm KCNS	(J/g KCNS)	cal/gm KCNS	(J/g KCNS)
.500	58.4	(244)	57.9	(242)
2.015	68.5	(286)		
5.019	63.2	(264)		
9.266	58.6	(245)	56.7	(237)
11.39	64.4	(269)		
20.00	65.4	(273)		
25.08	55.2	(231)		
48.40	53.1	(222)	44.3	(185) 67g
111.2	41.8	(175)		
147.0	38.5	(161)		
213.9	36.1	(151)	32.6	(136)

This salt was originally thought to have a heat of solution of 126 cal/gm (528 J/g) because of an erroneous listing in the International Critical Tables, Vol. 5, Page 205. The NBS circular 500, page 505 lists the heat of solution as 57.9 cal/gm (242 J/g) at infinite dilution, which would correspond to the first value given in Table XVI. This determination served as a check on the experimental procedures involved since the last column in Table XVI illustrates the close agreement between the NBS data and the data obtained in the present work.

Since KHF_2, potassium bifluoride is known to have a high negative heat of solution (Ref. 40) 76.6 cal/gm (320 J/g) as high dilution, and a fairly large solubility (Ref. 41) 39 g/100 g water, the heat of solution of ammonium bifluoride NH_4HF_2, unavailable in the literature was expected to have an even higher heat absorption since the NH_4^+ cation is larger than the K^+ cation. Ammonium fluoride, NH_4F, also has a heat of solution of 40.9 cal/gm (171 J/g) and the HF_2^- anion is larger than the F^- anion. Thus the compound NH_4HF_2 would be expected to exhibit a large negative heat of solution due to the fact that solute-solvent interactions should be at a minimum. Fortunately, the salt dissolves to the extent of about 60 g to 100 g of water. Table XVII shows the results of measurements of the heat of solution of ammonium bifluoride.

TABLE XVII

INTEGRAL HEAT OF SOLUTION, ΔH_s, OF NH_4HF_2

Concentration g NH_4HF_2/100g H_2O	ΔH_s cal/gm NH_4HF_2	(J/g NH_4HF_2)
10.0	99.6	(416)
20.0	96.6	(404)
50.0	95.3	(398)
58.9	92.6	(387)
66.7	86.0	(359)

The data in Table XVII indicate that not only is the heat of solution at low concentrations large (25 percent greater than the heat of fusion of water-ice) but that the high concentration of 58.9 g/100 g water still exhibits a high heat of solution. Since this concentrated solution contains about 60g of salt that can absorb 16 percent more heat than an equal amount of water-ice, the solution should be about 10 percent more effective in absorbing heat than water-ice. The regeneration experiments whose results are described in the following section revealed that even better performance is attainable when starting with the hydrate rather than the dry salt.

The heats of solution of potassium bifluoride (KHF_2) and sodium bifluoride ($NaHF_2$) were also measured and the results are shown in Table XVIII.

TABLE XVIII

INTEGRAL HEATS OF SOLUTION, ΔH_s, FOR KHF_2 AND $NaHF_2$

Concentration g KHF_2/100 g H_2O	ΔH_s cal/gm KHF_2	(J/g KHF_2)	Number of Determinations	σ (J/g)
5.0	58.9	(246)	3	22
10.0	88.4	(370)	2	70
15.0	76.6	(320)	3	14
20.0	73.4	(307)	4	3
g $NaHF_2$/100g H_2O	cal/gm $NaHF_2$	(J/g $NaHF_2$)		
5.0	90.0	(376)	3	70
10.0	84.2	(352)	1	--

Although the scatter in some of the data in Table XVIII is large, enough values for the heat absorbed were obtained that were above the heat of fusion of water ice (79.8 cal/gm) to warrant further study of the hydrated salt.

Heat Absorption by Combined Heat of Fusion and Heat of Solution

Regeneration experiments were run in the rotating bomb calorimeter to simulate the actual use of the salt and water mixtures. The salt was dissolved in the water and then the solution was frozen at dry ice temperatures, about -40°C (233K). A cooling curve was determined for a concentrated solution of ammonium bifluoride (NH_4HF_2) and showed that melting and heat absorption begin at a temperature of -14.5°C (258.5K). This curve is shown in Figure 52. Because of this, all runs were begun at about -15°C (258K). The results for ammonium bifluoride are shown in Table XIX.

TABLE XIX

COMBINED HEAT OF FUSION PLUS HEAT OF SOLUTION FOR NH_4HF_2 SOLUTIONS

Run #	Concentration g NH_4HF_2/100g H_2O	Electrical Energy In Joules	ΔT K	C_{TOTAL} J/K	Energy Out Joules	Heat Absorbed Joules	ΔH Cal/gm	ΔH (J/g)	% Improvement Over H_2O
1	18.8	184,800	11.10	12,578	139,616	45,184	91	(380)	14
2	18.8	201,600	12.30	12,578	154,709	46,891	94	(395)	18
3	18.8	277,200	18.00	12,578	226,404	50,796	102	(428)	28
4	18.8	230,400	15.00	12,578	188,670	41,699	84	(351)	5.3
5	39.9	273,600	17.50	12,578	220,115	53,485	92	(382)	15
6	39.9	273,600	17.02	12,578	214,077	59,522	102	(425)	27
7	39.9	273,600	16.86	12,962	218,532	55,068	94	(394)	18
8	39.9	277,200	17.15	12,959	222,251	54,949	94	(393)	18
9	45	326,400	22.73	11,883	270,102	56,298	93	(388)	16
10	45	302,400	21.42	11,159	239,028	63,372	105	(437)	31
11	45	310,800	22.74	11,235	255,474	55,326	91	(381)	14
12	50	331,800	24.12	11,107	267,912	63,888	102	(425)	27
13	50	310,800	22.43	10,940	245,383	65,417	104	(436)	31
14	50	310,800	22.44	10,981	246,840	64,378	103	(429)	29

The third column of Table XIX gives the heat input from the electrical heater, 60-80 watts for 45-70 minutes. This input was sufficient to raise the calorimeter temperature the amount indicated in the next column of Table XIX Figure 53 is a plot of both the calorimeter temperature and the jacket temperature during the course of run #4. This plot shows how close it was possible to maintain the jacket temperature and calorimeter temperature, the length of time and range of temperatures used. The C_{TOTAL} in column four of Table XIX for the first 6 runs was from the values obtained from tests using pure water. In subsequent runs, the C_{TOTAL} used was the initial slope of the curve of

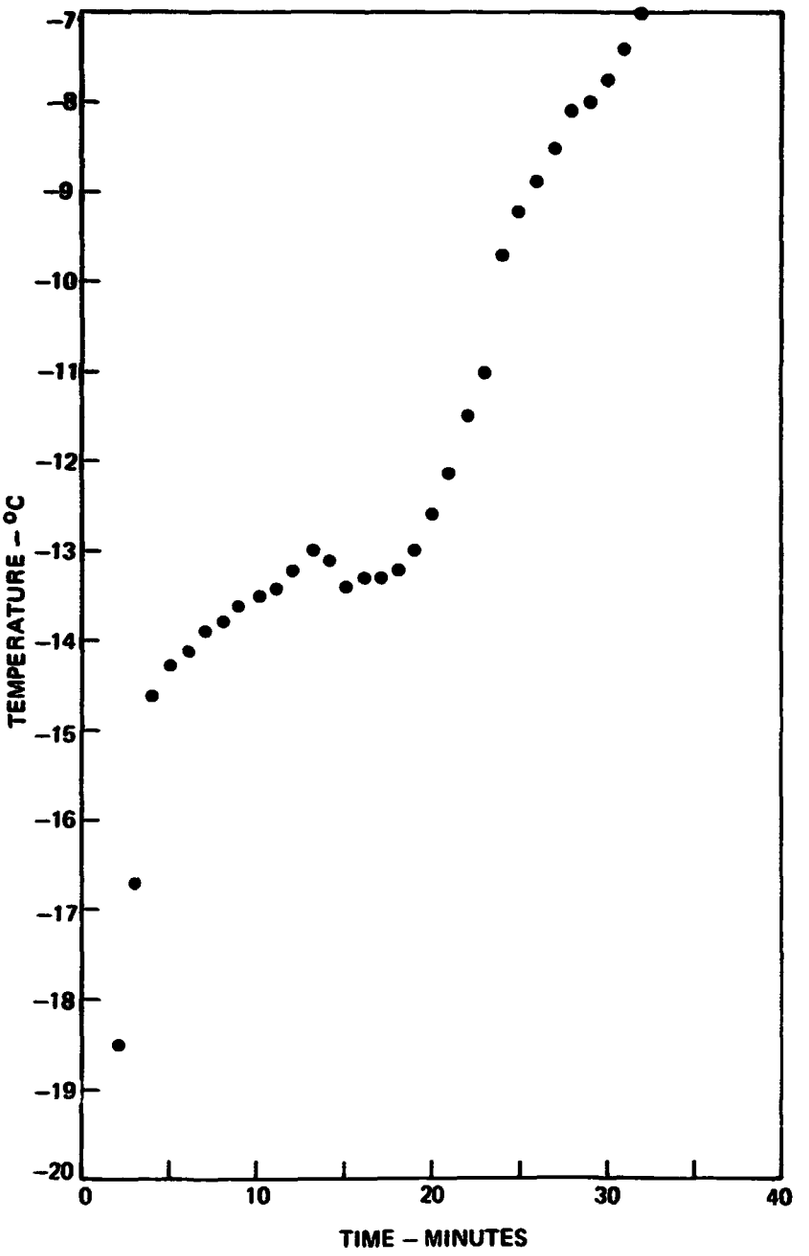

FIGURE 52 MELTING POINT OF NH_4HF_2 SOLUTION (65G / 100G H_2O)

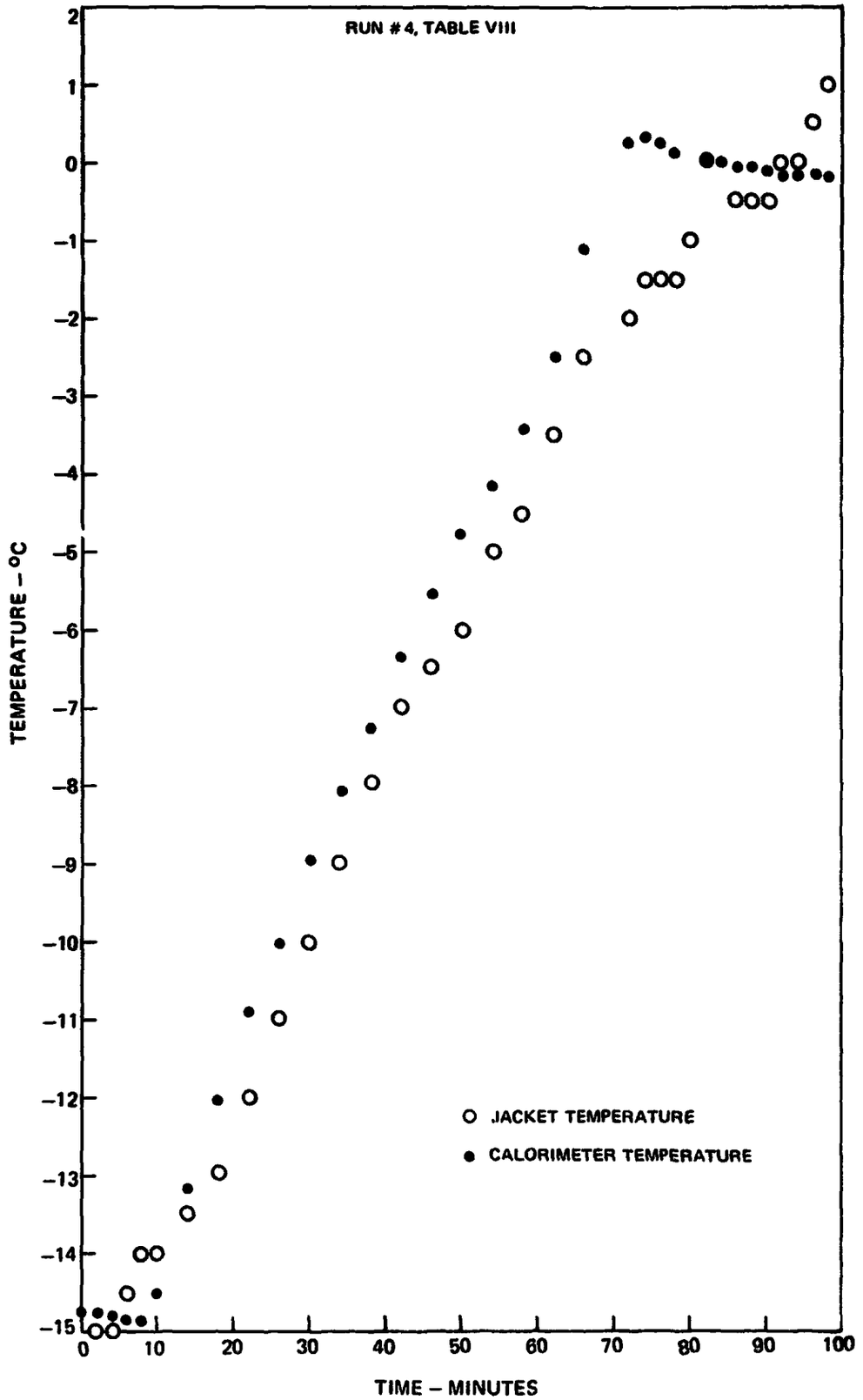

FIGURE 53 TEMPERATURE VS TIME FOR A TYPICAL MEASUREMENT OF HEAT OF SOLUTION

temperature rise vs. time. The first three points of such curves, it can be assumed, represented temperature rise of the calorimeter before any of the bomb contents could have altered it by heat absorption.

In addition to these runs, a solution of 60g NH_4HF_2 in water and a solution of 55.4g NH_4HF_2 in water were determined to have a 67.5 cal/gm (282 J/g) and a 64.8 cal/gm (271 J/g) heat absorption, respectively. At the end of these determinations, at a temperature of 273 K, some salt was still undissolved. Since the solubility is greater at 10 - 20°C (283 - 293K), this salt would dissolve if the experiment was run to higher temperatures, and large values for the heat absorbed per gram would be expected.

Table XX shows the average values for the four compositions along with the standard deviation σ and the average percent improvement over water-ice.

TABLE XX

AVERAGE VALUES OF HEAT ABSORBED - NH_4HF_2

Concentration g NH_4HF_2/100g H_2O	ΔH Absorbed		σ		Average % Improvement
	Cal/gm	(J/g)	Cal/gm	(J/g)	
18.8	93.0	(389)	7.6	(32)	16
39.9	95.4	(399)	4.3	(18)	20
45	96.1	(402)	7.4	(31)	20
50	103	(430)	1.4	(6)	29

The solution containing the highest amount of NH_4HF_2 in Table XX 50g/100g H_2O, exhibited an average of a 29 percent greater heat absorption than would have been possible by using 150g of water-ice. A possible explanation of the fact that the heat of solution of the dry salt in water indicated that only a 10 percent improvement could be expected is discussed in the following paragraphs.

Since equation (7) indicates that the heat of hydration must be a negative influence on the total heat of solution, it is apparent that compounds with no heat of hydration would be expected to have larger heat absorption upon dissolution. Certainly a hydrate would be expected to have a zero heat of hydration as long as the hydration number remains the same.

The effect of the heat of hydration upon the heat of solution can be seen in the following table of data taken from Ref. 42).

TABLE XXI

HEAT OF HYDRATION OF ALKALI METAL IONS
AND HEAT OF SOLUTION OF ALKALI METAL FLUORIDES

Ion	Radius Crystal (Å)	ΔH of Hydration		ΔH of Sclution of Fluoride			
		kcal/mole	(J/mole)	cal/gm	(J/g)	kcal/mole	(J/mole)
Li+	.60	121.2	(506,616)	39.8	(166)	1.03	(4305)
Na+	.95	94.6	(395,428)	11.4	(47.8)	.48	(2006)
K+	1.33	75.8	(316,844)	-71	(-287)	-4.12	(-17222)
Rb+	1.48	69.2	(289,256)	-56	(-234)	-5.85	(-24453)

The cations are listed in order of their ionic radius, and the heat of hydration is seen to decrease as the size of the cation increases. In the last columns the heat of solution of the corresponding fluorides can be seen to go from releasing heat in the lithium and sodium fluorides to absorbing heat in the potassium and rubidium fluorides. Thus, on a per mole basis, the compounds with high heat of hydration will exhibit less heat absorption upon dissolution, and high heat absorption upon dissolution is favored by large ionic size. However, one can argue that the water molecules tied up with the salt are unavailable for absorbing heat by melting. The magnitude of these two effects can be studied by looking at some examples of this effect from the literature.

It can easily be established that salt hydrates have higher heat absorption values than the dry salt. The following Table XXII shows the heats of solution of some anhydrous salt-hydrated salt pairs (Ref. 40) that will serve to illustrate this point.

In every case, the heat absorbed is larger for the hydrated salt than for the anhydrous salt. For compounds with one water molecule associated with them, an average increase in heat absorption of 69 percent is observed. Also in general, as the number of water molecules in the hydrate increases, the heat absorption ratio between hydrate and anhydrous forms increases. As an illustration of the magnitude of the hydrate effect, let us assume that each molecule of NH_4HF2 has one molecule of water associated with it as the hydrate. Then the 39.9 g of dry NH_4HF_2 combines with 12.6 g of water on a mole to mole basis. This leaves 87.4 g of water that is not effected by the hydrate. This amount of water will absorb 29,148 J upon melting. The average mono-hydrate in Table XXII absorbs 117.5 J/g more heat than its anhydrous counterpart. The

TABLE XXII

HEAT ABSORPTION OF ANHYDROUS-HYDRATED SALT PAIRS

Anhydrous Salt	ΔH_{soln} Cal/gm	ΔH_{soln} (J/g)	Hydrated Salt	ΔH_{soln} Cal/gm	ΔH_{soln} (J/g)	% Higher
$K_2S_2O_6$	29.9	(125)	$K_2S_5O_6 \cdot 1/2\ H_2O$	38.3	(160)	28
$NaHC_2O_4$	49.3	(206)	$NaHC_2O_4 \cdot H_2O$	73.7	(308)	50
$NaHC_4H_4O_6$	33.0	(138)	$NaHC_4H_4O_6 \cdot H_2O$	45.0	(188)	36
$(NH_4)_2C_2O_4$	36.4	(152)	$(NH_4)_2C_2O_4 \cdot H_2O$	81.1	(339)	123
$Ba(ClO_3)_2$	45.8	(191)	$Ba(ClO_3)_2 \cdot H_2O$	77.0	(322)	68
$Na_2S_2O_6$	27.8	(116)	$Na_2S_2O_6 \cdot 2H_2O$	48.3	(202)	74
$Sr(NO_3)_2$	22.0	(92)	$Sr(NO_3)_2 \cdot 4H_2O$	43.3	(181)	97
$Na_2H_2P_2O_7$	10.3	(43)	$Na_2H_2P_2O_7 \cdot 6H_2O$	42.1	(176)	309

heat of solution of a solution of 39.9g of NH_4HF_2 in 100g of water can be interpolated from Table XXII to be 398 J/g. Therefore, for the $NH_4HF_2 \cdot H_2O$ we have 398 + 117.5 = 515.5 J/g for 52.5g or 27,064 J. The combined heat absorbed for hydrate and uninvolved water-ice is 56,212 J. This amounts to 402 J/g for the 139.9g of NH_4HF_2 solution compared to 399 J/g actually measured. In the case of the solution containing 50g of NH_4HF_2 we have 66g of hydrate and 84g of water-ice. The heat absorbed for the hydrate would be 34,023 J and for the water-ice, 28,014 J, for a total of 62,037 or 413 J/g compared to 430 J/g actually found. Thus, although the calculated increase in heat absorption for the 50g/100g H_2O solution is only 6.6% based on the dry salt heat of solution, the calculated increase is 24% based on the hydrated salt. In view of the fact that the actual increase in heat absorbed for the monohydrates listed in Table XXII vary from 50 to 187 J/g, this simple arithmetic exercise cannot be considered definitive, but it does reveal how it is possible for the hydrate-water-ice system to absorb so much more heat than the anhydrous salt-water-ice system.

The question now arises -- what is the effect of changing the cation on the heat of solution of the hydrate. The potassium and sodium bifluorides have large heats of solution and their cations are both smaller than the ammonium cation. As shown earlier, the smaller the ion, the greater the field intensity surrounding it for a constant charge, and therefore, the greater the energy of hydration since the solvent-solute interactions will be stronger. Therefore, one would expect a greater difference in the heat absorption between the dry salts KHF_2 and $NaHF_2$ and their hydrated counterparts than between dry NH_4HF_2 and its hydrate.

The heats of fusion plus heats of solution for these compounds are given in Table XXIII. The C_{TOTAL} used in the first six runs was calculated from the initial slope of the curve of temperature versus heat-energy input with the bomb rotating. Variations in C_{TOTAL} for these runs are due primarily to differences in the amount of fluid in the calorimeter can. Runs 7 through 13 were made with no bomb rotation. The solution was frozen in the bottom of the bomb, and it was melted in that position with no stirring or disturbance at all, in order to more closely approach conditions as they would occur in actual use of the material in a backpack cooling system. The calorimeter stirrer alone was unable to bring the temperature into equilibrium while the heater was on in a short enough time span, and the initial slope was distorted. Therefore, the C_{TOTAL} used in the runs 7-13 was the value obtained from the calibrating experiments noted in the section on Experimental Methods. Since the C_{TOTAL} was sensitive to the amount of fluid present in the calorimeter, the amount used was very carefully measured to a constant 2,122g for these runs. Both the calculated C_{TOTAL} and the value obtained from the calibrating runs using water-ice in Table II were 11,500 J/K within ± 200 J/K.

The runs #5 and #6 were also part of an experiment to determine if a slower cooling cycle would result in significantly different performance due to a change in the separation rate of salt hydrate and water-ice. Run #5 used a slow cooling regime for freezing the bomb, shown in Fig. 54 along with the fast cooling schedule. Since no significant difference was found, the first six runs have been averaged together to obtain a mean value for the heat absorption. A cooling curve, shown in Fig. 55, showed that the 30g KHF_2 solution began to melt at about -10°C (263K), and, therefore, in runs 1-10 the initial temperature was about -12°C (261K). Runs 11, 12 and 13 were begun at higher temperatures than the preceding four runs, in order to test the loss of heat absorption capability when the salt-ice slush was not completely frozen. Table XIII contains a summary of the data presented in Table XXIII. For the 20% solution, the average heat absorption in runs 1-6 in Table XXIII was 42% more than that of water-ice and for the 30% solution, the average heat absorption in runs 7-10 in Table XXIII was 121 cal/gm (507 J/g) which is 52% more the value of 79.8 cal/gm (333.5 J/g) for water ice. The density of the 30% KHF_2 solution was determined to be 1.18 g/cm^3. Thus, the increase in heat absorbed over that of water-ice on an equal volume basis is 79%.

Table XXIV also shows the effect on the 30% concentration data when a higher value is used as the initial temperature. At an initial temperature of -6.9°C (266.1 K) 88 cal/gm (367 /g) was absorbed, only a 10% improvement over water-ice.

Another salt that has a large heat of solution (79.2 cal/gm·331 J/g), and a large solubility (118 g/100g H_2O) is NH_4NO_3, ammonium nitrate. Two regeneration type experiments were run to determine if a larger effect would be possible when starting with the wet salt. The results of these runs are in Table XXV.

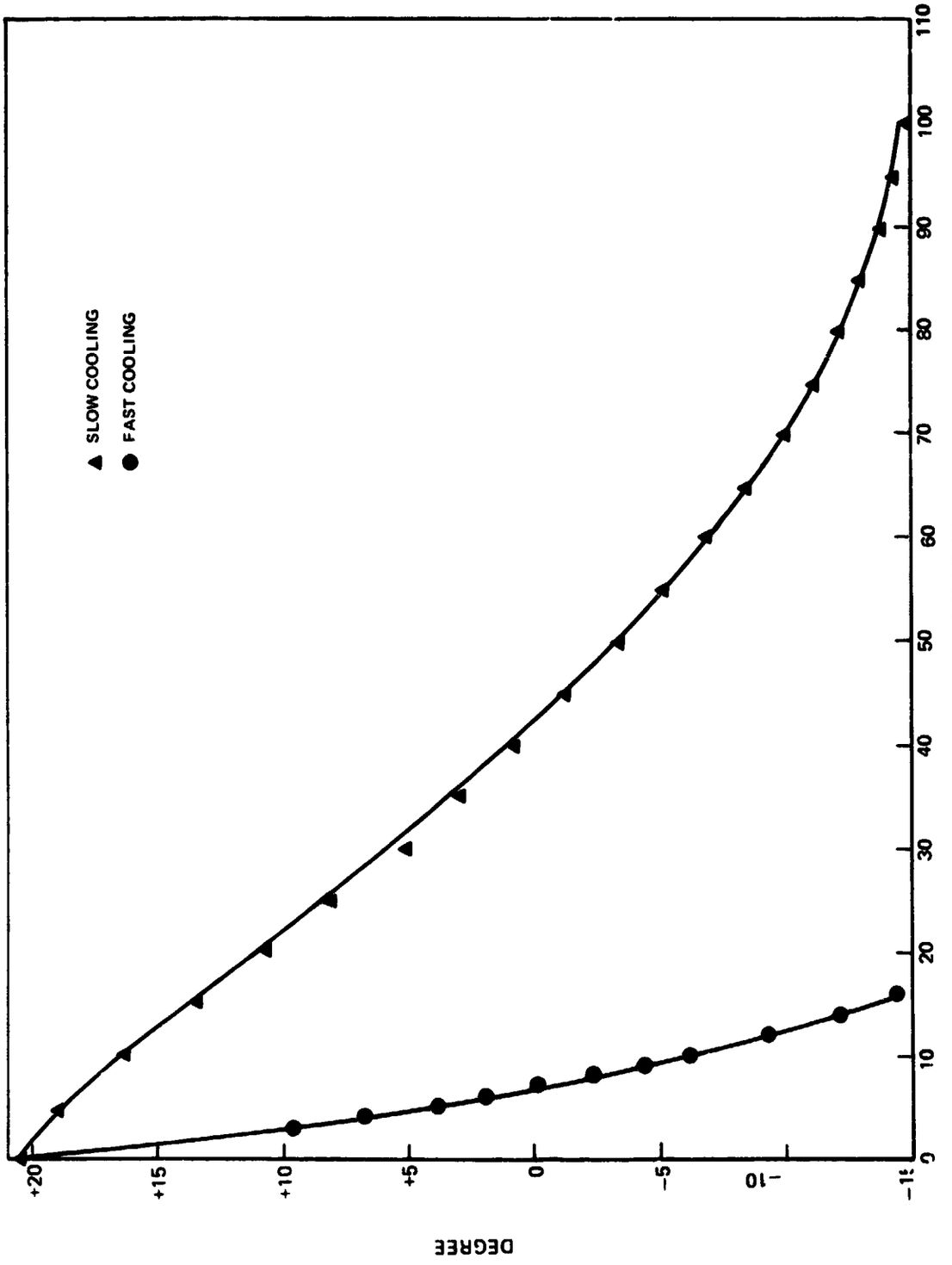

FIGURE 54 BOMB COOLING RATE IN REGENERATION EXPERIMENT

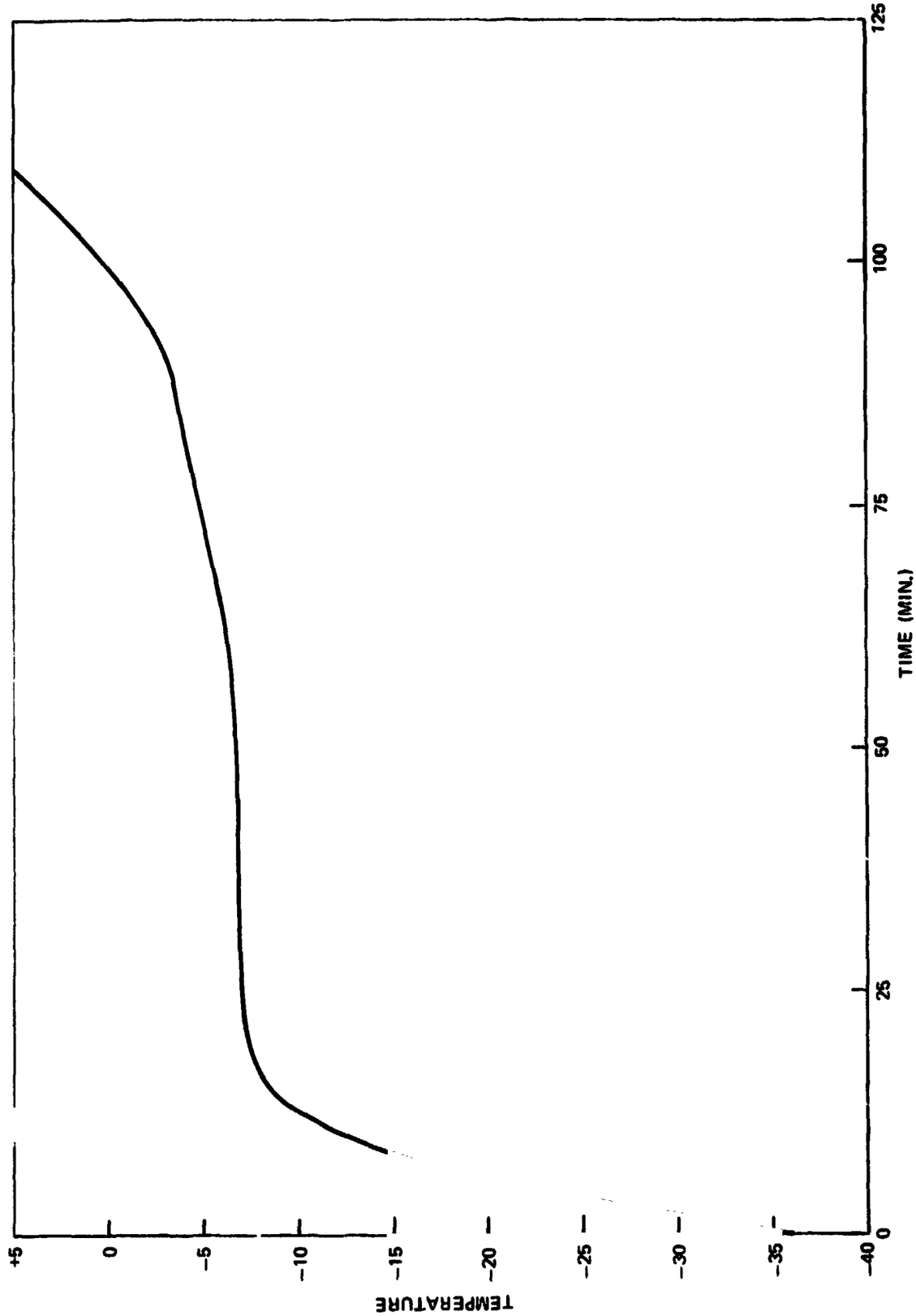

FIGURE 55 MELTING POINT OF KHF_2 SOLUTION

TABLE XXIII

HEAT OF FUSION-HEAT OF SOLUTION OF KHF_2

Run #	Concentration g KHF_2/100g H_2O	Electrical Energy In Joules	ΔT K	C_{TOTAL} J/K	Energy Out Joules	Heat Absorbed Joules	ΔH Cal/gm	ΔH (J/g)	% Improvement Over Water-ice
1	20	297,600	25.48	9,570	243,856	53,744	107	(448)	34
2	20	350,400	24.80	12,000	297,600	52,800	105	(440)	32
3	20	310,800	23.78	10,400	247,31,	63,481	127	(529)	59
4	20	316,800	24.34	10,545	256,710	60,090	120	(501)	50
5	20	252,000	20.21	9,538	192,763	59,237	118	(494)	48
6	20	312,000	21.79	12,000	261,480	50,520	101	(421)	26
7	30	336,000	23.12	11,500	265,846	70,155	129	(540)	62
8	30	297,906	20.54	11,500	236,233	61,673	113	(474)	42
9	30	272,964	17.92	11,500	206,080	66,884	123	(514)	54
10	30	316,953	21.91	11,500	251,971	64,982	120	(500)	50
11	30	240,000	16.72	11,500	192,280	47,720	88	(367)	10
12	30	240,000	16.40	11,500	188,600	51,400	95	(395)	18
13	30	278,400	19.19	11,500	220,685	57,715	106	(444)	33

TABLE XXIV

AVERAGE VALUES OF HEAT ABSORBED - KHF_2

Concentration g KHF_2/100g H_2O	ΔH Absorbed Cal/gm	ΔH Absorbed (J/g)	σ Cal/gm	σ (J/g)	Average Percent Improvement	Temp. Run Started °C	Temp. Run Started (K)
20	113	(472)	10	(42)	42	-12	(261)
30	121	(507)	7	(28)	52	-12	(261)
30	88	(367)	--	--	10	-6.944	(266.206)
30	95	(395)	--	--	18	-6.583	(259.623)
30	106	(444)	--	--	33	-8.844	(264.306)

TABLE XXV

HEAT OF FUSION PLUS HEAT OF SOLUTION OF NH_4NO_3

Concentration g NH_4NO_3/ H_2O	Electrical Energy In Joules	ΔT K	C_{TOTAL} J/K	Energy Out Joules	Heat Absorbed Joules	ΔH		Percent Improvement Over Water-ice
						Cal/gm	(J/g)	
50	288,000	20.80	11,282	234,658	53,342	85	(355)	6
50	352,800	25.12	11,908	301,392	51,408	82	(343)	3

The average value of 83 cal/gm (349 J/g) is only 5 percent better than can be obtained through the use of 150g of water-ice. In this case apparently, the heat of hydration does not play as large a role, and the heat of solution does not increase as much as with the bifluorides.

In space operation the heat absorbing material may not be under the influence of gravity, so its operation may be different. However, the influence of a zero gravity field on the melting and solidification of salt solutions is not expected to be much different than its effect on water-ice. Since segration of particles due to density differences is not possible in zero gravity, the salt will be more uniformly dispersed through the ice after the regeneration procedure. This can result in a higher dissolution rate upon melting.

The effect of the wicking material on the dispersion of the salt in water upon freezing may be greater than the effect of zero gravity, and while it was outside the scope of the present work, this effect should be measured.

Conclusions

1. The heat absorption available using a solution of 30 g of potassium bifluoride (KHF_2) in 100 g of water (H_2O) is 121 cal/gm (507 J/g) which is approximately 52 percent greater than the heat absorption available from an equal weight of water-ice, and approximately 79 percent greater than the heat absorption available from an equal volume of water-ice.

2. The heat absorption for the KHF_2-H_2O system begins at a temperature of -12°C (261 K)and continues through about 10°C (283 K).

3. The regeneration of the KHF_2-H_2O mixture is extremely simple -- a lowering of the temperature at virtually any rate with no stirring will produce the required separation of salt hydrate and water-ice. The maximum number of regeneration-melting cycles performed in this work was 4. No degradation as a function of repeated regeneration was noted.

4. A literature search has failed to uncover data relating directly to the corrosivity or toxicity of KHF_2. The following facts are known:

   - Repeated exposure of the platinum lined stainless steel calorimeter bomb to the KHF_2-H_2O solution produced no noticeable metal corrosion.

   - Overnight exposure of the aluminum differential scanning calorimeter sample holders to the KHF_2- H_2O solution produced no noticeable metal corrosion.

   - Exposure of laboratory personnel, including direct skin contact, to the KHF_2- H_2O solution produced no noticeable effects.

   - The Merck Index lists KHF_2 as being similar in toxicity to sodium flouride, which is toxic in amounts over 4 grams and causes severe symptoms when 0.5 gram is ingested. One ppm is commonly used in drinking water and a 2% solution is applied to the teeth routinely.

5. Based on the results of the KHF_2- H_2O testing, an ice chest containing a solution of KHF_2 in H_2O could conceivably be designed that would weigh 30 to 40 percent less than an equivalent ice chest containing pure H_2O.

6. Measurements of the heat of fusion of likely candidate compounds and eutectics has failed to reveal any with a higher heat of fusion than water-ice in the temperature range of -10 to 70°C (263 to 343 K).

FLIGHT EXPERIMENT PLAN

A Flight Experiment Plan has been prepared which outlines the steps necessary for developing the Ice Pack Heat Sink Subsystem into a candidate Shuttle/Spacelab flight experiment. This plan breaks down the effort into three phases:

Phase I - Configuration Support and Engineering Development, which includes concept generation and development.

Phase II - Flight Hardware Manufacture and Qualification, which includes manufacture, qualification, refurbishment, and acceptance testing of a qualification/flight backup unit; manufacture and acceptance testing of a flight unit; and design, manufacture, and test of Flight and Preflight checkout equipment.

Phase III - Field/Flight Test Support, includes effort required in support of the actual flight experiment.

This plan, Ice Pack Heat Sink Subsystem - Phase II, Flight Experiment Plan, SVHSER 6526, is contained under separate cover to allow its circulation independent of this final report (Ref. 43).

APPENDIX A

SMALL/LARGE SCALE INTERFACE DEVELOPMENT TEST PLAN

Hamilton Standard — Division of United Aircraft Corporation

ICE PACK HEAT SINK SUBSYSTEM - PHASE II

SMALL/LARGE SCALE INTERFACE DEVELOPMENT TEST PLAN

PREPARED UNDER CONTRACT NAS 2-7011

by

HAMILTON STANDARD

DIVISION OF UNITED AIRCRAFT CORPORATION

WINDSOR LOCKS, CONNECTICUT

for

NATIONAL AERONAUTICS AND SPACE ADMINISTRATION

AMES RESEARCH CENTER

MOFFETT FIELD, CALIFORNIA

OCTOBER 1973

Prepared by: _____
G. Roebelen
Program Engineer

Approved by: _____
F. H. Greenwood
Program Manager

1.0 SCOPE

This plan of test defines the development tests to be performed by Hamilton Standard on several small scale (6"x6") ice chest/ heat exchanger interface units as part of the effort to enhance thermal performance and life characteristics of this interface for the full size Ice Pack Heat Sink Subsystem. This testing will investigate different surface configurations.

2.0 TEST ITEM

This test program will consist of testing the following 6x6 inch surface configuration plates, inserted in the instrumented test fixture (figure 1), at pressure loadings of 8, 16, and 30 psi.

I. Plain aluminum on plain aluminum - this configuration is to be used as a baseline.

II. Lead plated aluminum on plain aluminum - this configuration represents the Phase I configuration.

III. Lead plated aluminum on plain aluminum with the lead plated part grooved to produce square pads approximately 0.25 in. (0.635 cm) x 0.25 in. (0.635 cm).

IV. Same as (II) but with every other pad removed to produce a checkerboard pattern.

V. Same as (III) but with square pads approximately 1.5 in. (3.81 cm) x 1.5 in. (3.81 cm).

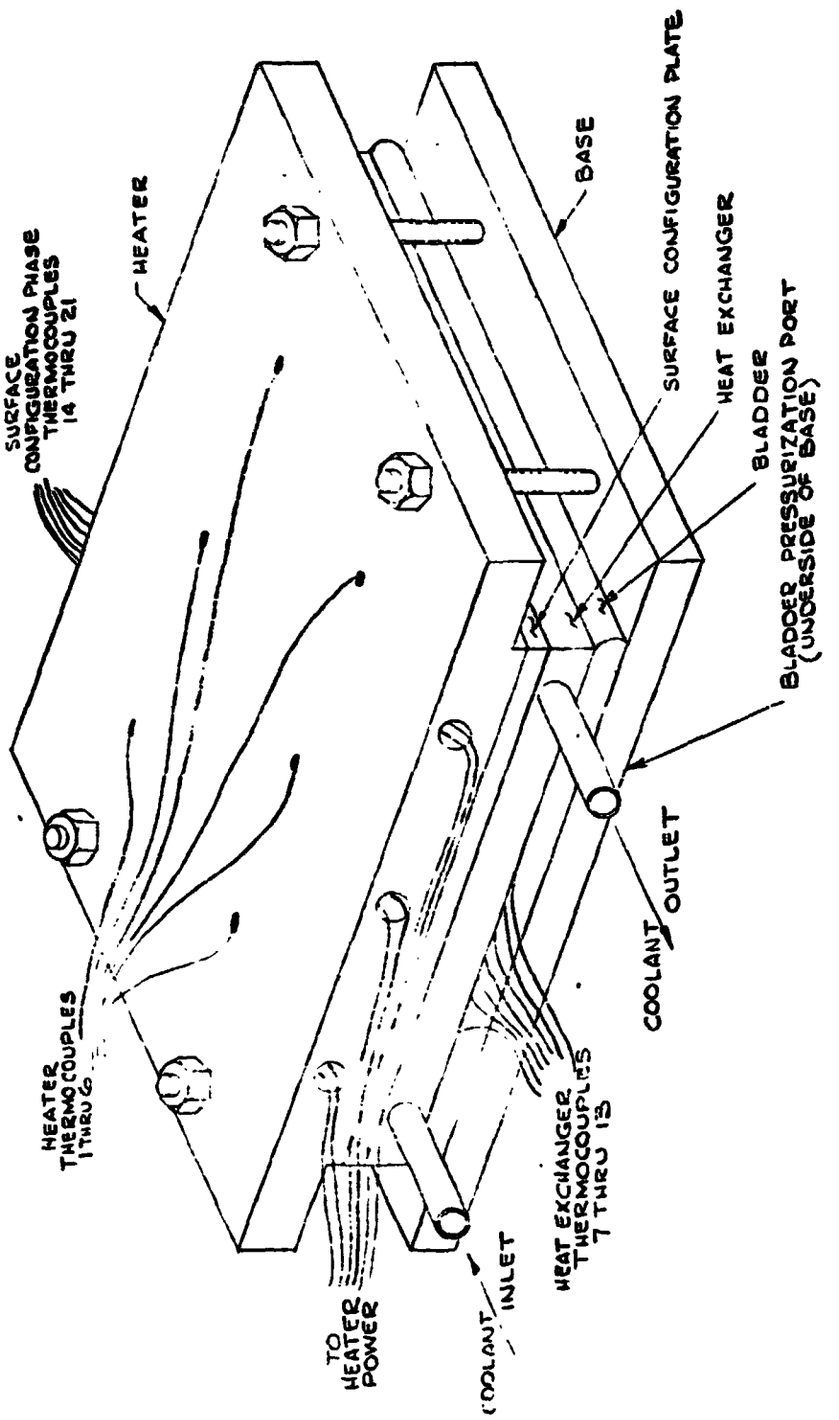

FIGURE 1 INSTRUMENTED SMALL/LARGE SCALE INTERFACE DEVELOPMENT TEST FIXTURE

2.0 (Continued)

VI. Same as (V) but with every other pad removed to produce a checkerboard pattern.

VII. Lead plated aluminum on plain aluminum, displaced 0.062 in. (0.157 cm) laterally after pressure mating.

VIII. Lead plated aluminum on chrome plated aluminum.

3.0 TEST MEDIA

The test media for all portions of this test will be:

Ambient: Pressure = Vacuum (~0.1 micron)

Temperature = Room Conditions

Coolant Liquid: Water (~40°F)

4.0 TEST EQUIPMENT

All portions of this test program will be performed in the Hamilton Standard Space Systems Department Space Laboratory (Reference Test Schematic Figure 2).

5.0 DEFINITION OF TESTS

5.1 TEST SETUP - The following steps will be taken for each sample plate test setup.

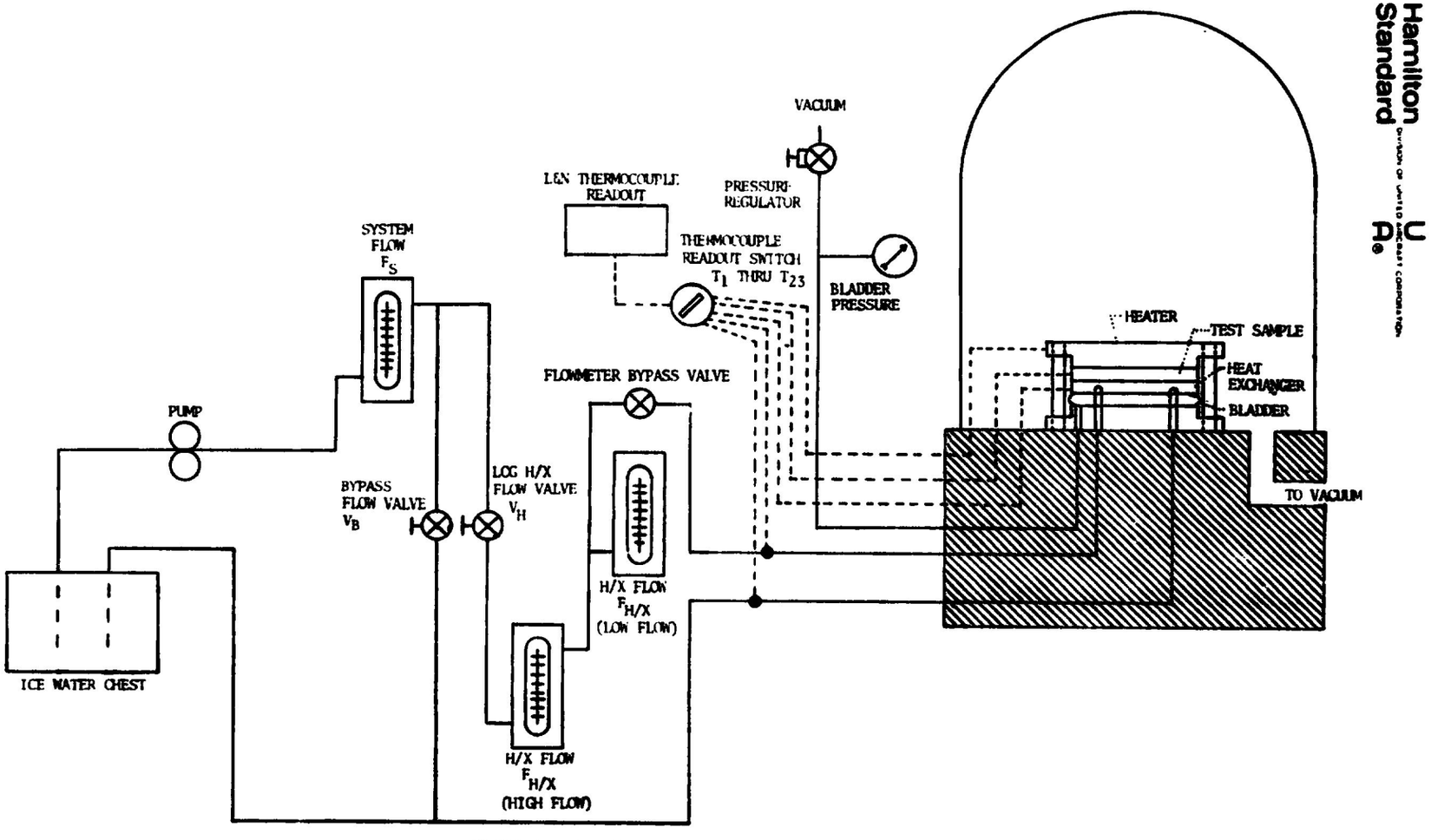

FIGURE 2 SMALL/LARGE SCALE INTERFACE DEVELOPMENT TEST SCHEMATIC

5.1 (Continued)

A. With the test fixture installed within the vacuum chamber, insert the surface configuration plate between the heater plate and the coolant plate and connect thermocouples.

B. Allow N_2 to slowly pressurize the test fixture bladder. Check squareness of test interface. Adjust to obtain maximum surface contact.

C. Vent bladder and evacuate it with external vacuum source.

D. Close test chamber and evacuate. Slowly vent the test fixture bladder to the chamber ambient. Evacuate chamber to 10^{-4} mmHg (0.1 micron).

5.2 TEST RUN - The following test runs will be performed on each surface configuration plate.

A. Load coolant reservoir with water and ice chips.

B. Slowly pressurize bladder to 8 psia (check squareness).

C. Close coolant by-pass valve and fully open heat exchanger valve.

D. Adjust the coolant pump power supply to 25 volts. Turn on pump and readjust power supply to 25 volts.

E. Close heat exchanger coolant valve to obtain 0.5 gpm flow.

F. Turn on heater and adjust powerstat to obtain 3.0 amps (AC).

G. Maintain this condition until the temperatures of the coolant water flowing into and out of the heat exchanger have stabilized. (Coolant water reservoir should always have sufficient ice present in it).

5.2 (Continued)

H. Take one complete set of data recordings. (Reference Sample Log Sheet Figure 3).

I. Turn off heater.

J. Slowly decrease test fixture bladder pressure. Evacuate with external vacuum supply before venting to chamber. There should be a gap between the test plate and the test fixture after bladder depressurization.

K. Slowly pressurize test fixture bladder to 16 psia (check squareness).

L. Repeat steps 5.2 (F) thru (J).

M. Slowly pressurize test fixture bladder to 30 psia (check squareness).

N. Repeat steps 5.2 (F) thru (J).

O. Turn off pump and pump power supply.

P. Slowly increase pressure in chamber to room ambient and open chamber door. Disconnect test plate thermocouples and remove test plate from test fixture.

5.3 TEST REQUIREMENTS - During each of the tests the coolant flow must be run for a sufficient length of time with the heater energized to allow the entire loop to come to equilibrium. This condition is achieved when the heat exchanger inlet and outlet temperatures remain unchanged for a period of at least five minutes.

Hamilton Standard — DIVISION OF UNITED AIRCRAFT CORPORATION
WINDSOR LOCKS, CONNECTICUT 06096

SPACE & LIFE SYSTEMS LABORATORY

LOG OF TEST

TYPE OF TEST: ICE PACK INTERFACE TEST

TEST ENGINEER

NAME OF RIG

PROJECT & ENG ORDER NO

SHEET OF DATE

TEST PLAN NO

MODEL NO.

PART NO.

SERIAL NO.

OPERATORS

RUN NUMBER:

INTERFACE CONDITION: (SURFACE CONFIGURATION PLATE TYPE)

HEAT EXCHANGER FLOW: (GPM)

INTERFACE PRELOAD PRESSURE: (PSIA) (BLADDER PRESSURE)

HEATER CURRENT: (AC AMPS)

HEATER VOLTAGE: (AC VOLTS)

CHAMBER WALL TEMPERATURE: (°F)

CHAMBER PRESSURE: (mm Hg)

THERMOCOUPLE READINGS: (°F)

T_1	T_2	T_3	T_4	T_5	T_6	T_7	T_8	T_9	T_{10}	T_{11}	T_{12}	T_{13}	T_{14}	T_{15}	T_{16}	T_{17}	T_{18}	T_{19}	T_{20}	T_{21}	T_{22}	T_{23}

REMARKS

SAMPLE DATA SHEET

7743

FIGURE 3 SAMPLE LOG SHEET

5.3 (Continued)

For each test run record the following steady state parameters:

1. Surface configuration plate type
2. Heat exchanger flow
3. Bladder pressure
4. Chamber pressure
5. Chamber wall temperature
6. Heater thermocouple readings (T_1 thru T_6)
7. Heat exchanger thermocouple readings (T_7 thru T_{13})
8. Surface configuration plate thermocouple readings (T_{14} thru T_{21})
9. Heat exchanger inlet thermocouple reading (T_{23})
10. Heat exchanger outlet thermocouple reading (T_{22})

5.4 INSTRUMENTATION

Quantity	Item	Range	Accuracy
1	Flowmeter	0-0.6 gpm	±0.025 gpm
1	AC Ammeter	0-3.0 amp	±0.1 amp
1	AC Voltmeter	0-120 volt	±2 volt
1	Pressure gauge	0-45 psia	±0.1 psi
1	L&N Thermocouple Readout	0-90°F	±0.5°F

NO. 340-M DIETZGEN GRAPH PAPER
MILLIMETER

EUGENE DIETZGEN CO.
MADE IN U. S. A.

GAL TO CC
GAL x 3785 = CC

HAMILTON STANDARD
FLOWMETER CALIBRATION CURVE

SIZE 1/4-16 FLOAT 55

SCFM AIR

16
15
14
13
12
11
10
9
8
7
6
5
4
3
2
1
0

0 5 10 15 20 25 30 35 40 45x10

CC/MIN. H2O @ 70°F

F12 5/30/73

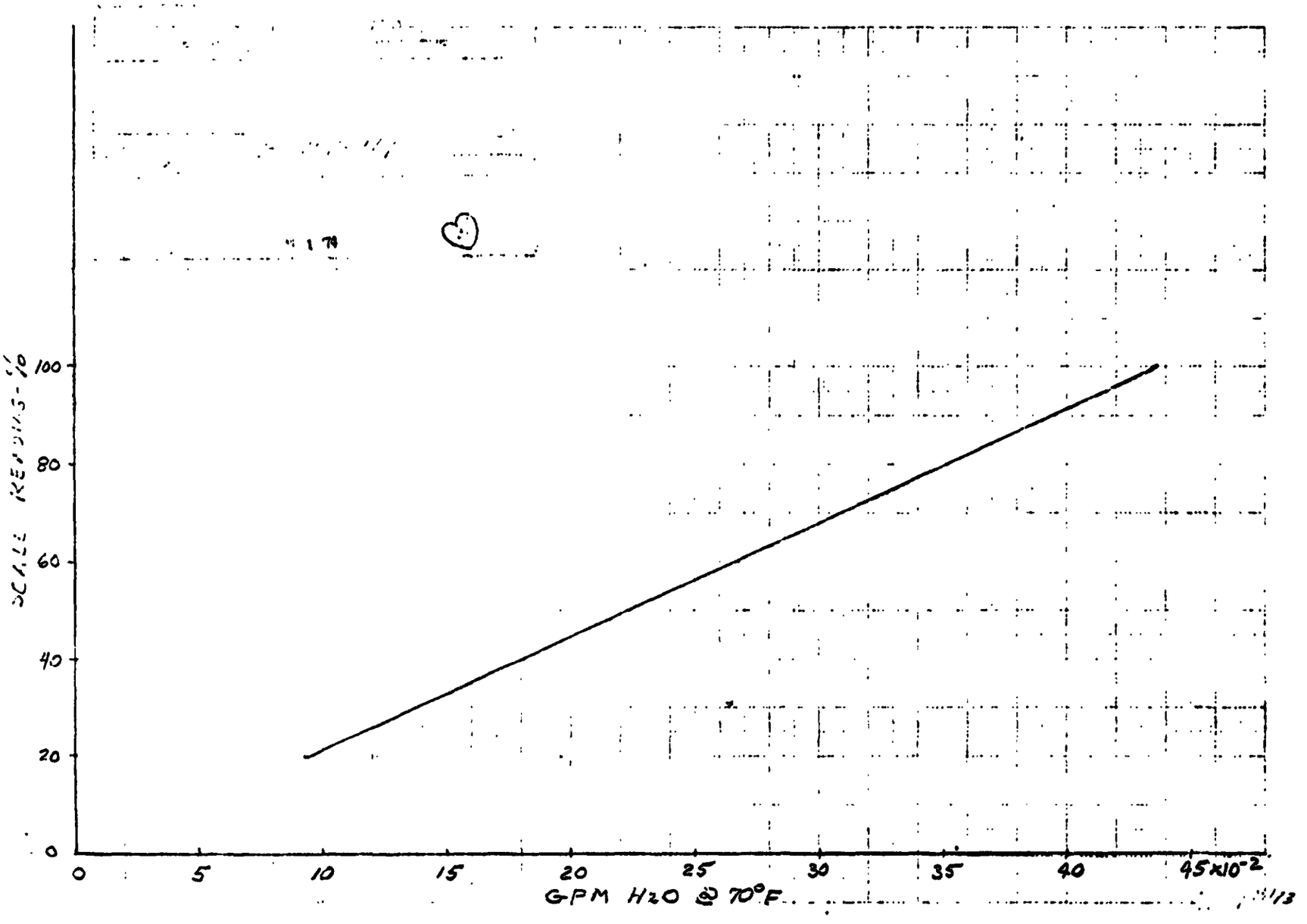
SCALE READING - %
100
80
60
40
20
0
0
5
10
15
20
25
30
35
40
45 X 10⁻²
GPM H2O @ 70°F

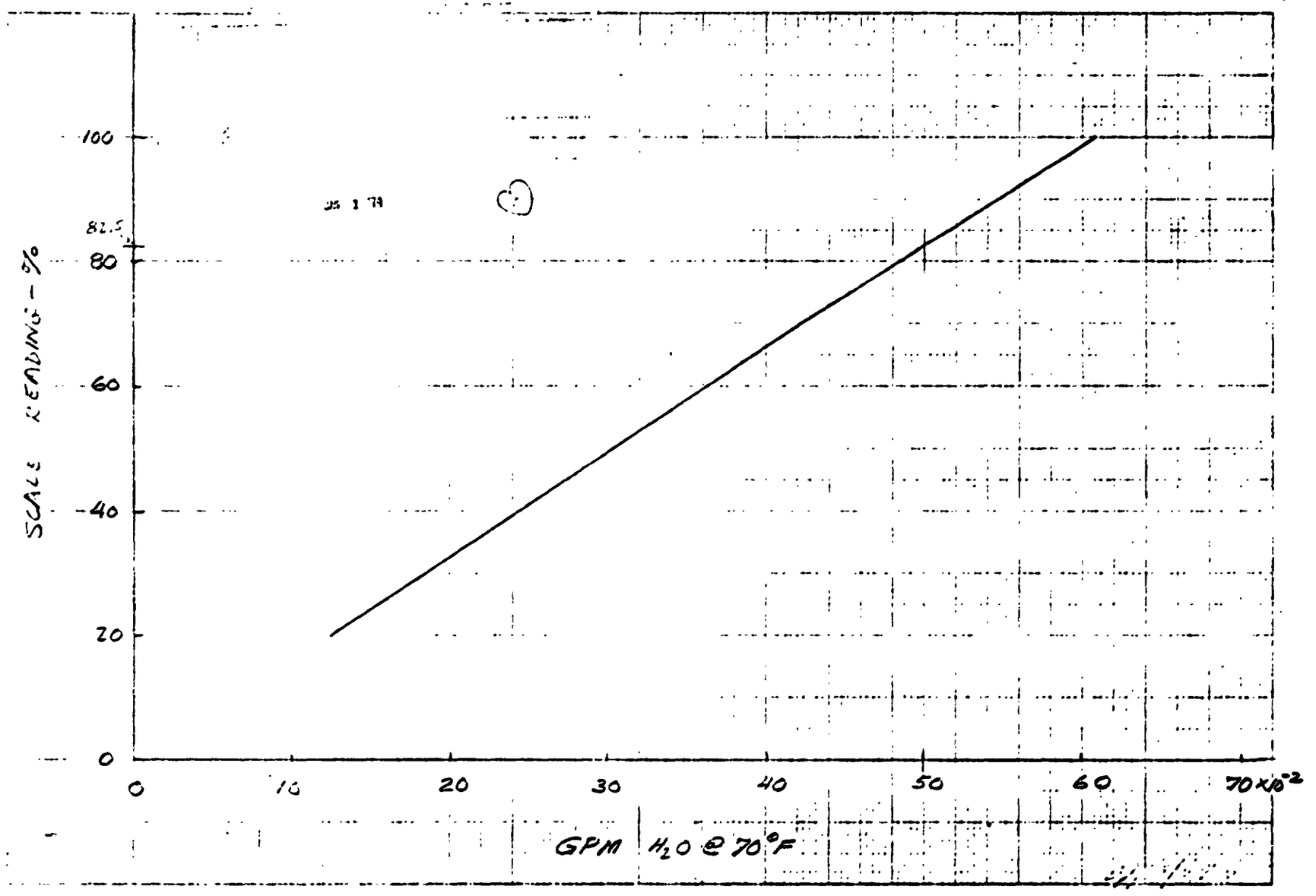
100
82.5
80
60
40
20
0
SCALE READING - %
0
10
20
30
40
50
60
70 x 10^-2
GPM H2O @ 70°F

APPENDIX B

SMALL/LARGE SCALE INTERFACE DEVELOPMENT TEST LOG SHEETS

HSF 301C 2/62

Hamilton Standard — UA

TEMPERATURE LOG OF REFRIGERATION UNIT TEST

TURBINE ACCESSORY DEVELOPMENT GROUP

SHEET No 1

DATE 10-29-73

OPERATORS LASZCLYK

ENGINEER SUPERVISING TEST Boe[illegible]

BOOTH No 35 TYPE OF TEST ICE PACK HEAT SINK SUBSYSTEM INTERFACE DEVELOPMENT

UNIT ____ SERIAL No ____ ASSEMBLY No ____ TEST SPEC ____ ENG PROJECT AND PLAN No BE9-5CC-200B

HEAT EXCHANGER SER No ____ (PRIMARY) ____ (SECONDARY) ENGINEERING INSTRUCTION No ____

E W I No ____ WRITTEN BY ____

Margin note	Reading No	Time	Running Time	Speed RPM	HX In (25)	HX Out (26)	Top Plate °F 1 (27)	2 (28)	3 (29)	4 (30)	5 (31)	6 (32)	Bottom Plate °F 7 (33)	8 (34)	9 (35)	10 (36)	11 (37)	12 (38)	Middle Plate °F 13 (39)	14 (40)	15 (41)	16 (42)	17 (43)	18 (44)	19 (49)	20 (50)	21 (51)	Tank (16)	% FR	Heater Volts AC	Heater Amps AC	Δ Press at Pump	Δ Press at Reservoir	Bladder PSIA
LEAD PLATED	1	11:02			36	39	115	117	121.5	116	120.5	114	40	40	39. ~~40~~	46.5	40.5	40	39	78	84.5	66	72	77	67	72.5	72.5		62.5	98	2.5	4x10^-5	7.x10^-5	8.0
	2	11:25			36	34.5	92.5	97	98.5	92	106	94.5	41	41	41	44.5	41	41	40	66.5	77.	69	62	65	60.5	61.5	65.5		62.5	98	2.5	6.5x10^-5	6.8x10^-5	16.0
	3	11:45			36	39.5	68	66	71	65.5	73	69.	41	41	41.5	42.	40	40.5	40.	51.5	56.5	51	50	51	50	50	52.		62.5	98.	2.5	6.5x10^-5	7.5x10^-5	30.0
NOT PLATED	4	14:10			34	35	221	221	222	221	219	215	35.5	35.5	35.5	61	37	37	36.5	176	193	165	169	176	180	200	188	71.	62.5	69.5	1.75	8x10^-5	6.5x10^-5	8.0
	5	15:10			35	36.5	171	171	171	170	166	161	37	37	37	56	39	39	38	132	147	145	125	132	133	154	142	71.	62.5	69.5	1.75	6.2x10^-5	6.x10^-5	16.0
	6	15:50			35	36.5	88	91	93	93	89	85	36.5	38	36.5	44.5	38	38	37	73	78	76	69	70	72	81	76	71	62.5	69.5	1.73	5.5x10^-5	6.5x10^-5	30.
		10-30-73																																
1/4" SQUARES	7	10:20			35	38	177	173	178	170	169	163.5	39	38	38	38.5	41.5	40	38	132	144	156	128.5	141.5	109	134	124	71.5	62.5	98.	2.5	7.x10^-5	4.4x10^-5	8.
	8	10:50			34.5	38	120	113	120	114	112	104	40	38	38	45.5	41	41.5	38	78	89	99	71.5	85	73	81.5	78	71.	62.5	98.	2.5	4.2x10^-5	4.1x10^-5	16.
	9	11:15			34.5	38	79.5	75	80	75	71.5	68	40	38	38.5	43.5	39	40.5	37.5	57	59	65	50.5	55.5	54	52.5	55.5	71	62.5	98	2.5	3.6x10^-5	5.3x10^-5	30.
1/2" SQUARES	10	1355			34.5	37.5	206	211	212	209	207	196	38.5	-	42	56.5	38	38	38	105	102	103	88	120	115	103	113	74	62.5	98	2.5	6.5x10^-5	4.2x10^-5	8
	11	1425			34.5	37.5	133	139	142	140	139.5	132	39.5	-	41	47	38.5	38.5	38.	71	77.5	76.5	71.5	87	84	83.5	87.	74	62.5	98	2.5	4.x10^-5	4.6x10^-5	16
	12	1455			36.5	40.	85.5	91	93.5	93.5	93.5	88	42	-	42	41.5	40.5	40.5	40.	58	60	59	55.5	66	62.5	64	67	74	62.5	98	2.5	4.x10^-5	5.x10^-5	30

REMARKS ____

INSPECTION

OPERATOR ____

INSPECTOR ____

NAVY ____

TEST ACCEPTED ____ REJECTED ____

MAKE INSPECTION STAMP

HSF 50-1-C 2/62

Hamilton Standard U A

TEMPERATURE LOG OF REFRIGERATION UNIT TEST

TURBINE ACCESSORY DEVELOPMENT GROUP

BOOTH No 25 TYPE OF TEST ICE PACK HEAT SINK SUBSYSTEM INTERFACE DEVELOPMENT

UNIT ____ SERIAL No ____ ASSEMBLY No ____ TEST SPEC ____ ENG PROJECT AND PLAN No B69-500-200A

HEAT EXCHANGER SER No ____ (PRIMARY) ____ (SECONDARY) ENGINEERING INSTRUCTION No ____

E W I No ____ WRITTEN BY ____

SHEET No 1
DATE 11-2-73
OPERATORS Laszczyk
ENGINEER SUPERVISING TEST Raibelon

	READING NO	TIME	RUNNING TIME	SPEED RPM	HX IN 25	HX OUT 26	TOP PLATE 1 (27)	2 (28)	3 (29)	4 (30)	5 (31)	BOTTOM PLATE 6 (32)	7 (33)	8 (34)	9 (35)	10 (36)	11 (37)	12 (38)	13 (39)	MIDDLE PLATE 14 (40)	15 (41)	16 (42)	17 (43)	18 (44)	19 (45)	20 (50)	21 (51)	T wall (16)	% FR	Heater Volts AC	Heater Amps AC	Vac at Plate	Vac at Reading	Header PSIA
1½" SQ T/C UP	1	1020			38	41	178	146	167	186	184	174	42	42	44	54	41.5	41	40.5	108	107	123	126	122	123	113	118	69	52.5	98	2.5	1.4x10^-4	1.2x10^-4	8
	2	1050			36	39	122	130	132	131	131	123	41.5	41.5	41.5	46.5	40.5	40.5	40	78	78	88	90	89	86	88	88.5	69	62.5	98	2.5	1.2x10^-4	8.4x10^-5	16
	3	1120			35.5	39	75	56	69	69	69	53	41.5	41.5	40.5	41.5	40	39.5	39	58	60	63	62.5	66	63.5	64.5	66	69	62.5	98	2.5	2.3x10^-5	8.6x10^-5	30
1½" SQ. T/C Down	4	1355			35.5	36.5	175.5	182	182	188	186	197	41	40.5	38	37	37.5	37	38	141	149	112	127	124	121	129	128	71	82.5	98	2.5	6.4x10^-5	6.0x10^-5	8
	5	1435			35.5	39	114	119	120	122	120	125	41	41	38	47	39	38.5	38.5	78	161	62	69	90	87	90	58	71	62.5	98	2.5	5.6x10^-5	5.5x10^-5	16
	6	1450			36	39.5	74	77	81.5	81.5	80	80.5	41	41	39	46	40	40	39.5	70	69	63	64	66	64	63	62	71	82.5	98	2.5	5.0x10^-5	6.5x10^-5	30
		11-6-73																																PSIG
1½" SQ T/C UP	7	0930			34.5	37.5	52	53	54.5	54	55.5	53	40	40	40	39.5	38.5	38.5	36.5	44	44.5	44.5	44.5	44.5	46.5	45	42.5	69	82.5	97.5	2.5	AMB	AMB	8.0
	8	0950			34.5	37.5	49	50.5	51.5	50.5	52	50	40.5	40	40	39.5	38.5	38.5	38.5	41	44	43.5	43	43	43	43.5	44.5	69	62.5	97.5	2.5	AMB	AMB	16.0

REMARKS ____

INSPECTION

OPERATOR ____
INSPECTOR ____
NAVY ____
TEST ACCEPTED ____ REJECTED ____
MARK INSPECTION STAMP

HSF 30-C 2/62

Hamilton Standard — U A

TEMPERATURE LOG OF REFRIGERATION UNIT TEST

TURBINE ACCESSORY DEVELOPMENT GROUP

BOOTH No 25 TYPE OF TEST Ice Pack Heat Sink Subsystem Interface Development

UNIT ______ SERIAL No ______ ASSEMBLY No ______ TEST SPEC ______ ENG PROJECT AND PLAN No DSY-SDC 200A

HEAT EXCHANGER SER No ______ (PRIMARY) ______ (SECONDARY) ENGINEERING INSTRUCTION No ______

E W I No ______ WRITTEN BY ______

SHEET No 1

DATE 11-5-73

OPERATORS Laszczyk

ENGINEER SUPERVISING TEST Rerbaum

TEMPERATURES °F →

Note	Reading No	Time	Running Time	Speed RPM	NA In (25)	NA Out (26)	1 (27)	2 (28)	3 (29)	4 (30)	5 (31)	6 (32)	7 (33)	8 (34)	9 (35)	10 (36)	11 (37)	12 (38)	13 (39)	14 (40)	15 (41)	16 (42)	17 (43)	18 (44)	19 (45)	20 (50)	21 (51)	Turb (16)
							← Top Plate					← Bottom Plate							→ ← Middle Plate								→	
1½" sq T/C w/ ½ load rated (alt sets)	1	1030			30	37	76.5	76.5	81	76.5	78	73.5	37	36.5	36.5	36.5	36.5	36.5	38	54	56.5	58	51	51.5	53	56	54	69
	2	1055			35	34	66	64	70	66	67	62.5	39.5	39.5	39	39	39	39	38	50	51.5	51	47.5	47.5	48.5	51.5	50	69
1½" sq T/C w/ ½ load rated (alt sets)	3	1305			34.5	37.5	135	139	142	140	138	130.5	31.5	38.5	37.5	37	39.5	40	37.5	95	99	101.5	84	90.5	88.5	94	91	70
	4	1335			35	31	94	99	102	99.5	97.5	41	39.5	39.5	36	36.5	39.5	40	38.5	67.5	70	65	62	68.5	67	61.5	68	69
	5	1405			34.5	32.5	71.5	76	78	76	73	69	39	39	31	39	39	37	38	54	54.5	52.5	51	51	53	55	53.5	68
	11-6-73																											
1½" sq T/C down ½ load rated (alt sets)	6	1110			34.5	37.5	216	235	230	231	223	206	38	37	37.5	50.5	39	39.5	38	116	111	127	121	138	86	102	100	69
	7	1220			36	38.5	131	153	149	149	142	129	39.5	42	39.5	47.5	41	41	39.5	42	82	100	81	99	64	82	75	69
	8	1225			35.5	34	89	92	96	100	94.5	87	37	43	34.5	45	40	40	40	61	70	74.5	66	78	54	64	61	69

Reading No	% FR	Sec Duct: TR Heater Volts	Sec Duct: TE Heater Amps	Bearings: at rate	Bearings: at reading	Bearings: Chamber Psia
1	62.5	92.5	2.5	Amb	Amb	8.0 Psig
2	62.5	97.5	2.5	Amb	Amb	16. Psig
3	62.5	98	2.5	6.2×10^-5	5.8×10^-5	8
4	62.5	98	2.5	4.8×10^-5	4.6×10^-5	16
5	62.5	94.5	2.5	6.0×10^-5	5.3×10^-5	30
6	62.5 / 69	94.5	2.5	4.1×10^-5	2.8×10^-5	8
7	62.5	96.5	2.5	2.6×10^-5	2.8×10^-5	16
8	62.5	94.5	2.5	2.0×10^-5	3.7×10^-5	30

REMARKS ______

INSPECTION

OPERATOR ______
INSPECTOR ______
NAVY ______
TEST ACCEPTED ______ REJECTED ______ MARK INSPECTION STAMP

HSF 90-C 2/62

Hamilton Standard — U A

TEMPERATURE LOG OF REFRIGERATION UNIT TEST
TURBINE ACCESSORY DEVELOPMENT GROUP

SHEET No 1
DATE 11-7-73
OPERATORS LASZCZYK

BOOTH No 25 TYPE OF TEST ICE PACK HEAT SINK SUBSYSTEM INTERFACE DEVELOPMENT
UNIT ____ SERIAL No ____ ASSEMBLY No ____ TEST SPEC ____ ENG PROJECT AND PLAN No B89-560 J0CA
HEAT EXCHANGER SER No ____ (PRIMARY) ____ (SECONDARY) ENGINEERING INSTRUCTION No ____
E W I No ____ WRITTEN BY ____
ENGINEER SUPERVISING TEST ROE BOLLEN

	Reading No	Time	Running Time	Speed RPM	HX IN (35)	HX OUT (36)	Top Plate 1 (27)	2 (28)	3 (29)	4 (30)	5 (31)	6 (32)	Bottom Plate 7 (33)	8 (34)	9 (35)	10 (36)	11 (37)	12 (38)	13 (39)	Middle Plate 14 (40)	15 (41)	16 (42)	17 (43)	18 (44)	19 (44)	20 (50)	21 (51)	Tube (16)	% F.R.	Heater Volts AC	Heater Amps AC	AP Rate		AP Bearing		Bladder PSIA	
1/8" SQ T/C 4P	1	1425			35	38	66	66.5	69	69.5	70.5	65.5	42	40	41	31.5	31	32.5	32.5	50	50	52	51.5	53.5	52	55.5	51	68	82.5	97.5	2.5	AMB		AMB		8 PSIG	
1/8" (LOAD) PLATED (Al' sq)	2	1445			34.5	37.5	59.5	60.5	62.5	63	64	59.5	48	40.5	41	36.5	37.5	37.5	31	46.5	48.5	48	50	49.5	50	52	49	68	82.5	97.5	2.5	AMB		AMB		16 PSIG	
	3	1025			35	38	166	168	173	173	179	176	42.5	39	42	40	38	38	37	98	98.5	115	116	115	129	133	116	69	82.5	98.5	2.5	7.5x10^-5		6.4x10^-5		8	
T/C 4P	4	1105			34	37	113	119	125.5	126	127	120.5	41.5	38.5	39.5	38	37	37.5	36.5	74	75.5	83	86.5	87	82.5	104	82.5	69	82.5	96.5	2.5	5.0x10^-5		4.5x10^-5		16	
⋮	5	1130			35	38.5	60	87.5	92.5	92	93	89	42.5	40.5	40.5	39	38.5	39	38	60.5	62	64	67.5	64.5	67.5	79	66	69	82.5	96.5	2.5	3.9x10^-5		5.3x10^-5		30	
TC Down	6	1420			33	36	176	183	179	180	181	190	37.5	38.5	36	36.5	36.5	36	36	130	132.5	96	108	107	116	116	112	70	82.5	98.5	2.5	5.5x10^-5		3.2x10^-5		8	
	7	1450			33.5	37	121	127.5	125	125	125	129	37.5	37.5	37	47	38	32.5	37	46.5	47.5	82	83.5	83.5	86	86	84	70	82.5	98.5	2.5	3.1x10^-5		3.3x10^-5		16	
	8	1510			34	37.5	64.5	89	89	88	87.5	87.5	39.5	39.5	38	44	39	38.5	38	71	71	67	65	64.5	65	65	63.5	70	82.5	98.5	2.5	3.6x10^-5		4.5x10^-5		30	

REMARKS ____

INSPECTION

OPERATOR ____
INSPECTOR ____
NAVY ____
TEST ACCEPTED ____ REJECTED ____ MARK INSPECTION STAMP

HSF 90-1C 2/62

Hamilton Standard

TEMPERATURE LOG OF REFRIGERATION UNIT TEST

TURBINE ACCESSORY DEVELOPMENT GROUP

SHEET No 1
DATE 12-5-73
OPERATORS Laszczyk
ENGINEER SUPERVISING TEST Roebozen

BOOTH No 25 TYPE OF TEST ICE PACK HEAT SINK SUB ASSEMBLY INTERFACE DEVELOPMENT
UNIT ______ SERIAL No ______ ASSEMBLY No ______ TEST SPEC ______ ENG PROJECT AND PLAN No B89-500-200A
HEAT EXCHANGER SER No ______ (PRIMARY) ______ (SECONDARY) ENGINEERING INSTRUCTION No ______
E W I No ______ WRITTEN BY ______

TEMPERATURES °F → ; ← TOP PLATE → ; ← BOTTOM PLATE → ; ← MIDDLE PLATE →

Note	Reading No	Time	Running Time	Speed RPM	HX IN (25)	HX OUT (26)	1 (27)	2 (28)	3 (29)	4 (30)	5 (31)	6 (32)	7 (33)	8 (34)	9 (35)	10 (36)
Flat 6" load plate T/C up	1	1325			35.5	38.5	225	227	229	225	228	226	41	-	38	-
	2	1350			36	39.	203	206	209	203	206	202	43	-	40	-
	3	1425			36	39.5	153	156	159	154	159	152	42.5	-	40.5	-
1/4" square T/C up	4	1655			35	36.5	261	263	266	264	267	261	40	-	~~40~~ 37.	-
	5	1725			35	37	196	197	201	201	202	197	41	-	38	
	6	1755			35	37.5	133	134	137	137.5	136	134	40		38	

Reading No	11 (37)	12 (38)	13 (39)	14 (40)	15 (41)	16 (42)	17 (43)	18 (44)	19 (45)	20 (50)	21 (51)	T amb (16)	% FR	Heater Volts AC	Heater Amps AC	Vacuum at plate	Vacuum at pump	PSIA bladder
1	40.5	40.	39	171	174	154	155	165	155	162	169	-	82.5	98.0	2.5	1.0x10^-4	7.2x10^-5	8.
2	42.5	41.5	40.5	122	125	117	116	119	117	132	119	-	82.5	96.	2.5	7.2x10^-5	6.7x10^-5	16.
3	41.5	42.	41.	86.5	89.	81.5	87	86	89	91	89	-	82.5	98	2.5	6.2x10^-5	7.5x10^-5	30.
4	40	38.5	38.5	146	145	148	152	150	145	142	145	73	82.5	79.	2.0	6.1x10^-5	6.1x10^-5	8.
5	40	39	39	117	116	119	125	124	116	113	116	73	82.5	79.5	2.0	5.9x10^-5	5.8x10^-5	16.
6	39.5	39.5	39	88	87	90	93	95	85	83.5	86	74	82.5	79.5	2.0	5.0x10^-5	6.5x10^-5	30.

REMARKS ______

INSPECTION

OPERATOR ______
INSPECTOR ______
NAVY ______
TEST ACCEPTED ______
REJECTED ______
M.RK INSPECTION STAMP

APPENDIX C

ICE CELL CONDUCTANCE VARIATIONS

SINGLE VERSUS MULTIPLE NODES

To correlate the difference between analytical and computer calculations of the ice cell conductance as a function of the amount of ice which has melted, the following discussion is presented. Bear in mind, however, that the discussion below does not represent the actual model size of conductance values but rather demonstrates the expected trends on the ice conductance as the number of nodes in the model varies.

Consider two generalized ice cell models, each of constant volume and cross-sectional area, per figure A-I. With the assumption of equal cross-sectional areas for the same material, each connector can be defined as follows:

$$C = f\left(\frac{1}{\Delta x}\right)$$ where Δx is the distance from the plate to node.

At the start of the melt cycle, the conductance C to the single node model is

$$C = \left(\frac{1}{L/2}\right) = (2/L).$$

However, the conductance at the start of the melt cycle for the 4 node model is

$$C = \left(\frac{1}{L/8}\right) = (8/L).$$

Thus, at the start of the melt cycle, the conductance to the 4 node model is greater than to the single node model.

Now, consider the case where the ice has almost completely melted. In this case, the conductance to the single node model is still (2/L) but the conductance through the four node model is approximately

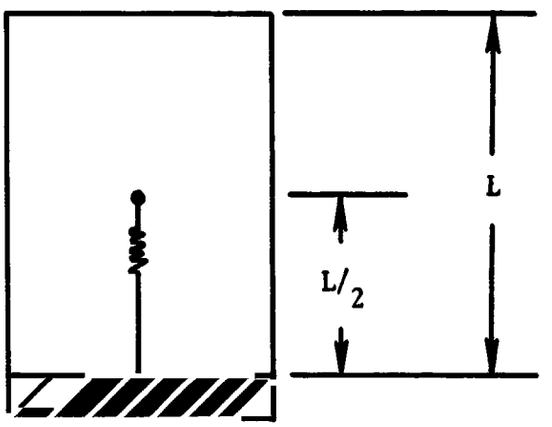

A) SINGLE NODE

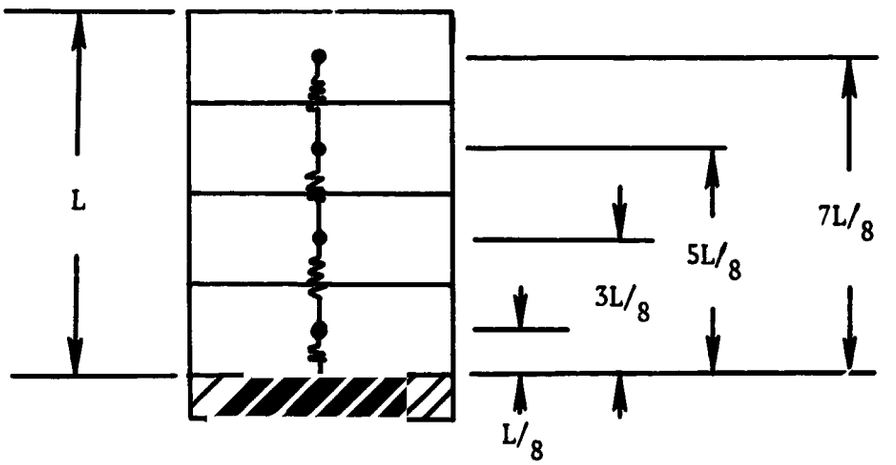

B) MULTIPLE NODE (4)

FIGURE A-1

$$C = \frac{1}{\frac{7}{8}L} = \frac{8L}{7}$$

Therefore, at the end of the melt cycle, the conductance to the single node model is larger than that of the 4 node model.

The result of these nodal effects is a change in slope of the ice cell conductance curve, per figure 25 of the main text.

APPENDIX D

SAMPLE ICE PACK HEAT SINK SUBSYSTEM

PRINT-OUT

Hamilton Standard

The attached print-out is a partial run of the full size Ice Pack Heat Sink Subsystem model with an LCG water flow rate of 240 lbm/hr at an LCG water inlet temperature of 70° F.

The time heading of each series of numbers is the time in minutes since the start of the melt cycle. All nodes of a major segment (reference figures 4 and 5, main text) are printed together on one line. All numbers under any time heading should be read per Table B-I.

TABLE B-I

PRINT-OUT LEGEND

** TIME = XXXXX						
Line 1	(Segment 1)	T_{LCG} Water (°F)	T_{HX} (°F)	T_{PLATE} (°F)	T_{ICE} Cell (°F)	Fraction of ice melted in cell
.	.	.	.	.	.	.
.	.	.	.	.	.	.
.	.	.	.	.	.	.
.	.	.	.	.	.	.
.	.	.	.	.	.	.
.	.	.	.	.	.	.
.	.	.	.	.	.	.
8	8	.	.	.	.	.

```
end
READY
loadgo icecst
INPUT HA OF LCG WATER
?
326.35
INPUT WATER INLET TEMP. AND STOP TIME(MINS.)
?
70. 40.
INPUT TIME STEP(MIN.), PRINT LOOPS, WCP OF LCG
?
.001 4000 240.
** TIME =   3.99872
  67.840   66.252   34.178   32.001    0.173
  65.824   64.341   34.148   32.001    0.161
  63.921   62.522   34.027   32.001    0.151
  62.139   60.828   33.916   32.001    0.142
  60.427   59.169   33.761   32.001    0.129
  58.825   57.647   33.661   32.001    0.122
  57.313   56.201   33.562   32.001    0.113
  55.896   54.855   33.477   32.001    0.107
** TIME =   7.98984
  67.855   66.278   34.425   32.001    0.368
  65.859   64.391   34.297   32.001    0.339
  63.973   62.587   34.348   32.001    0.321
  62.205   60.904   34.210   32.001    0.305
  60.504   59.254   34.005   32.001    0.279
  58.910   57.738   33.877   32.001    0.265
  57.404   56.297   33.754   32.001    0.249
  55.993   54.955   33.651   32.001    0.236
** TIME =  11.98097
  67.874   66.311   34.741   32.001    0.557
  65.905   64.457   34.974   32.001    0.512
  64.042   62.673   34.778   32.001    0.490
  62.293   61.007   34.603   32.001    0.466
  60.606   59.366   34.326   32.001    0.428
  59.022   57.858   34.154   32.001    0.408
  57.524   56.423   34.000   32.001    0.384
  56.118   55.085   33.871   32.001    0.365
** TIME =  15.97210
  67.900   66.356   35.165   32.001    0.750
  65.970   64.552   35.665   32.001    0.677
  64.139   62.793   35.378   32.001    0.656
  62.417   61.150   35.157   32.001    0.626
  60.748   59.522   34.760   32.001    0.573
  59.178   58.023   34.523   32.001    0.549
  57.689   56.596   34.323   32.001    0.518
  56.290   55.262   34.157   32.001    0.494
** TIME =  19.96321
  67.937   66.420   35.771   32.001    0.946
  66.069   64.696   36.748   32.001    0.830
  64.234   62.972   36.253   32.001    0.819
  62.602   61.365   35.984   32.001    0.783
  60.959   59.751   35.379   32.001    0.716
  59.406   58.264   35.035   32.001    0.690
  57.930   56.845   34.768   32.001    0.652
  56.539   55.517   34.547   32.001    0.623
** TIME =  23.95435
  68.397   67.220   43.522   41.862    1.000
  66.659   65.382   39.395   32.001    0.992
  64.944   63.684   38.058   32.001    0.984
  63.312   62.113   37.540   32.001    0.938
  61.683   60.487   36.377   32.001    0.854
  60.132   58.993   35.836   32.001    0.830
```

Hamilton Standard

APPENDIX E

PROTOTYPE HARDWARE PARTS LIST

ICE PACK ASSEMBLY

BOILER ASSEMBLY

ICE CHEST ASSEMBLY

NS P-1023.10

PARTS LIST

PARTS LIST NO. PLSVSK87308

PARTS LIST FOR ICE PACK ASSEMBLY

CODE IDENT. NO. 75030

MODEL ICE PACK HEAT SINK SUBSYSTEM - PHASE II

PAGE 001

NO. REQ'D.	1	2	3	4	5	6	7	8	PART IDENTIFICATION	CONFIGURATION NO.	SEMI-FINISHED NO.	Ltr	Item
1	S	V	S	K	8	7	3	0	8 ASSY, ICE PACK				
1		S	V	S	K	8	7	3	08-100 ASSY, MNTG & HARNESS				
1			S	V	S	K	8	7	308-200 ASSY, MOUNTING				
1				S	V	S	K	8	7206 ASSY MANIFOLD				
1					S	V	S	K	87306-104 PLATE GUIDE				
1					S	V	S	K	87306-105 STEM, ACTUATOR				
1					S	V	S	K	87306-106 HOUSING				
4					S	V	S	K	87306-107 TUBE				
2					S	V	S	K	87306-108 TUBE				
2					S	V	S	K	87306-109 PLUG				
1					S	V	S	K	87306-110 SEAL, O-RING				
1					S	V	S	K	87306-111 SEAL, SLIPPER				
1					A	N	8	1	4-12L PLUG				
1					M	S	9	0	20-04 SEAL, O-RING				
1					M	S	9	0	20-12 SEAL, O-RING				
1					M	S	2	4	693-C-372 [illegible] MACH F.H.				
1					S	2	4	T	-4½-4 VALVE CHECK			A	
1					L	C	-	0	45H-155 SPRING			B	
1				S	V	S	K	8	7307 ASSY ACCUMULATOR & PLATE				
1					S	V	S	K	87307-100 ASSY, ACCUMULATOR				
1						S	V	S	K 87307-102 BRACKET, MTG				
1						S	V	S	K 87307-103 BRACKET, LEVER				
1						S	V	S	K 87307-104 LEVER				
1						S	V	S	K 87307-105 BRACKET, LEVER				
1						S	V	S	K 87307-106 LINK				
1						S	V	S	K 87307-107 ACCUMULATOR				
1						S	V	S	K 87307-108 SPRING				
1						S	V	S	K 87307-110 ROD				
1						S	V	S	K 87307-113 SPRING				
4						A	N	5	01AD10-8 SCREW, MACH				
4						A	N	5	01AD10-10 SCREW, MACH				
2						A	N	5	10 C8R10 SCREW, MACH F.H.				
1						A	N	9	60C8L WASHER				
9						A	N	9	60C10L WASHER				
1						M	S	9	245-22 PIN, COTTER				
1						M	S	9	390-450 PIN, STRAIGHT-HDLESS				
1						M	S	2	1043-08 NUT, SELF-LOCKING				
5						M	S	2	1043-3 NUT, SELF-LOCKING				
1						6	9	2	91C4-18 PIN, STRAIGHT-HD'D				
1						9	X	2	5-0646 BOLT, SHOULDER			C	
1						9	X	2	5-0848 BOLT, SHOULDER			C	

PREPARED BY	DATE	CHECKED BY	DATE	PRELIMINARY DRAFTING APPR.	DATE
R Loeffler	10/14/74				
FINAL DRAFTING APPROVAL	DATE I-1	APPROVED BY			DATE 10/15/74

HS P-1028.10

PARTS LIST

PARTS LIST NO. PLSVSK87308

PARTS LIST FOR ICE PACK ASSEMBLY

CODE IDENT. NO. 78030

MODEL ICE PACK HEAT SINK SUBSYSTEM - PHASE II

NO. REQ'D.	1	2	3	4	5	6	7	8	PART IDENTIFICATION	CONFIGURATION NO.	SEMI-FINISHED NO.	AIR	Item
1					S	V	S	K	87307-200 ASSY, PLATE				
1						S	V	S	K87307-121 PLATE, MOUNTING				
1						S	V	S	K87307-122 PLATE, SPACER				
2						S	V	S	K87307-130 BASE, LATCH				
3						M	S	2	1209-F1-10 INSERT, HELICOIL				
1				S	V	S	K	8	7309-101 LATCH				
AR				S	V	S	K	8	7303-102 TUBING, FLEXIBLE				
12				S	V	S	K	8	7309-103 CLAMP, AERO SEAL				
2				S	V	S	K	8	7308-104 PLUG				
1				S	V	S	K	8	7302-105 TUBE				
1				S	V	S	K	8	7304-106 TEE				
1				S	V	S	K	8	7308-107 PLUG				
2				S	V	S	K	8	7308-108 ADAPTER				
2				S	V	S	K	8	7308-109 ELBOW				
1				S	V	S	K	8	7302-110 TUBE				
AR				S	V	S	K	8	7303-111 TUBING, FLEXIBLE				
1				S	V	S	K	8	7303-112 TUBE				
1				S	V	S	K	8	7314 BRACKET, MOUNTING				
1					S	V	S	K	87314-1 BRACKET				
5					S	V	S	K	87314-2 RING, CLIP				
10					M	S	2	0	470AD6-5 RIVET, RD HD				
1				S	V	S	K	S	88478 ASSY, HX/BLADDER				
2					S	V	S	K	88476 ASSY, HEAT EXCHANGER				
2						S	V	S	K88472 NIPPLE, HOSE				
1						S	V	S	K88473 COVER, HX				
1						S	V	S	K88474 HOUSING, HX				
3						S	V	S	K88475-103 FIN, RUFFLED				
2						S	V	S	K88475-104 FIN, RUFFLED				
2						S	V	S	K88475-105 FIN, RUFFLED				
1					S	V	S	K	88477 FRAME, HX RETAINER				
1					S	V	S	K	88479 ASSY, BLADDER				
1						S	V	S	K88479-102 BLADDER				
1						S	V	S	K88479-104 NIPPLE, BLADDER				
1						S	V	S	K88479-105 TUBE, INLET				
1						S	V	S	K88479-106 FLANGE				
AR						S	T	S	V090-2 THREAD				
AR						S	T	S	V098-1 TAPE, SEALING				
6					S	V	S	K	88490 SPRING				
2					A	N	5	0	0A32-5 SCREW, MACH				
2					A	N	9	6	08CL WASHER				
2					M	S	2	1	043-09 NUT, SELF LOCKING				

PREPARED BY	DATE	CHECKED BY	DATE	PRELIMINARY DRAFTING APPR.	DATE
[signature]	10/14/74				
FINAL DRAFTING APPROVAL	DATE F-2	APPROVED BY			DATE 10/15/74

NB P-1038.10

PARTS LIST

PARTS LIST NO. PLSVSK87308

PARTS LIST FOR ICE PACK ASSEMBLY

CODE IDENT. NO. 78030

MODEL ICE PACK HEAT SINK SUBSYSTEM - PHASE II

NO. REQ'D.	1	2	3	4	5	6	7	8	PART IDENTIFICATION		CONFIGURATION NO.	SEMI-FINISHED NO.	FIR	Item
11				A	N	5	0	1	AD 10-12	SCREW, MACH				
4				A	N	5	0	1	AD 10-14	SCREW, MACH				
1				A	N	7	4	2	66C	CLAMP, CUSHION				
16				A	N	9	6	0	C8L	WASHER				
28				A	N	9	6	0	C10L	WASHER				
8				M	S	1	6	7	96-14	SCREW, INT HEX				
AR				M	S	2	0	9	95C20	LOCKWIRE				
8				M	S	2	1	0	43-08	NUT, SELF LOCKING				
13				M	S	2	1	0	43-3	NUT, SELF LOCKING				
1				6	9	2	8	5	-258	SCREW, INT HEX				
18				5	9	3	6	0	1-5	WASHER, SHOULDER				
4			S	V	S	K	8	7	309	ASSY, HARNESS				
1				S	V	S	K	8	7309-1	WEB, ADJUSTABLE				
1				S	V	S	K	8	7309-2	WEB, FIXED				
2				S	V	S	K	[illegible]	7309-3	FITTING, HOOK END				
1				S	V	S	K	[illegible]	7309-4	ADJUSTER, WEB				
AR				S	T	S	V	0	93-4	THREAD				
		S	V	S	K	[illegible]	[illegible]	-	32-500	ASSY, BOILER	P1			
		S	V	S	K	8	9	4	32-600	ASSY, ICE CHEST	P1			

NOTE A - OBTAINABLE FROM JAMES POND & CLARK, INC

NOTE B - OBTAINABLE FROM LEE SPRINGS CO, BKLYN N.Y.

NOTE C - OBTAINABLE FROM STOCK DRIVE PRODUCTS, NEW HYDE PARK, N.Y.

- FINAL PAGE -

PREPARED BY	DATE	CHECKED BY	DATE	PRELIMINARY DRAFTING APPR.	DATE
[signature]	10/14/74				
FINAL DRAFTING APPROVAL	DATE E-3	APPROVED BY			DATE
		[signature]			10/15/74

NS P-1028.10

PARTS LIST

PARTS LIST NO. PL SVSK 88482-500

PARTS LIST FOR BOILER ASSEMBLY

CODE IDENT. NO. 78030

MODEL ICE PACK HEAT SINK SUBSYSTEM - PHASE II

NO. REQ'D.	1	2	3	4	5	6	7	8	PART IDENTIFICATION	CONFIGURATION NO.	SEMI-FINISHED NO.	PIR	Item
1	S	V	S	K	8	8	4	8	2-500 ASSY, BOILER				
2		S	V	S	K	8	7	3	15-100 FITTING, CAP				
1			S	V	S	K	8	7	315-110 FITTING, QUICK DISCON.				
1			A	N	9	1	3	-	22 PLUG, PIPE				
2		S	V	S	K	8	7	3	15-200 FITTING, PLUG				
2		S	V	S	K	9	8	4	02-100 BOILER				
1			S	V	S	K	8	8	02-101 PLATE, BOILER				
19			S	V	S	K	8	8	482-103 PANEL, DIVIDER				
20			S	V	S	K	8	8	482-104 PLATE, PERFORATED				
2			S	V	S	K	8	8	482-105 PANEL, END				
1			S	V	S	K	8	8	482-106 PANEL				
1			S	V	S	K	8	8	482-107 PANEL, REAR				
4			S	V	S	K	8	8	482-108 BOSS				
1			S	V	S	K	8	8	482-109 FLANGE				
1			S	V	S	K	8	8	482-111 HEADER				
10			S	V	S	K	8	8	482-118 RIB				
8			S	V	S	K	8	8	482-119 SID				
1			S	V	S	K	8	8	482-121 BOSS				
1			S	V	S	K	8	8	482-[illegible] BOSS				
1			A	N	9	0	5	6	C1032-10 SCREW, SET				
4			M	S	2	1	2	0	2C0820 INSERT, HELICOIL				
1			M	S	2	1	2	0	9F1-15 INSERT, HELICOIL				
2		S	V	S	K	8	8	4	82-110 COVER				
108		S	V	S	K	8	8	4	82-116 WICK				
8		S	V	S	K	8	8	4	82-117 WICK				
2		S	V	S	K	8	8	4	82-120 SPACER				
2		S	V	S	K	8	8	4	82-122 SEAL				
2		S	V	S	K	8	8	4	82-123 GUIDE				
2		S	V	S	K	8	8	4	82-124 HOOK				
36		S	V	S	K	8	9	4	82-300 ASSY, EXPANSION LIM				
2			S	V	S	K	8	9	482-112 PLATE, EXPANSION LIM				
1			S	V	S	K	8	9	482-113 SPACER, RUBBER				
AR			S	T	S	V	0	8	3-20 THREAD				
12		S	V	S	K	8	8	4	82-400 ASSY, EXPANSION LIM				
2			S	V	S	K	8	8	482-114 PLATE, EXPANSION LIM				
1			S	V	S	K	8	8	482-115 SPACER, RUBBER				
AR			S	T	S	V	0	8	3-20 THREAD				
AR		S	V	7	1	2	8	2	5 CABLE, STRANDED FLEX				
8		S	V	7	2	1	7	8	2 SLEEVE, COMPRESSION				

PREPARED BY	DATE	CHECKED BY	DATE	PRELIMINARY DRAFTING APPR.	DATE
[signature]	10/14/74				
FINAL DRAFTING APPROVAL	DATE	APPROVED BY	DATE
	E-4	[signature]	10/15/74

HS P-1028.10

PARTS LIST

PARTS LIST NO. PLSVSK88482-500

PARTS LIST FOR BOILER ASSEMBLY

CODE IDENT. NO. 73030

MODEL ICE PACK HEAT SINK SUBSYSTEM - PHASE II

PAGE 002

NO. REQ'D.	1	2	3	4	5	6	7	8	PART IDENTIFICATION	CONFIGURATION NO.	SEMI-FINISHED NO.	NR	Item
12		A	N	5	0	0	A	D	3-8	SCREW, MACH			
12		A	N	5	0	0	A	D	8-10	SCREW, MACH			
44		A	N	5	0	0	A	D	8-12	SCREW, MACH			
4		A	N	5	0	7	C	8	2288	SCREW, MACH F.H.			
2		A	N	9	1	2	-	1	D	PLUG, PIPE			
96		A	N	9	6	0	C	2	L	WASHER			
18		M	S	1	6	5	5	5	-636	PIN, STRAIGHT - HDLESS			
56		M	S	2	1	0	4	3	-08	NUT, SELF LOCKING			
4		S	V	0	0	8	K	1	6-000C11	TUBING, SHRINKABLE			
8		-	-	8	9	7	-	A	E	WASHER, SEAL			
										- FINAL PAGE -			

PREPARED BY [signature]	DATE 10/14/74	CHECKED BY	DATE	PRELIMINARY DRAFTING APPR.	DATE
FINAL DRAFTING APPROVAL	DATE F-5	APPROVED BY [signature]			DATE 10/15/74

HB P-1028.1D

PARTS LIST

PARTS LIST NO. PL SVSK 88482-600

PARTS LIST FOR ICE CHEST ASSEMBLY

CODE IDENT. NO. 78030

MODEL ICE PACK HEAT SINK SUBSYSTEM - PHASE II

NO. REQ'D.	1	2	3	4	5	6	7	8	PART IDENTIFICATION	CONFIGURATION NO.	SEMI-FINISHED NO.	NR	Item
1	S	V	S	K	8	8	4	8	2-600 ASSY, ICE CHEST				
2		S	V	S	K	9	9	4	82-200 ICE CHEST				
1			S	V	S	K	9	8	482-102 PLATE, BOILER				
21			S	V	S	K	8	8	482-103 PANEL, DIVIDER				
2			S	V	S	K	8	9	482-106 PANEL				
4			S	V	S	K	9	8	482-108 BOSS				
1			S	V	S	K	8	9	482-109 FLANGE				
10			S	V	S	K	9	8	482-118 RIB				
8			S	V	S	K	9	5	482-119 RIB				
1			S	V	S	K	F	9	482-139 BOSS				
1			A	N	S	6	5	E	C1032-10 SCREW, SET				
4			M	S	2	1	2	0	9C0820 INSERT, HELICOIL				
1			M	S	2	1	2	0	9F1-15 INSERT, HELICOIL				
2			S	V	S	K	8	9	4	82-110 COVER				
108			S	V	S	K	9	0	4	82-116 WICK				
8			S	V	S	K	8	9	4	82-117 WICK				
2			S	V	S	K	9	9	-	82-120 SPACER				
2			S	V	S	K	8	9	4	82-122 SEAL				
2			S	V	S	K	9	9	-	82-123 GLIDE				
2			S	V	S	K	8	8	4	82-124 HOOK				
36			S	V	S	K	8	8	4	82-300 ASSY, EXPANSION LIM				
2				S	V	S	K	8	9	482-112 PLATE EXPANSION LIM				
1				S	V	S	K	8	8	482-113 SPACER, RUBBER				
AR				S	T	S	V	0	8	3-20 THREAD				
12			S	V	S	K	8	8	4	82-400 ASSY, EXPANSION LIM				
2				S	V	S	K	8	9	482-114 PLATE, EXPANSION LIM				
1				S	V	S	K	8	8	482-115 SPACER, RUBBER				
AR				S	T	S	V	0	8	3-20 THREAD				
12			A	N	S	0	0	A	D	8-8 SCREW, MACH				
56			A	N	S	0	0	A	D	8-12 SCREW, MACH				
4			A	N	S	0	7	C	P	832R8 SCREW, MACH F.H.				
2			A	N	9	1	3	-	1	L PLUG, PIPE				
96			A	N	9	6	0	C	8	L WASHER				
18			M	S	1	6	5	5	5	-336 PIN, STRAIGHT-HDLESS				
56			M	S	2	1	0	4	3	-08 NUT, SELF LOCKING				
8			A	N	9	9	7	-	A	5 WASHER, SEAL				

— FINAL PAGE —

PREPARED BY	DATE	CHECKED BY	DATE	PRELIMINARY DRAFTING APPR.	DATE
[signature]	10/14/74				
FINAL DRAFTING APPROVAL	DATE	APPROVED BY			DATE
	E-6	[signature]			10/15/74

APPENDIX F

PERFORMANCE TEST PLAN

Hamilton Standard — Division of United Aircraft Corporation

ECS-2124-L-079

ICE PACK HEAT SINK SUBSYSTEM - PHASE II

PERFORMANCE TEST PLAN

PREPARED UNDER CONTRACT NAS 2-7011

BY

HAMILTON STANDARD

DIVISION OF UNITED AIRCRAFT CORPORATION

WINDSOR LOCKS, CONNECTICUT

FOR

NATIONAL AERONAUTICS AND SPACE ADMINISTRATION

AMES RESEARCH CENTER

MOFFETT FIELD, CALIFORNIA

JUNE 1974

Prepared by: G. Roebelen
Program Engineer

Approved by: F. H. Greenwood
Program Manager

1.0 SCOPE

This plan of test defines the performance tests to be performed by Hamilton Standard on the Phase II Ice Pack Heat Sink Subsystem, SVSK 87308. The acceptance test program is intended to verify the functional operation of the Phase II Ice Pack Heat Sink Subsystem.

2.0 TEST SEQUENCE

The performance test program consists of the following tests performed in the sequence defined:

1. Evaluation of ice chest freeze/thaw performance.
2. Evaluation of water boiler freeze/thaw performance.
3. Evaluation of water boiler boiling performance.

Deviation from the test sequence or test procedure requires approval of the cognizant program engineer.

3.0 TEST ENVIRONMENT

The test environment for all portions of this test will be vacuum.

4.0 TEST EQUIPMENT

All portions of this test program will be performed in the Hamilton Standard Space Systems Department Space Laboratory. Except for the Rig 25 vacuum facility, portable equipment compatible with the test unit and the test requirements as defined by this plan of test will be utilized.

5.0 DEFINITION OF TESTS

5.1 Evaluation of Ice Chest Freeze/Thaw Performance

5.1.1 Instrumentation and Equipment

Qty	Item	Range	Accuracy
1	DC Power Supply	0-30 VDC @ 3 ampere	± 0.1 volt
1	DC Voltmeter	0-30 VDC	± 0.05 volt
1	DC Ammeter	0-3 ampere	± 0.05 ampere
1	AC Voltmeter	0-120 VAC	± 1.0 volt
1	AC Ammeter	0-10 amp	± 0.1 ampere
1	Flowmeter	0-0.1 gpm	± 0.005 gpm
1	Flowmeter	0-0.425 gpm	± 0.025 gpm
1	Flowmeter	0-0.58 gpm	± 0.025 gpm
4	Pressure Gauge	0-30 psia	± 0.05 psi
1	Pressure Gauge	0-20 mmHg ABS	± 0.05 mmHg
1	Coolant Pump	0.48-0.53 gpm	± 0.02 gpm
1	Heat Load	0-2000 Btu/hr	± 20 Btu/hr
1	L&N Thermocouple . Readout	0-100°F	± 0.4°F
4	Thermocouple	0-100°F	± 0.1°F

5.1.2 Test Set-up

This test is performed on Rig 25 in the Space Systems Department Space Laboratory. Figure 1 schematically illustrates the test set-up.

5.1.3 Test Procedure

a. Install the ice pack heat exchanger assembly in the vacuum chamber of Rig 25 and plumb the hardware and wiring per Figure 1.

b. Close the vapor passage valve.

c. Set the power supply to 27 vdc and start the pump/motor. Close the bypass flow valve. Open the flowmeter bypass valve. Adjust the heat exchanger flow valve to obtain a system flow of 0.5 gpm. Fill system with water through water fill port. Bleed air from system utilizing water fill port valve and air bleed vent valve and pressurize pump inlet to 5 psig.

d. Check thermocouples T_1, T_2, T_3, T_4.

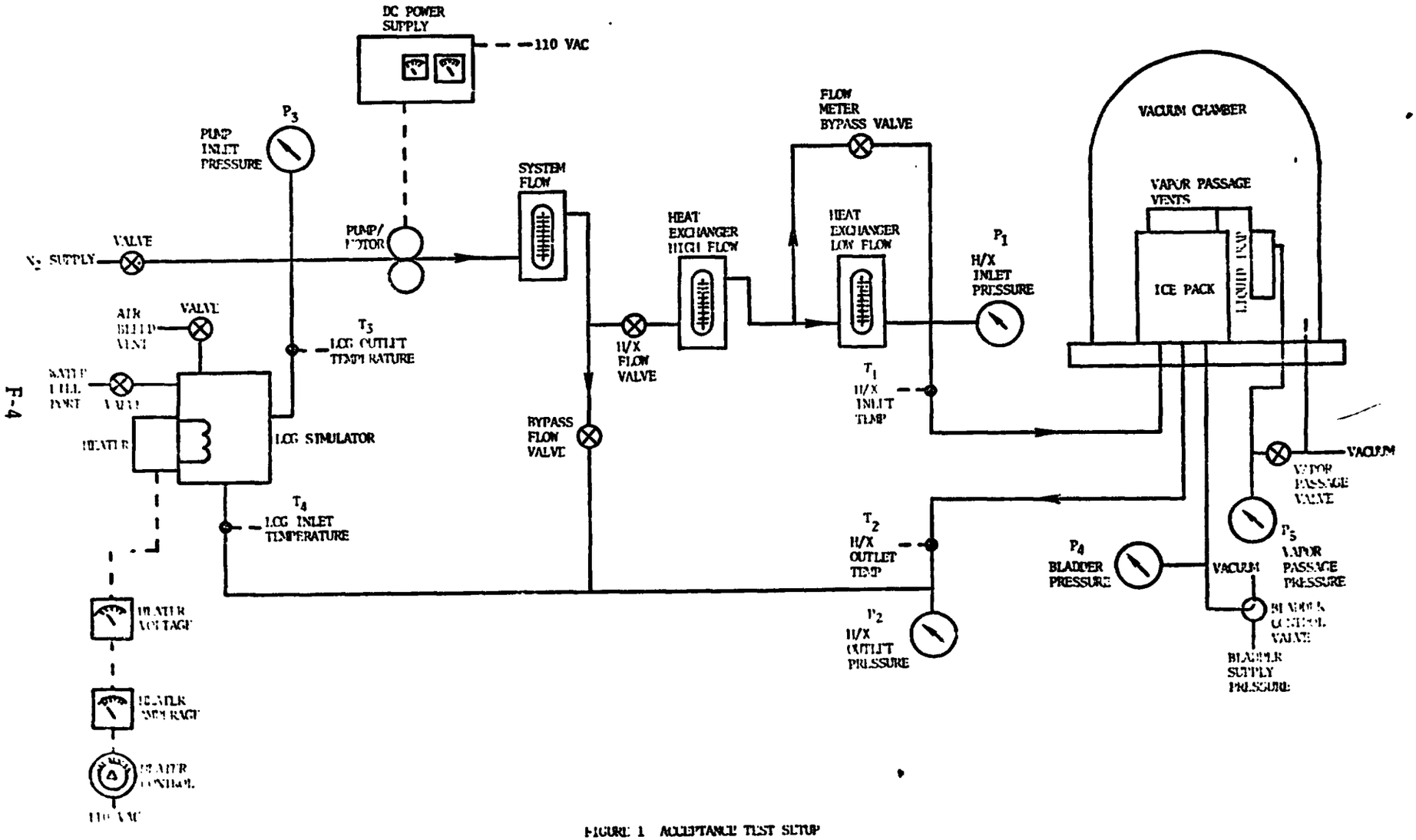

FIGURE 1 ACCEPTANCE TEST SETUP

5.1.3 Test Procedure - Continued

e. Switch the bladder control valve to vacuum.

f. Chill the system to 45°F using an external cooling pack applied to heat exchanger.

g. Install an insulated frozen ice chest on the heat exchanger assembly. Close the vacuum chamber and evacuate to 10^{-4} mmHg (0.1 micron).

h. Adjust the heater control to apply 2000 Btu/hr (587 volt amperes) to the LCG simulator.

i. When the outlet temperature of the LCG simulator reaches 58°F pressurize the bladder to 20 psia.

j. Adjust the heat exchanger flow valve and bypass flow valve to maintain the LCG inlet temperature at 50°F and the system flow at 0.5 gpm. When the bypass flow reaches zero, continue running until the heat exchanger outlet temperature reaches 65°F. Shut off the heater and the pump/motor. Repressurize the chamber and remove the ice chest. Refreeze the ice chest.

k. Repeat c., d., e., and g..

l. Adjust the heater control to apply 1500 Btu/hr (440 volt-amperes) to the LCG simulator.

m. When the outlet temperature of the LCG simulation reaches 76°F pressurize the bladder to 20 psia.

n. Adjust the heat exchanger flow valve and bypass flow valve to maintain the LCG inlet temperature at 70°F and the system flow at 0.5 gpm. When the bypass flow reaches zero, continue running until the heat exchanger outlet temperature reaches 80°F. Shut off the heater and the pump/motor. Repressurize the chamber and remove the ice chest. Refreeze the ice chest.

o. Repeat k., l., m., n., except adjust heater control to 75° Btu/hr (220 volt-amperes) and pressurize the bladder when the outlet temperature of the LCG simulator reaches 88°F. Adjust valves to maintain the LCG in - let temperature at 85°F and shut down when the heat exchanger outlet temperature reaches 90°F.

5.1.4 Test Requirements

Each of the tests must be run until the heat exchanger outlet temperature cannot be maintained at the specified temperature. For each run record the following condition vs time:

1. Heater voltage
2. Heater amperage
3. System flow
4. Heat exchanger flow
5. Pump inlet pressure
6. Bladder pressure
7. Heat exchanger inlet pressure
8. Heat exchanger outlet pressure
9. Heat exchanger inlet temperature
10. Heat exchanger outlet temperature
11. LCG inlet temperature
12. LCG outlet temperature
13. Vacuum chamber pressure

5.2 Evaluation of Water Boiler Freeze/Thaw Performance

5.2.1 Instrumentation and Equipment

Qty	Item	Range	Accuracy
1	DC Power Supply	0-30 VDC @ 3 ampere	± 0.1 volt
1	DC Voltmeter	0-30 VDC	± 0.05 volt
1	DC Ammeter	0-3 ampere	± 0.05 ampere
1	AC Voltmeter	0-120 VAC	± 1.0 volt
1	AC Ammeter	0.10 ampere	± 0.1 ampere
1	Flowmeter	0-0.1 gpm	± 0.005 gpm
1	Flowmeter	0-0.425 gpm	± 0.025 gpm
1	Flowmeter	0-0.58 gpm	± 0.025 gpm
4	Pressure Gauge	0-30 psia	± 0.05 psi
1	Pressure Gauge	0-20 mmHg ABS	± 0.05 mmHg
1	Coolant Pump	0.48-0.53 gpm	± 0.02 gpm
1	Heat Load	0-2000 Btu/hr	± 20 Btu/hr
1	L&N Thermocouple Readout	0-100°F	± 0.4°F
4	Thermocouple	0-100°F	± 0.1°F

5.2.2 Test Set-up

This test is performed on Rig 25 in the Space Systems Department Space Laboratory. Figure 1 schematically illustrates the test set-up.

5.2.3 Test Procedure

a. Install the ice pack heat exchanger assembly in the vacuum chamber of Rig 25 and plumb the hardware and wiring per Figure 1.

b. Close the vapor passage valve.

c. Set the power supply to 27 vdc and start the pump/motor. Close the bypass flow valve. Open the flowmeter bypass valve. Adjust the heat exchanger flow valve to obtain a system flow of 0.5 gpm. Fill system with water through air bleed vent valve. Close water fill port valve and air bleed vent valve and pressure pump inlet to 5 psig.

d. Check thermocouples T_1, T_2, T_3, T_4.

e. Switch the bladder control valve to vacuum.

f. Chill the system to 45°F using an external cooling pack applied to heat exchanger.

g. Install an insulated frozen water boiler with the two vapor passage vents plugged onto the heat exchanger assembly. Close the vacuum chamber and evacuate to 10^{-4} mmHg (0.1 micron).

h. Adjust the heater control to apply 2000 Btu/hr (587 volt amperes) to the LCG simulator.

i. When the outlet temperature of the LCG simulator reaches 58°F pressurize the bladder to 20 psia.

j. Adjust the heat exchanger flow valve and bypass flow valve to maintain the LCG inlet temperature at 50°F and the system flow at 0.5 gpm. When the bypass flow reaches zero, continue running until the heat exchanger outlet temperature reaches 65°F. Shut off the heater and the pump/motor. Repressurize the chamber and remove the ice chest. Refreeze the ice chest.

5.2.3 Test Procedure - Continued

k. Repeat c., d., e., and g..

l. Adjust the heater control to apply 1500 Btu/hr (440 volt-amperes) to the LCG simulator.

m. When the outlet temperature of the LCG simulation reaches 76°F pressurize the bladder to 20 psia.

n. Adjust the heat exchanger flow valve and bypass flow valve to maintain the LCG inlet temperature at 70°F and the system flow at 0.5 gpm. When the bypass flow reaches zero, continue running unitl the heat exchanger outlet temperature r ches 80°F. Shut off the heater and the pump/motor. P ressurize the chamber and remove the ice chest. Refreeze the ice chest.

o. Repeat k., l., m., n., except adjust heater control to 75°F Btu/hr (220 volt-amperes) and pressurize the bladder when the outlet temperature of the LCG simulator reaches 88°F. Adjust valves to maintain the LCG in - let temperature at 85°F and shut down when the heat exchanger outlet temperature reaches 900F.

5.2.4 Test Requirements

Each of the tests must be run until the heat exchanger outlet temperature cannot be maintained at the specified temperature. For each run record the following condition vs time:

1. Heater voltage
2. Heater amperage
3. System flow
4. Heat exchanger flow
5. Pump inlet pressure
6. Bladder pressure
7. Heat exchanger inlet pressure
8. Heat exchanger outlet pressure
9. Heat exchanger inlet temperature
10. Heat exchanger outlet temperature
11. LCG inlet temperature
12. LCG outlet temperature
13. Vacuum chamber pressure

5.3 Evaluation of Water Boiler Boiling Performance

5.3.1 Instrumentation and Equipment

Qty	Item	Range	Accuracy
1	DC Power Supply	0-30 VDC @ 3 ampere	± 0.1 volt
1	DC Voltmeter	0-30 VDC	± 0.05 volt
1	DC Ammeter	0-3 ampere	± 0.05 ampere
1	AC Voltmeter	0-120 VAC	± 1.0 volt
1	AC Ammeter	0-10 ampere	± 0.1 ampere
1	Flowmeter	0-0.1 gpm	± 0.005 gpm
1	Flowmeter	0-0.425 gpm	± 0.025 gpm
1	Flowmeter	0-0.58 gpm	± 0.025 gpm
4	Pressure Gauge	0-30 psia	± 0.05 psi
1	Pressure Gauge	0-20 mmHg ABS	± 0.05 mmHg
1	Coolant Pump	0.48-0.53 gpm	± 0.02 gpm
1	Heat Load	0-2000 Btu/hr	± 20 Btu/hr
1	L&N Thermocouple Readout	0-100°F	± 0.4°F
4	Thermocouple	0-100°F	± 0.1°F

5.3.2 Test Set-up

This test is performed on Rig 25 in the Space Systems Department Space Laboratory. Figure 1 schematically illustrates the test set-up.

5.3.3 Test Procedure

a. Install the ice pack heat exchanger assembly in the vacuum chamber of Rig 25 and plumb the hardware and wiring per Figure 1.

b. Close the vapor passage valve.

c. Set the power supply to 27 vdc and start the pump/motor. Close the bypass flow valve. Open the flowmeter bypass valve. Adjust the heat exchanger flow valve to obtain a system flow of 0.5 gpm. Fill system with water through air bleed vent valve. Close water fill port valve and air bleed vent valve and pressure pump inlet to 5 psig.

d. Check thermocouples T_1, T_2, T_3, T_4.

5.3.3 Test Procedure - Continued

e. Switch the bladder control valve to vacuum.

f. Install an insulated unfrozen water boiler on the heat exchanger assembly. Unplug the vapor passage vents and hook up to the vacuum line.

g. Close the vapor passage valve. Close the vacuum chamber and evacuate to 10^{-4} mmHg (0.1 micron). Pressurize the bladder to 20 psia.

h. Adjust the heater control to apply 2000 Btu/hr (587 volt amperes) to the LCG simulator.

i. Open the vapor passage valve and run until the heat exchanger outlet temperature stabilizes.

j. Adjust the heater control to apply 1500 Btu/hr (440 volt-amperes) to the LCG simulator.

k. Run until the heat exchanger outlet temperature stabilizes.

l. Adjust the heater control to apply 750 Btu/hr (220 volt-amperes) to the LCG simulator.

m. Run until the heat exchanger outlet temperature stabilizes or reaches 32°F.

n. Shut off the heater and repressurize the chamber.

o. Switch the bladder control valve to vacuum.

p. Replug one of the vapor passage vents

q. Close the vapor passage valve. Close the vacuum chamber and evacuate to 10^{-4} mmHg (0.1 micron). Pressurize the bladder to 20 psia.

r. Adjust the heater control to apply 750 Btu/hr (220 volt-amperes) to the LCG simulator.

s. Run until the heat exchange outlet temperature stabilizes.

t. Adjust the heater control to apply 1500 Btu/hr (440 volt-amperes) to the LCG simulator.

u. Run until the heat exchange outlet temperature stabilizes.

5.3.3 Test Procedure - Continued

v. Shut off the heater and pump/motor. Repressurize the chamber and remove the water boiler.

5.3.4 Test Requirements

Each of the tests must be run until the heat exchanger outlet temperature has stabilized or reached 32°F. For each run record the following conditions vs time:

1. Heater voltage
2. Heater amperage
3. System flow
4. Heat exchanger flow
5. Pump inlet pressure
6. Bladder pressure
7. Heat exchanger inlet pressure
8. Heat exchanger outlet pressure
9. Heat exchanger inlet temperature
10. Heat exchanger outlet temperature
11. LCG inlet temperature
12. LCG outlet temperature
13. Vacuum chamber pressure
14. Vapor passage pressure

APPENDIX G

PERFORMANCE TEST LOG SHEETS

HSF 175 1A 1/66

Hamilton Standard DIVISION OF UNITED AIRCRAFT CORPORATION
WINDSOR LOCKS, CONNECTICUT 06096

SPACE & LIFE SYSTEMS LABORATORY
LOG OF TEST

TYPE OF TEST: ICE PACK ICE CHEST
TEST ENGINEER: G. ROEBELEN
NAME OF RIG: 35
PROJECT & ENG ORDER NO: 389-500-300A

SHEET 1 OF 2 DATE 10-2-74
TEST PLAN NO ECS-2124-L-079
MODEL NO
PART NO.
SERIAL NO.
OPERATORS LASZCZYK

TIME	TEST TIME	Volts	Amps	Amps	WATTS		FLOW System	FLOW HX	FLOW HX	HX IN	HX OUT	HX IN	HX IN	HX OUT	ΔT 37-38	LCG IN	LCG OUT	HX OUT	WALL TEMP	BLADDER PRESS		CHAMB PRESS
	MIN	AC	AC	AC			%	%	%	PSIA	PSIA	°F 23	°F 37	°F 38	mV	°F 1	°F 2	°F 24	°F 19	PSIG		TORR
0922	0	0	0	0			82.5	35.	-	16.4	15.		64	64	.015	64.5	64.		65	OPEN TO CHAMB		1.2×10^{-4}
0948		53.5	4.12	—			82.5	12	9.	15.3			81.5	78.5	.090	87.5	88			CLOSED TO CHAMB		7.4×10^{-5}
0950	START						~~8~~	~~8~~	~~6~~											20		
	6	53.5	4.12	~~220.42~~	220.42		82.5	8	6.	15.2	15.		84.5	39.5	1.013	85.	87.5			20		6.8×10^{-5}
	11	53.5	4.12	-	220.42		82.5	8	6	15.2	15		84.5	38.0	—	85	87.5			20		6.5×10^{-5}
	30	53.5	4.12	—			82.5	8	6	15.2	15.	84.5	—	39	-	85.2	88	40	66	20		6.0×10^{-5}
	35	53.5	4.12	—			82.5		6.5	15.2	15.	84.	—	40	—	84.5	87	40.5		20		5.6×10^{-5}
	45	53.5	4.12	-			82.5	8	6	15.2	15	83.	-	39.5	-	85	87.5	40.5		20		5.4×10^{-5}
	55	53.5	4.12	-			82.5	8	6	15.2	15.	83.5	-	37.5	-	85	87.5	40.5		20		5.2×10^{-5}
	62	53.5	4.12	-			82.5		6.1	15.2	15.	83.5	-	34.5	-	85	87.5	40	67	20		5.0×10^{-5}
	71	53.5	4.12	-			82.5		6.1	15.2	15.	82.5		37		85	87.5	40		20		4.8×10^{-5}
	79	53.5	4.12	-			82.5		6.1	15.2	15	82.0		37.5		85	87	40.		20		4.7×10^{-5}
	90	53.5	4.12	-			82.5		6.1	15.2	15.	82.0		40		85	87.5	41		20		4.6×10^{-5}
	97	53.5	4.12	-			82.5		6.1	15.2	15.	82.0		40.5		85	87.5	41.5		20		4.4×10^{-5}
	104	53.5	4.12	-			82.5		6.1	15.2	15	82.0		41		85	87.5	42	68	20		4.2×10^{-5}
	112	53.5	4.12	-			82.5		6.2	15.2	15.	82.0		42		85	87.5	43		20		4.2×10^{-5}
	119	53.5	4.12	-			82.5		6.2	15.2	15	82.0		43		85	87.5	44		20		4.1×10^{-5}
	126	53.5	4.12	-			82.5		6.2	15.2	15	82.0		44		85	87.5	45		20		4.0×10^{-5}
	131	53.5	4.12	-			82.5		6.4	15.2	15	82.5		45		85	87.5	46	69	20		4.0×10^{-5}
	136	53.5	4.12		220.42		82.5		6.6	15.2	15	83		46.5		85	87.5	47		20		4.0×10^{-5}

REMARKS
A 750 Btu/hr
#1

10510

HSF 170 1A 1/66

Hamilton Standard DIVISION OF UNITED AIRCRAFT CORPORATION
WINDSOR LOCKS, CONNECTICUT 06096

SPACE & LIFE SYSTEMS LABORATORY

LOG OF TEST

TYPE OF TEST: ICE PACK ICE CHEST
TEST ENGINEER: G. ROLLBULLEN
NAME OF RIG: 25
PROJECT & ENG ORDER NO: B89-500-300A

SHEET 2 OF 2 DATE 10-2-74
TEST PLAN NO.
MODEL NO.
PART NO.
SERIAL NO
OPERATORS LASZCZYK

TIME	TEST TIME	VOLTS	AMPS	AMPS	WATTS		F LCG SYST.	F LCG HX	HX IN	HX IN	HX IN	HX IN	HX OUT	AT	LCG IN	LCG OUT	HX OUT	WALL TEMP	BLADDER PRESS		CHAMB PRESS
	MIN	AC	AC	AC			%	%	%	PSIA	PSIA	°F 23	°F 27	°F 28	MV	°F 1	°F 2	°F 24	°F 29	PSIA	TORR
	141	53.5	4.12		220.42		82.5		6.8	15.2	15.	63	-	46	-	85	87.5	46.5		20	3.4 X10-5
	146	53.5	4.12				82.5	4.5	7.0	15.7	15.	63	-	50.5	-	85	87.5	50.5	70	20	3.9X10-5
	150	53.5	4.12				82.5	10.	7.4	15.1	15.	63	-	53.5	-	85	87.5	53.		20	3.8X10-5
	155	53.5	4.12				82.5		7.4	15.2	15	63		56.5		85	87.5	56		20	3.5X10-5
	160	53.5	4.12				82.5		8.0	15.2	15	63.5		60		85	87.5	59.5		20	3.8X10-5
	165	53.5	4.12				82.5		9.0	15.25	15.	64.		63.5		85	88	63.	71	20	3.8X10-5
	170	53.5	4.12				82.5	14.	10.0	15.3		64.5		67		85	87.5	67		20	3.8X10-5
	174	53.5	4.12				82.5	18.	12.2	15.4		65		70.5		85	87.5	70.5		20	3.7X10-5
	179	53.5	4.12				82.5	21.5	14	15.5		65		73.5		85	87.5	73.5		20	3.7X10-5
	184	53.5	4.12				82.5	25.	16	15.7		65		76.5		85	87.5	76.5		20	3.6X10-5
	189	53.5	4.12				82.5	42	-			56		60		85	87.5	60		20	3.5X10-5
	193	53.5	4.12				82.5	55		17.2		66		67.5		85	87.5	62.5		20	3.5X10-5
1307	197	53.5	4.12		220.42		82.5	100+		32.6		67		65		85.5	88.	65	72	20	3.5X10-5

REMARKS

10511

(2-2)

NSP 170 1A 1/66

Hamilton Standard DIVISION OF UNITED AIRCRAFT CORPORATION
WINDSOR LOCKS, CONNECTICUT 06096

SPACE & LIFE SYSTEMS LABORATORY

LOG OF TEST

TYPE OF TEST: ICE PACK ICE CHEST
TEST ENGINEER: G ROEBUCK
NAME OF RIG: 35
PROJECT & ENG ORDER NO.: 889-500-300A

SHEET 1 OF
DATE 10-1-79
TEST PLAN NO. ECS-2124-L-079
MODEL NO.
PART NO.
SERIAL NO.
OPERATORS LASZCZYK

TIME	TEST TIME	VOLTS AC	AMPS AC	AMPS AC	WATTS	SYST %	HX %	HX %	HX IN PSIA	HX OUT PSIA	HX IN °F 27	HX OUT °F 28	AT 27-28 MV	LCG IN °F 1	LCG OUT °F 2	WALL TEMP °F 29	BLADDER PRESS PSIA	CHAM PRESS TORR
1245	START	0	0	0	0	82.5	58	-	17.7	15.0	65.5	65.5	.005	66	66	69	OPEN TO CHAMB	6.5 X10^{-5}
1250		75.5	3.59	2.33	434.4	82.5	56		17.4		72.5	71.5	.030	74	76		CLOSED TO CHAMB	
1253	0																20	
	3	75.5	3.56	2.23		82.5	40				77.5	47.5	.635	66	75			6.0X10^{-5}
	8	75.5	3.58	2.34	434.41	82.5	15.5		15.5		73	42	.702	70	75			5.5X10^{-5}
	13	76	3.58	2.35	443.08	82.5	19		15.6	15.0	74.5	41	.742	70	76		20	5.3X10^{-5}
	19	76	3.58	2.35	443.08	82.5	19		15.6	15.0	74.5	42	.720	70	76		20	5.2X10^{-5}
	24	76	3.58	2.35	443.08	82.5	22		15.7	15.0	74.5	41	.681	70	76		20	5.2X10^{-5}
	28	76	3.58	2.35	443.08	82.5	22		15.7	15.0	74.5	45.5	.640	70	76		20	5.0X10^{-5}
	32	76	3.58	2.35	443.08	82.5	22		15.7	15.0	74.5	46.5	.600	70	76		20	4.8X10^{-5}
	37	76	3.58	2.35	443.08	82.5	27		15.9	15.0	74.5	51	.536	70	76		20	4.5X10^{-5}
	41	76	3.58	2.35	443.08	82.5	31		16.1	15.	75	55	.444	70	76		20	4.8X10^{-5}
	46	76	3.58	2.35	443.08	82.5	41		16.6	15.	75	61	.328	70.5	76.5		20	4.8 X10^{-5}
	50	76	3.58	2.35	443.08	82.5	64		18.5	15	75	67	.185	70	76		20	4.8 X10^{-5}
	53	76	3.58	2.35	443.08	82.5	100+		23.1	15.0	75.5	71	.098	72	77		20	5.0 X10^{-5}
	57	76	3.58	2.35	443.08	82.5	100+		23.1	15	77	73.5	.086	74	79		20	5.0 X10^{-5}
	61	76	3.58	2.36	443.54	82.5	100+		23.	15.	74.5	76	.078	76.5	81		20	5.5 X10^{-5}
	65	76	3.58	2.36	443.54	82.5	100+		22.9	15.	81.5	78.5	.075	79	84.		20	5.0 X10^{-5}
1401	68	76	3.58	2.36	443.54	82.5	100+		22.6	15.0	83.5	80.5	.075	81	86	69	20	6. X10^{-5}

REMARKS
A 1500 Btu/hr
+1

10509

C-3

HSF 175 1A 1/56

Hamilton Standard DIVISION OF UNITED AIRCRAFT CORPORATION
WINDSOR LOCKS, CONNECTICUT 06096

SPACE & LIFE SYSTEMS LABORATORY

LOG OF TEST

TYPE OF TEST: ICE CHEST
TEST ENGINEER: G ROEBELEN
NAME OF RIG: 25
PROJECT & ENG ORDER NO: B69-500-300A

SHEET 1 OF DATE 9-30-71
TEST PLAN NO. LECS-4124-L-079
MODEL NO.
PART NO.
SERIAL NO.
OPERATORS LASZCZYK

TIME	TEST TIME	HEATER VOLTS	HEATER AMPS	HEATER AMPS	WATTS		SYST FLOW	HX FLOW	HX FLOW	HX IN PRESS	HX OUT PRESS		LCG IN TEMP	LCG OUT TEMP	C. HAMB IN TEMP	C. HAMB OUT TEMP	HX HEAT TEMP	HX COOLANT TEMP	WALL TEMP	BLADDER PRESS		C. HAMB PRESS
	MIN.	AC	AC	AC			%	%	%	PSIA	PSIA		°F 1	°F 2	°F 3	°F 4	27	28	29	PSIA		TORR.
1140	0	0	0	0	0		82.5	60	—	18.1	15.		61	61	62	62	61	60	63	.2		1.8×10^{-4}
	10	87.	4.08	2.72			82.5	97	-	22.1	15.2		49	56	58	51	56.5	46.5	63	20.		4×10^{-4}
	20	90	4.23	2.74			82.5	100		22.3	15.1		50	58	60	53	58	46.5	63	20		5×10^{-4}
	25	90	4.23	2.74			82.5	100+		23.8	15.1		51	59	61	55	50.5	63.5	63	20		6.3×10^{-4}
	35	90	4.33	2.73			83.5	100+		23.8	15.1		51	60.	61	55	51.5	60	63	20		50μ
	45	90	4.31	2.73			82.5	100+		23.5	15.1		53.5	62.	63	56.5	53.	61.5	63	20		300μ
	55	90	4.32	2.73			82.5	100+		23.7	15.1		55	63.5	64	58.	55	63	63	20		600μ
	65	90.	4.31	2.73			82.5	100+		23.5	15.1		58	67	67	61	58.5	65.5	63	20		750μ
1255	75	90.	4.32	2.74			82.5	100+		23.2	15.1		65.5	73	71.5	66	65	71	64	20		600μ

G-4

REMARKS
A 2000 Btu/hr
#1 -

10467

HSP 178 1A 1/66

Hamilton Standard DIVISION OF UNITED AIRCRAFT CORPORATION
WINDSOR LOCKS, CONNECTICUT 06096

SPACE & LIFE SYSTEMS LABORATORY

LOG OF TEST

TYPE OF TEST: ICL PACK ICE CHEST
TEST ENGINEER: G. ROEMELLER
NAME OF RIG: 25
PROJECT & ENG ORDER NO: BSG-500-300A

SHEET 1 OF
DATE 10-3-74
TEST PLAN NO ECS-2124-L-079
MODEL NO.
PART NO.
SERIAL NO.
OPERATORS LASZCZYK

TIME	TEST TIME MIN	VOLTS AC	AMPS AC	AMPS AC	WATTS	FLOW SYST %	FLOW HX %	HX %	HX IN PSIA	HX OUT PSIA	HX IN °F 17	HX OUT °F 35	ΔT 17-24 MV	LCG IN °F 1	LCG OUT °F 2	WALL TEMP °F 29	BLADDER PRESS PSIA	CHAM PRESS TORR
1455		0	0	0	0	82.5	100+	-	23.7	15	57.	57.	.010	54	58	64.	0	1.5×10^{-4}
1500	0	87.5	4.1	2.65	590.62												20.	
	4	87.5	4.1	2.65	590.62	82.5	100+		23.4	15	54	49.5	.215	51.5	60.5		20	7.2×10^{-5}
	8	87.5	4.08	2.66	589.75	82.5	100+		23.4	15	58.5	50	.204	53	59.5		20	6.4×10^{-5}
	14	87.5	4.08	2.66	589.75	82.5	100+		23.4	15	58.5	56	.192	52	59.5		20	$6. \times 10^{-5}$
	19	87.5	4.08	2.66	589.75	82.5	100+		23.4	15	56.5	50.5	.186	52	59.5		20	5.7×10^{-5}
	24	87.5	4.09	2.67	591.5	82.5	100+		23.4	15	58.6	51.	.186	53	60.5		20	5.5×10^{-5}
	29	87.5	4.09	2.67	591.5	82.5	100+		23.8	15	60	52	.186	54	61		20	5.3×10^{-5}
	34	87.5	4.08	2.67	590.62	82.5	100+		23.8	15	61	52.5	.179	54	62		20	$5. \times 10^{-5}$
	39	87.5	4.09	2.67	591.5	82.5	100+		23.8	15	61.5	53.5	.174	55	62.5		20	$5. \times 10^{-5}$
	44	87.5	4.09	2.67	590.62	82.5	100+		23.7	15	62.	54.5	.176	56	63.5		20	$5. \times 10^{-5}$
	49	87.5	4.08	2.67	590.62	82.5	100+		23.7	15	62	56.	.170	57.5	65		20	$5. \times 10^{-5}$
	54	87.5	4.08	2.67	590.62	82.5	100+		23.6	15	64.5	57.5	.160	59.	66		20	5.4×10^{-5}
	59	87.5	4.08	2.67	590.62	82.5	100+		23.6	15	66.5	60	.142	61.5	68		20	4.8×10^{-5}
1605	65	87.5	4.08	2.67	590.62	82.5	100+		23.5	15	69.5	64	.125	65	71.5		20	4.4×10^{-5}

REMARKS:
A 2000 Ctn/hr
#2

10518

HSF 179 1A 1/66

Hamilton Standard DIVISION OF UNITED AIRCRAFT CORPORATION
WINDSOR LOCKS, CONNECTICUT 06096

SPACE & LIFE SYSTEMS LABORATORY

LOG OF TEST

TYPE OF TEST: ICE PACK ICE CHEST
TEST ENGINEER: C. ROEBELEN
NAME OF RIG: 25
PROJECT & E.O. ORDER NO: 849-500-300A

SHEET 1 OF   DATE 10-7-74
TEST PLAN NO ECS-2124-L-079
MODEL NO
PART NO.
SERIAL NO
OPERATORS LASZCZYK

Time	Test Time	Volts AC	Amps AC	Amps AC	Watts		Syst. %	Flow HX %	HX %	HX In PSIA	HX Out PSIA		HX In °F	HX Out °F	ΔT 27-28 MV	LCG In °F 1	LCG Out °F 2		Wall Temp °F 29	Bladder Pres PSIA		Chamb Press TORR
0925		0	0	0	0		82.5	100+	-	23.4	15		57.5	57.5	.007	57.5	57.5		63	0		1.2×10^{-4}
~~0930~~		~~87.5~~																				
0930	START	87.5	4.1	2.64	589.75		82.5						5							30		
	3	87.5	4.1	2.64	589.75		82.5	100+		24.2	15		59	46	.375	46	55.5			30		$1.\times10^{-4}$
	7	87.5	4.08	2.66			82.5	100+		24.2	15		55	45	.222	45	53.5			30		$1.\times10^{-4}$
	12	87.5	4.08	2.66			82.5	100+		24.2	15		54	45	.190	45.5	53.5			30		$1.\times10^{-4}$
	17	87.5	4.08	2.66			82.5	100+		24.2	15		54.5	45.5	.158	46	53.5			30		1×10^{-4}
	22	87.5	4.08	2.66			82.5	100+		24.2	15		55	46.5	.164	47	54.5			30		1×10^{-4}
	27	87.5	4.08	2.66			82.5	100+		24.1	15		56	47.5	.164	48	55			30		1×10^{-4}
	32	87.5	4.08	2.66			82.5	100+		24.1	15		56.5	48	.160	48.5	56			30		1×10^{-4}
	37	87.5	4.08	2.66			82.5	100+		24.1	15		57	49	.178	49.5	56.5			30		1×10^{-4}
	42	87.5	4.08	2.66			82.5	100+		24.0	15		58	50.5	.177	50.5	58			30		9.8×10^{-5}
	47	87.5	4.08	2.66			82.5	100+		24.0	15		59	51.5	.171	52	59			30		9.6×10^{-5}
	52	87.5	4.08	2.66			82.5	100+		23.9	15		60.5	53.5	.165	53.5	60.5			30		9.4×10^{-5}
	57	87.5	4.08	2.66			82.5	100+		23.5	15		63.5	56	.145	56	63.5			30		9.0×10^{-5}
	62	87.5	4.08	2.66			82.5	100+		23.6	15		65.5	60	.130	60	66			30		8.8×10^{-5}
1037	67	87.5	4.08	2.66	589.75		82.5	100+		23.5	15		69.5	64	.119	64	69.5			30		8.5×10^{-5}

REMARKS
A 2000 Btu/h
#1 - 30 psia

10524

HSP-175 1A 1/66

Hamilton Standard DIVISION OF UNITED AIRCRAFT CORPORATION
WINDSOR LOCKS, CONNECTICUT 06096

SPACE & LIFE SYSTEMS LABORATORY

LOG OF TEST

TYPE OF TEST: ICE PACK WATER BOILER
TEST ENGINEER: G ROEBELEN
NAME OF RIG: 25
PROJECT & ENG. ORDER NO.: B69-500-300A

SHEET 1 OF — DATE 10-4-72
TEST PLAN NO. ECS-2124-L-079
MODEL NO —
PART NO. — —
SERIAL NO. —
OPERATORS LASZCZYK

TIME	TEST TIME	VOLTS AC	AMPS AC	WATTS		PLCW SYST. %	PLCW HX %	HX °/o	HX IN PSIA	HX OUT PSIA		HX IN °F 27	HX OUT °F 28	ΔT 27-28 MV	LCG IN °F 1	LCG OUT °F 2	WALL TEMP. °F 29		BLADDER PRESS PSIA		CHAM. PRESS TORR
0980		0	0	0		82.5	36	-	16.3	15.		62	62	.015	62	62	—		0		7.2×10^{-5}
0942		53.5	4.1	219.35		82.5	34					56	63	.069	65.5	67.5			0		5.5×10^{-5}
0945	START																		20		
	5	54	4.12	222.48		82.5	-	6.3	15.15	15.		64.5	39.	1.020	64.5	67.			20		5.2×10^{-5}
	11	54	4.12	222.48		82.5		5.6	15.16	15.		63	36.5	.992	65	67.5			20		5×10^{-5}
	15	54	4.12	222.48		82.5		5.6	15.15	15.		62	38.	.981	65	67.5			20		4.8×10^{-5}
	20	54	4.11	221.94		82.5		6.0	15.2	15.		62.5	37.5	1.000	65	67.5			20		4.7×10^{-5}
	26	54	4.12	222.48		82.5		5.6	15.2	15.		63	38.	1.000	65	67.5			20		4.5×10^{-5}
	31	54	4.12	222.48		82.5		5.6	15.2	15		63	38	.996	65	67.5			20		4.4×10^{-5}
	36	54	4.12	222.48		82.5		5.8	15.2	15.		63	38	.996	65	67.5			20		4.4×10^{-5}
	41	54	4.13	223.02		82.5		5.9	15.2	15.		63	38	1.000	65	67.5			20		4.3×10^{-5}
	46	54	4.13	223.02		82.5		5.9	15.2	15.		63	38	1.003	65	67.5			20		4.2×10^{-5}
	51	54	4.12	222.48		82.5		5.9	15.2	15.		63	38	1.003	65	67.5			20		4.2×10^{-5}
	56	54	4.12	222.48		82.5		5.9	15.2	15.		63	38	1.003	65	67.5			20		4.1×10^{-5}
	61	54	4.12	222.48		82.5		5.9	15.2	15.		63	38	1.001	65	67.5			20		4.1×10^{-5}
	66	54	4.13	223.02		82.5		5.9	15.2	15.		63.5	38	.995	65	67.5			20		4.1×10^{-5}
	71	54	4.12	222.48		82.5		5.9	15.2	15.		63.5	38	.993	65	67.5			20		4×10^{-5}
	76	54	4.12	222.48		82.5		5.9	15.2	15		63.5	38	.991	65	67.5			20		4.1×10^{-5}
	81	54	4.12	222.48		82.5		5.9	15.2	15		63.5	38	.988	65	67.5			20		4×10^{-5}
	86	54	4.12	222.48		82.5		5.9	15.2	15.		63	38.5	.985	65	67.5			20		$4. \times 10^{-5}$

REMARKS:
B 750 Btu/hr
#1

10520

HSF 175 1A 1/66

Hamilton Standard DIVISION OF UNITED AIRCRAFT CORPORATION
WINDSOR LOCKS, CONNECTICUT 06096

SPACE & LIFE SYSTEMS LABORATORY

LOG OF TEST

TYPE OF TEST: ICE PACK WATER BOILER
TEST ENGINEER: G BOLBELLER
NAME OF RIG: 25
PROJECT & ENG. ORDER NO.: BSG-500-300A

SHEET 2 OF
DATE 10-4-74
TEST PLAN NO. GCS-2124-L-078
MODEL NO.
PART NO.
SERIAL NO.
OPERATORS LASZCZYK

TIME	TEST TIME	VOLTS	AMPS	AMPS	WATTS		F/CW SYST.	F/CW HX	HX	HX IN	HX OUT		HX IN	HX OUT	AT 27-28	LCG IN	LCG OUT	WALL TEMP		BLADDER PRESS	STEAM PRESS.	CHAM. PRES.
		AC	AC	AC			%	%	%	PSIA	PSIA		°F 27	°F 28	MV	°F 1	°F 2	°F 29		PSIA	M	TORR
1116	91	54	4.13	~~22302~~	223.02		82.5	-	6.0	15.2	15		82.5	38.5	.940	85	87.5	-		20	—	9×10^{-5}
1121	96	54	4.13	-	223.02		82.5		6.0	15.2	15		83	39	.980	85	87.5			20		3.9×10^{-5}
	101	54	4.13		223.02		82.5		6.0	15.2	15		83	39	.974	85	87.5			20		3.8×10^{-5}
	106	54	4.13		223.02		82.5		6.0	15.2	15		83	39.5	.971	85	87.5			20		3.8×10^{-5}
	111	54	4.12		222.48		82.5		6.0	15.2	15		83	39.5	.961	85	87.5			20		3.7×10^{-5}
1141	116	54	4.12		222.48		82.5		6.0	15.2	15		83	40	.950	85	87.5			20		3.7×10^{-5}
1220	155	54	4.12		222.48		82.5		6.2	15.2	15		83	45	.855	85	87.5			20		8 M
	160	54	4.12		222.48		82.5		6.5	15.2	15		83.5	46.5	.828	85	87.5			20		8
	165	54	4.12		222.48		82.5		6.6	15.2	15		83.5	48.	.800	85	87.5			20		8
	170	54	4.12		222.48		82.5		6.5	15.2	15		84	49.5	.772	85	87.5			20		8
	175	54	4.12		222.48		82.5		7.0	15.2	15		84	52	.710	85	87.5			20		8
	180	54	4.12		222.48		82.5		7.0	15.2	15		84	54.5	.654	85	87.5			20		8
	185	54	4.12		222.48		82.5		7.7	15.2	15		84	58	.592	85	87.5			20		8
	190	54	4.12		222.48		82.5		8.0	15.25	15		84	61.5	.540	85	87.5			20		8
	195	54	4.13		223.02		82.5		9	15.3	15		85	66	.440	85	87.5			20		8
	200	54	4.13		223.02		82.5	15	10.5	15.3	15		85.5	70	.360	85	87.5			20		8

REMARKS:

10521

G-8

NSP 170 1A 1/66

Hamilton Standard DIVISION OF UNITED AIRCRAFT CORPORATION
WINDSOR LOCKS, CONNECTICUT 06096

SPACE & LIFE SYSTEMS LABORATORY

LOG OF TEST

TYPE OF TEST: ICE RACK WATER BOILER
TEST ENGINEER: G. ROEBELEN
NAME OF RIG: 25
PROJECT & ENG. ORDER NO.: B89-500 300A

SHEET 1 OF DATE 10-3-74
TEST PLAN NO. ECS-2124-L-079
MODEL NO.
PART NO.
SERIAL NO.
OPERATORS LASZCZYK

TIME	TEST TIME MIN	VOLTS AC	AMPS AC	AMPS AC	WATTS		FLOW SYST. %	FLOW HX %	HX %	HX IN PSIA	HX OUT PSIA		HX IN °F 27	HX OUT °F 28	ΔT 27-28 MV	LCG IN °F 1	LCG OUT °F 2	WALL TEMP °F 29		BLADDER PRESS PSIA	STEAM PRESS M	CHAM. PRES. TORR
0950		0	0	0	0		82.5	56	-	17.5	15		62	62	.009	63	63	65		0	2 BIA *	1.1 X10⁻⁴
1000													74	73	.035	75	76.5					6.2X10⁻⁵
1002	0	75.5	3.55	2.25	437.90															20.		
	4	75.5	3.55	2.25	437.90		82.5	24		15.6	15		75.5	41.	.785	68.5	76			20		7.4 X10⁻⁵
	9	75.5	3.54	2.25	437.14		82.5	18		15.6	15		74	38.5	.790	70	75.5			20		7.2X10⁻⁵
	14	75.5	3.54	2.25	437.14		82.5	18		15.6	15		74	38.0	.790	70	75.5	65		20		6.8 X10⁻⁵
	19	75.5	3.55	2.26	436.65		82.5	18.		15.6	15		74	34.5	.761	70	76			20		6.5 X10⁻⁵
	24	76.	3.58	2.27	444.60		82.5	20		15.7	15		74.5	40.5	.753	70	76			20		6.2 X10⁻⁵
	31	76	3.57	2.27	443.84		82.5	20		15.7	15		-	-	.730	70	76			20		6.1X10⁻⁵
	36	76	3.56	2.27	443.08		82.5	20		15.7	15		73.5	41.	.720	70	75.5			20		6.0X10⁻⁵
	41	76	3.56	2.27	443.08		82.5	20		15.7	15		74.	42.5	.695	70	75.5			20		5.9 X10⁻⁵
	45	76	3.56	2.27	443.08		82.5	20		15.7	15		74	43.5	.673	70	75.5			20		5.7X10⁻⁵
	50	76	3.56	2.27	443.08		82.5	22.5		15.7	15		74.5	46.5	.630	70	76			20		5.6X10⁻⁵
	55	76	3.57	2.27	443.84		82.5	25.5		15.8	15		74.5	49.5	.560	70	76			20		5.4 X10⁻⁵
	60	76	3.57	2.27	443.84		82.5	30.		16	15		75.	53.5	.477	70	76			20		5.4 X10⁻⁵
	65	76	3.57	2.27	443.84		82.5	40		16.5	15		75	59.	.360	70	76			20		5.4 X10⁻⁵
	69	76	3.57	2.27	443.84		81.5	60.		18.3	15		75	66	.310	70	76			20		5.4X10⁻⁵
	75	76	3.57	2.27	443.84		82.5	100+		23.1	15		75.5	71.5	.102	72	77			20		5.7X10⁻⁵
	80	76	3.57	2.27	443.84		82.5	100+		23.1	15		76.5	74.5	.084	76	56.5	66		20		6.0 X10⁻⁵
1127	96	76	3.57	2.27	443.84		82.5	100+		23.0	15		82	79	.072	79.5	84			20	2 PSIA	6.4 X10⁻⁵

REMARKS: * 1 SIDE OF WATER BOILER OPEN TO 2. PSIA PRESS. - OTHER SIDE CAPPED

10516

B 1500 Btu/h
#1

HSF-178 1A 1/66

Hamilton Standard DIVISION OF UNITED AIRCRAFT CORPORATION
WINDSOR LOCKS, CONNECTICUT 06096

SPACE & LIFE SYSTEMS LABORATORY

LOG OF TEST

TYPE OF TEST: ICE PACK - BOILER
TEST ENGINEER: G ROEBELEN
NAME OF RIG: 75
PROJECT & ENG. ORDER NO.: B69-500-3, C/T

SHEET 1 OF
DATE 9-30-74
TEST PLAN NO. LCS-2124-L-079
MODEL NO.
PART NO.
SERIAL NO.
OPERATORS LASZCZYK

TIME	TEST TIME	VOLTS	AMPS	AMPS	WATTS		SYST. FLOW	HX FLOW	HX FLOW	HX INLET PRESS	HX OUTLET PRESS	ΔT 27-28	LCG INLET TEMP 1	LCG OUT TEMP 2	CHAM IN TEMP 3	CHAMB OUT TEMP. 4	HX IN TEMP. 27	HX OUT TEMP 26	WALL TEMP. 29	BLADDER PRESS		CHAMB PRESS
	MIN	AC	AC	AC			%	%	%	PSIA	PSIA	M.U.	°F	°F	°F	°F			°F	PSIA		TORR
1430	0	0	0	0	0		62.5	66	-	16.6	15.	.018	56.5	58.5	60.	60.	58	57.5	-	.2		2.3×10^{-4}
	10	90	4.21	2.73			62.5	100+	-	24.	15.1	.18	51.5	59.5	61	55	58.5	50.5	-	20.		1.6×10^{-4}
	30	90	4.22	2.74			62.5	100+	-	23.8	15.1	.18	54	62	63	57	61	53.5		20.		1.5×10^{-4}
	30	90	4.20	2.73			62.5	100+	-	23.6	15.1	.18	57	65	66	59.5	64	56.5		20		1.4×10^{-4}
	40	90	4.22	2.74			62.5	100+		23.6	15.1	.182	59	67	67	61.5	66.5	58.5		20		1.4×10^{-4}
	50	90.5	4.24	2.75			62.5	100+		23.4	15.1	.17	62.5	70.5	70.5	64	68.5	61.		20		1.3×10^{-4}
	60	90.5	4.24	2.75			62.5	100+		23.4	15.1	.16	65.5	73			72	65		20		1.2×10^{-4}

REMARKS:
B 2000 Btu/hr
#1 -

10506

HSP-179 1A 1/66

Hamilton Standard DIVISION OF UNITED AIRCRAFT CORPORATION
WINDSOR LOCKS, CONNECTICUT 06096

SPACE & LIFE SYSTEMS LABORATORY

LOG OF TEST

TYPE OF TEST: ICE PACK WATER BOILER
TEST ENGINEER: G. BUEBELEN
NAME OF RIG: 25
PROJECT & ENG ORDER NO.: B59-300-300A

SHEET 1 OF
DATE 10-1-74
TEST PLAN NO. ECS-3124-L-079
MODEL NO.
PART NO.
SERIAL NO.
OPERATORS LASZCZYK

TIME	TEST TIME MIN.	VOLTS	AMPS	AMPS	WATTS		SYSTEM %	FLOW HX %	HX %	HX IN PSIA	HX OUT PSIA	READING TIME MIN	HX IN °F 27	HX OUT °F 28	ΔT 27-28 MV.	LCG IN °F 1	LCG OUT °F 2	READING TIME MIN	WALL TEMP °F 29	BLADDER PRESS. PSIA		CHAMB PRESS TORR
10:00	START	0	0	0	0		82.5	100 T	—	23.5	15.		61.5	61.5	.011	62.5	62.		64	OPEN TO CHAMB		1.1 X 10^{-4}
	3	0	0	0	0		82.5	100T		24.2	15	3	56.5	50.5	.151	51	54	5	64	30.		1.0 X 10^{-4}
	9	88	4.15	2.64	597.52		82.5	100 T		24.0	15	9	55.5	49.	.157	50.5	56.5	11	64	30		9.5 X 10^{-5}
	14	88	4.13	2.66	597.52		82.5	100 T		23.8	15	14	58	51.	.165	52.	59	16	64	30.		9.0 X 10^{-5}
	21	88.	4.13	2.67	596.40		82.5	100T		23.7	15	21	60.5	53.5	.174	54	62	23	64	30		8.4X 10^{-5}
	26	88.	4.13	2.68	599.28		82.5	100 T		23.7	15	26	62	55	.166	56	63	28	64	30		8.0X 10^{-5}
	31	88	4.13	2.68	599.28		82.5	100T		23.6	15	31	64	57	.157	58	66	33	64	30		7.8X 10^{-5}
	36	88.5	4.13	2.68	602.66		82.5	100T		23.5	15	36	66.5	60	.145	61	67	38	64	30		7.5X 10^{-5}
	40	88.5	4.13	2.68	602.68		82.5	100T		23.4	15	40	68.5	63	.132	64	70.5	42	64	30		7.4X 10^{-5}
1044	44	88.5	4.13	2.68	602.68		82.5	100T		23.4	15	44	71.5	66	.122	67	73.5	46	64	30		7.0 X 10^{-5}

REMARKS:
B 2000 Btu/hr
#2 - 30 psia b.p.

10508

G-11

HSF 175 1A 1/66

Hamilton Standard DIVISION OF UNITED AIRCRAFT CORPORATION
WINDSOR LOCKS, CONNECTICUT 06096

SPACE & LIFE SYSTEMS LABORATORY

LOG OF TEST

TYPE OF TEST: ICE PACK WATER BOILER
TEST ENGINEER: G. ROEBELEN
NAME OF RIG: 25
PROJECT & ENG ORDER NO.: 869 - 500 - 30MA

SHEET 1 OF DATE 10-2-74
TEST PLAN NO. ECS-3124-L-079
MODEL NO.
PART NO.
SERIAL NO.
OPERATORS: LASZCLIK

TIME	TEST TIME	VOLTS	AMPS	AMPS	WATTS	FLOW SYST.	FLOW HX	HX	HX IN	HX OUT	HX IN	HX OUT	AT 27-28	LCG IN	LCG OUT	WALL TEMP	BLADDER PRESS	CHAMB PRESS
	MIN	AC	AC	AC		%	%	%	PSIA	PSIA	°F 37	°F 28		°F 1	°F 2	°F 29	PSIA	TORR
1443		0	0	0		52.5	100+	-	23.2	15	64.5	69.5	.007	70.	70.	71	OPEN TO CHAMB.	1.1x10⁻⁴
1445	START																20	
	4:30	87.	4.1	2.62	584.69									52	58			
	9	87.5	4.1	2.63	586.87	52.5	100+		24.1	15	55	46	.198	46	55		20	6x10⁻⁵
	13	87.5	4.1	2.63	586.87	52.5	100+		24.1	15	54	46.5	.186	48	56		20	5.7x10⁻⁵
	17	87.5	4.1	2.63	586.87	52.5	100+		24.1	15	55.5	47.5	.180	49	56	71	20	5.5x10⁻⁵
	22	87.5	4.1	2.63	586.87	52.5	100+		24.0		56.5	48.5	.180	49.5	57		20	5.3x10⁻⁵
	27	87.5	4.1	2.64	589.75	52.5	100+		23.9		57.	49.	.180	51	58		20	5.2x10⁻⁵
	32	87.5	4.1	2.63	586.87	52.5	100+		23.9		56	50	.160	51.5	54		20	5.0x10⁻⁵
	37	87.5	4.1	2.64	589.75	52.5	100+		23.8		59	51	.172	53	60	71.5	20	4.9x10⁻⁵
	42	87.5	4.1	2.64	589.75	52.5	100+		23.7		60	52.5	.167	54	62		20	4.7x10⁻⁵
	50	87.5	4.1	2.63	586.87	52.5	100+		23.7		63.5	57.5	.131	59	65		20	4.7x10⁻⁵
	54	87.5	4.1	2.64	589.75	52.5	100+		23.6		66.	61	.123	62	68.5		20	4.7x10⁻⁵
1543	58	87.5	4.1	2.64	589.75	52.5	100+		23.4		64	59	.110	65.5	72	71.5	20	4.6x10⁻⁵

REMARKS:
B 2000 Btu/hr
#3

10512

HSP-178 1A 1/66

Hamilton Standard DIVISION OF UNITED AIRCRAFT CORPORATION
WINDSOR LOCKS, CONNECTICUT 06096

SPACE & LIFE SYSTEMS LABORATORY

LOG OF TEST

TYPE OF TEST: ICE PACK WATER BOILER
TEST ENGINEER: G. BOEBLEEN
NAME OF RIG: 25'
PROJECT & ENG. ORDER NO.: B59-300-300A

SHEET 2 OF
DATE 10-3-74
TEST PLAN NO. ECS-2124-L-079
MODEL NO.
PART NO.
SERIAL NO.
OPERATORS LASZCZYK

TIME	TEST TIME	VOLTS	AMPS	AMPS	WATTS	FLOW SYST.	FLOW HX	HX	HX IN	HX OUT	HX IN	HX OUT	AT	LCG IN	LCG OUT	WALL TEMP	BLADDER PRESS	STEAM PRESS	CHAMBER PRESS
	MIN	AC	AC	AC		%	%	%	PSIA	PSIA	°F 27	°F 28	MV	°F 1	°F 2	°F 29	PSIA	M *	TORR
1235	0	53.5	4.11	–	219.85	62.5	100+	–	23.1	15.	60.5	56	.093	57	60.	65	30.	900.	4.5×10^{-5}
1330	5	53.5	4.10		219.35	62.5	100+		23.7	15	60.	55.5	.093	56.5	59.5		30	900	4.6×10^{-5}
1240	15	53.5	4.10		219.35	62.5	100+		23.6	15	59.	55	.091	56.	59.		30	900	4.6×10^{-5}
1250	25	53.5	4.10		219.35	62.5	100+		23.5	15	58	54	.090	55.5	58.5		30	900	4.4×10^{-5}
1300	35	53.5	4.10		219.35	62.5	100+		23.6	15	58	54	.090	55	56.5	65	30	900	4.3×10^{-5}

REMARKS: 1 side of water boiler open to vacuum - other side capped

C 750.0 Btu/in
#1

10517

G-13

HSF 178 1A 1/66

Hamilton Standard DIVISION OF UNITED AIRCRAFT CORPORATION
WINDSOR LOCKS, CONNECTICUT 06096

SPACE & LIFE SYSTEMS LABORATORY

LOG OF TEST

TYPE OF TEST: ICE PACK WATER BOILER
TEST ENGINEER: E. ROEBELEN
NAME OF RIG: 25
PROJECT & ENG. ORDER NO.: 1389-500-300A

SHEET 3 OF DATE 10-4-74
TEST PLAN NO. ECS-2124-L-079
MODEL NO.
PART NO.
SERIAL NO.
OPERATORS LASZCZYK

TIME	TEST TIME	VOLTS	AMPS	AMPS	WATTS		FLOW SYST.	FLOW HX	HX		HX IN	HX OUT	HX IN	HX OUT	ΔT	LCG IN	LCG OUT	WALL TEMP		BLADDER PRESS	STEAM PRESS	CHAMB PRESS
	MIN	AC	AC	AC			%	%	%		PSIA	PSIA	°F 37	°F 38	MV	°F 1	°F 2	39		PSIA	MM	TORR
1400		0	0	0	0		82.5	100+	-		23.1	15	77.5	77.5	.007	77.5	77.5			0	4.2 MM	5.5X10⁻⁵
1403		0	0	0	0															20		
1405	0	87	4.12	2.58	582.9											62	67					
1416	10	87.5	4.15	2.60	590.62		82.5	100+			23.6	15	65.5	56	.210	56	64.5			20	4.15 MM	4.6X10⁻⁵
1425	20	87.5	4.13	2.62	590.62		82.5	100+			23.8	15	64	55.	.200	54.5	63.5			20	4.10 MM	4.6X10⁻⁵
1435	30	87.5	4.13	2.62	590.62		82.5	100+			23.6	15	63	54.5	.197	54	62.			20	4.06 MM	4.3X10⁻⁵
1445	40	87.5	4.15	2.62	592.37		82.5	100+			23.6	15	62.5	54.	.197	54	62			20	4.0	4.4X10⁻⁵
1455	50	87.5	4.13	2.62	590.62		82.5	100+			23.6	15	62.5	54	.197	54	62			20	4.0	4.4X10⁻⁵
1605	0	76.	3.6	2.24	443.84		82.5	100+			23.4	15	58	51	.160	51	57			20	3.9	4.2X10⁻⁵
1615	10	76	3.6	2.24	443.84		82.5	100+			24.	15	57	50.5	.158	50.5	56.5			20	3.9	4.1X10⁻⁵
1625	20	76	3.6	2.24	443.84		82.5	100+			24	15	57.	50	.156	50	56.			20	3.85	4.X10⁻⁵
1635	30	76	3.6	2.24	443.84		82.5	100+			24	15	56.5	49.5	.152	49.5	55.5			20	3.85	4.5 MM
1645	40	76	3.6	2.24	443.84		82.5	100+			24	15.	56.5	49.5	.152	49.5	55.5			20	3.85	4.0 MM

REMARKS:

BOTH SIDES OF WATER BOILER OPEN TO VAC.
165 CC H_2O IN H_2O TRAP IN CHAMBER 1650 CC IN Cold TRAP
@ 1500 Btu/hr #1
@ 2000 Btu/hr #1

10522

HSP-178 1A 1/66

Hamilton Standard DIVISION OF UNITED AIRCRAFT CORPORATION
WINDSOR LOCKS, CONNECTICUT 06096

SPACE & LIFE SYSTEMS LABORATORY

LOG OF TEST

TYPE OF TEST: ICE PACK
TEST ENGINEER: G. ROEBELEN
NAME OF RIG: 25
PROJECT & ENG. ORDER NO.: 869-500-300A

SHEET 1 OF DATE 10-7-74
TEST PLAN NO.
MODEL NO
PART NO.
SERIAL NO.
OPERATORS: LASZCZYK

TEST TIME MIN	Volts AC	Amps AC	Amps AC	WATTS	LCG IN °F1	LGG OUT °F2		TEST TIME MIN	Volts AC	Amps AC	Amps AC	WATTS	LGG IN °F1	LCG OUT °F2
	0	0	0	0	49	49			0	0	0	0	48	48
0	87.5	4.1	2.64		50	50		0	76	3.56	2.28		49	49
1					50.5	52		1	76	3.55	2.29		49	50
2					52	55		2					50	52
3					54.5	57		3					52	54
4					56.5	59		4					53.5	55.5
5					59	62		5					55.5	57.5
6					61	64		6					57	59
7					63	66		7					58.5	61
8					65	68		8					60	62.5
9					67	70		9					62	64
10					69	72		10					63	65.5
11					71	73.5		11					65	67
12					72.5	76.		12					66	68.5
13					74.5	77.5		13					68	70
14					76	79.5		14					69	72
15					78	82		15					71	73
16	87.5	4.1	2.64		79.5	83		16					72	74.5
								17					73.5	75.5
								18					74.5	77.5
								19					76	78.8
								20					77	80
								21					78.5	81
								22	76	3.55	2.29		79.5	83

REMARKS

10525

G-15

Hamilton Standard DIVISION OF UNITED AIRCRAFT CORPORATION
WINDSOR LOCKS, CONNECTICUT 06096

SPACE & LIFE SYSTEMS LABORATORY

LOG OF TEST

TYPE OF TEST: ICE PACK
TEST ENGINEER: G ROEBELEN
NAME OF RIG: 35
PROJECT & ENG. ORDER NO.: B&G-300-300A

SHEET 2 OF
DATE 10 7-76
TEST PLAN NO.
MODEL NO.
PART NO.
SERIAL NO.
OPERATORS: LASZLO YK

TEST TIME	VOLTS	AMPS	AMPS	WATTS	LCG IN	LCG OUT	TEST TIME	VOLTS	AMPS	AMPS	WATTS	LCG IN	LCG OUT	TEST TIME	VOLTS	AMPS	AMPS	WATTS	LCG IN	LCG OUT
MIN	AC	AC	AC		°F 1	°F 2	MIN	AC	AC	AC		°F 1	°F 2						°F 1	°F 2
	0	0	0		47.5	47.5	19	53.5	4.1	–		64.5	65.5	39	53.5	4.1	–		78	79
0	53.5	4.1	–		48.5	48	20	53.5	4.1	–		65	66	40	"	"			78	80
1	"	"			49	49	21	"	"			66	67	41	"	"			79	80.5
2	"	"			49.5	50	22	"	"			67	68	42	53.5	4.1	–		79.5	81
3	"	"			50.5	51	23	"	"			68	68.5							
4	"	"			51.5	52	24	"	"			69	70							
5	"	"			52.5	53.5	25	"	"			69	70							
6	"	"			53.5	54	26	"	"			69.5	70.5							
7	"	"			54.5	55	27	"	"			70.5	71.5							
8	"	"			55.5	56	28	"	"			71	72							
9	"	"			56	57	29	"	"			72	73							
10	"	"			57	58	30	"	"			72	73.5							
11	"	"			58	59	31	"	"			73	74							
12	"	"			59	60	32	"	"			73.5	75							
13	"	"			60	61	33	"	"			74	75.5							
14	"	"			60.5	61.5	34	"	"			75	76.5							
15	"	"			61.5	62.5	35	"	"			75.5	77							
16	"	"			62.5	63	36	"	"			76	77.5							
17	"	"			63	64	37	"	"			76.5	78							
18	53.5	4.1	–		64	65	38	53.5	4.1			77	78.5							

REMARKS:

10527

G-16

APPENDIX H

REFERENCES

REFERENCES

1. "Thermal Conductance of Metallic Contacts in a Vacuum." E. Fried and M. J. Kelley (General Electric Co.). AIAA Paper 65-661, September 13, 1965.

2. "Thermal Contact Resistance of Selected Low Conductance Interstitial Materials." L. S. Fletcher and P. A. Smuda (Arizona State University). AIAA Paper 68-31, January 22, 1968.

3. "A Review of Thermal Control Materials for Metallic Junctions." L. S. Fletcher (Rutgers University). AIAA Paper 72-284, April 10, 1972.

4. "Ice Pack Heat Sink Subsystem - Phase I, Volume I." George J. Roebelen, Jr. (Hamilton Standard) SVSHER 6223; NASA CR 114624, June 1973.

5. "First Quarterly Report, Ice Pack Heat Sink Subsystem." George J. Roebelen, Jr. (Hamilton Standard) Contract NAS 2-7011, Report ECS-2124-L-015.

6. "Design Manual." (Hamilton Standard).

7. "Ice Chest Computer Models." J. Wehner (Hamilton Standard) SSD Analysis Memo 74-7, April 1974.

8. "Prospects for Thermal Energy Storage." Manfred Altman (Pennsylvania, University, Towne School of Civil and Mechanical Engineering, Institute for Direct Energy Conversion, Philadelphia, Pa.). In: Combustion and Propulsion; Agard Colloquium on Energy Sources and Energy Conversion, 6th, Cannes, France, March 16-20, 1964, Papers. [A68-22514 09-03]

9. "Manufacture of Thermal Storage Materials." Spikins, Paul Brit. 1,291,057 (Cl C 08b), 27 September 1972, Appl. 50,026/68, 22 October 1968.

10. "Heat-Storage System." N. V. Philips' Gloeilampenfabrieken Neth. Appl. 70 12,830 (Cl. C 09k, F 02g), 02 Mar 1972, Appl. 29 Aug 1970; 7 pp.

11. "Heat-Storage Materials and Devices." Accessair S. A. Brit. 1,255,331 (Cl. F 24h, B 01j, C 01gd), 01 Dec 1971, Austrian Appl. 27 Nov 1967-22 Nov 1968; 9 pp.

REFERENCES (CONTINUED)

12. "Heat-Storage Module Comprising an Anhydrous Alkali-metal Hydroxide Composition and Aluminized Walls." Mekjean, Matthew (Hooker Chemical Corp.) U. S. 3,517,151 (Cl. 219-10.49; H 05b), 23 Jun 1970, Appl. 03 Sep 1968.

13. "Prediction of Transient Heat Transfer Performance of Thermal Energy Storage Devices." Manfred Altman, D. P. Ross, and Han Chang (Univ. of Pennsylvania, Philadelphia). Chem. Eng Progr., Symp. Ser. 61(57), 289-98 (1965) (Eng).

14. "Chemical Aspects of Heat Storage." Martin Goldstein. Scuola Azione Pt. 1 1962, No. 18, 178-96.

15. "Design of a Chemical Heat Accumulator." Kh. A. Kistoryan. Trudy Nauch.-Tekh. Konf. po Geliotekh., Erevan 1959, 87-93.

16. "The Storage and Transfer of Low Potential Heat." J. W. Hodgins, T. W. Hoffman. Can. J. Tech. 33, p. 293-302 (1955).

17. "Hydrazine: Heat Capacity, Heats of Fusion and Vaporization, Vapor Pressure, Entropy, and Thermodynamic Functions." D. W. Scott, G. D. Oliver, Margaret E. Gross, W. N. Hubbard, and Hugh M. Huffman (U. S. Bur. Mines, Bartlesville, Okla). J. Am. Chem. Soc. 71, 2293-7 (1949).

18. "Handbook of the Physiochemical Properties of the Elements." Ed. by G. V. Samsonov IFI/plenum (1968).

19. "Study of Heat Storage Cells for Space Solar Power Plants." V. M. Matveev (Akademiia Nauk SSSR, Moscow, USSR). IN: International Astronautical Federation, International Astronautical Congress, 18th, Belgrade, Yugoslavia, September 24-30, 1967, Proceedings. Volume 2 - Spacecraft Systems, Education, Edited by Michal Lunc. Oxford, Pergamon Press, Ltd.; Warsaw, Panstwowe Wydawnictwo Naukowe, 1968, p. 147-151. In Russian.

20. "Heat-Transfer Processes in Solar Energy Storage Systems for Orbital Applications. Frank Matinek (Vermont, University, Burlington, Vt). Journal of Spacecraft and Rockets, Vol. 7, Sept 1970, p. 1032-1037. 15 refs.

REFERENCES (CONTINUED)

21. "Design and Fabrication of Brayton Cycle Solar Heat Receiver." Final Report. I. Mendelson, (ed.) Jul 1971 329 p. refs. Contract NAS3-10944. (NASA-CR-72872 GESP-519) Avail. NTIS HC $6.00/MF $.95 CSCL 10C.

22. "Filling Heat Storage Tubes for Solar Brayton-Cycle Heat Receiver with Lithium Fluoride." P. A. Gnadt, Jul 1970 90 p. refs. (NASA Order C-90089-A; Contract W-7405-eng-26). NASA-CR-110776; ORNL-TM-2732 Avail: NTIS CSCL 10B.

23. "Thermal Energy Storage/Converter Prototype Design, Fabrication and Testing." Final Report. B. Gunther, S. Merra, and P. Pantazzelos, Jan 1968, 42 p. refs. Prepared for JPL. (Contracts NAS7-100; JPL 950976). (NASA-CP-93177; TE-4049-30-68) CFSTI: HC $3.00/MF $0.65 CSCL 10A.

24. "The Solar Collector Thermal Power System - Its Potential and Development Status." E. T. Mahefkey, Jr. (USAF, Aero Propulsion Laboratory, Wright-Patterson AFB, Ohio). In: Intersociety Energy Conversion Engineering Conference, 7th, San Diego, Calif., September 25-29, 1972, Proceedings. (A73-22751-09-03) Washington, D. C., American Chemical Society, 1972, p. 512-521, 28 refs.

25. "Heat of Fusion, A Thermodynamic Constant." Popovici, Vasile. Rev. Fiz. Chim., Ser. A 1969, 6(5), 161-6 (Rom).

26. "A Correlation of the Entropy of Fusion of Molecular Crystals with Molecular Structure." A. Bondi (Shell Develop. Co., Emeryville, Calif.). Chem. Rev. 67(5), 565-80 (1967) (Eng).

27. "Relations Between the Crystal Structure, Temperature, and Heat of Fusion of Solids." N. N. Stulov (Mining Inst., Leningrad). Zapiski Vesesoyuz. Mineral. Obshchestva 89, 143-51 (1960).

28. "How to Estimate Engineering Properties." Wallace R. Gambill (Union Carbide). Find Heat of Fusion and Sublimation Chem.Eng. 64, No. 5, 147-9 (1957).

29. "The Relation Among Some Physiochemical Constants of the Elements." S. D. Gertsriken. Dopovodi Akad. Nauk Ukr. R. S. R. 1956, No. 1 72-3 (Russian summary 74).

REFERENCES (CONTINUED)

30. "Correlating Vapor Pressures and Other Physical Properties." Donald F. Othmer, Paul W. Maurer, Charles J. Molinary, and Ronald C. Kowalski (Polytech. Inst. of Brooklyn, Brooklyn, N.Y.) Ind. Eng. Chem. 49, 125-37 (1957).

31. "Correlating Vapor-Pressure and Latent-Heat Data: A New Plot." Donald F. Othmer. Ind. Eng. Chem. 32, 841-56 (1940).

32. "A Relation Between the Heat of Fusion of Intermetallic Compounds and Their Melting Points and the Calculation of Heats of Formation and Heats of Solution." Oswald Kubaschewski and Friedrich Weibke. Z. Metallkunde 30, 325-6 (1938).

33. "Latent Heat of Fusion." Nath S. Binayendra. Gazz. Chim. Ital. 67, 714-15 (1937).

34. "Relation Between Molecular Structure and the Value of the Heat of Fusion of Organic Compounds. II." Synthesis of 1, 4 -endoazocyclohexane. Josef Pirsch and Josef Jorgl. Ber. 68B, 1324-30 (1935).

35. Turkdogan and Pearson. J. Appl. Chem. 3, 495 (1953).

36. Glasstone, S.: "Textbook of Physical Chemistry", 2nd Edition, D. Van Nostrand Co., Inc., Princeton, New Jersey (1946).

37. Ubbelohde, A. R.: "Melting and Crystal Structure", Clarendon Press, Oxford (1965).

38. "Condensation of Ammonium Bifluoride." Sudarikov, B. N.; Rakov, E. G.; Bratishko, V. D.; Cherkasov, V. A. (USSR). Tr. Mosk. Khim.-Tekhnol. Inst. 1967, No. 56, 228-31 (Russ).

39. "System Ammonia + Carbon Dioxide + Ammonium Carbamate. I. Equilibrium of Thermal Dissociation of Ammonium Carbamate." R. N. Bennett, P. D. Ritchie, D. Roxburgh, and J. Thomson (Royal Tech. Coll., Glasgow, Scot.). Trans. Faraday Soc. 49, 925-9 (1953).

REFERENCES (CONCLUDED)

40. "Lange's Handbook of Chemistry." N. A. Lange, Ed. Handbook Publishers Inc., Ohio.

41. Harshaw Bulletin 82074 (Harshaw Chemical Co.).

42. "Electrolyte Solutions." Robinson and Stokes. Academic Press (1959), p. 68-70.

43. "Ice Pack Heat Sink Subsystem - Phase II Flight Experiment Plan". George J. Roebelen, Jr. Hamilton Standard, SVHSER 6526, December 1974.